

Charles University in Prague

Faculty of Science

Study program: Biology

Field of study: Cell and Developmental Biology



**Jarmila Tvarůžková**

**The role of CSL proteins in oxidative stress response of *Schizosaccharomyces pombe***

Role proteinů rodiny CSL v odpovědi na oxidativní stres u *Schizosaccharomyces pombe*

*Diploma thesis*

Supervisor: RNDr. Martin Převorovský, Ph.D.

PRAGUE 2015

## **Prohlášení**

Prohlašuji, že jsem závěrečnou práci zpracovala samostatně a že jsem uvedla všechny použité informační zdroje a literaturu. Tato práce ani její podstatná část nebyla předložena k získání jiného nebo stejného akademického titulu.

V Praze, 4.5.2015

Jarmila Tvarůžková

## **Acknowledgements**

I wish to thank my supervisor RNDr. Martin Převorovský, Ph.D. for the support and encouragement I have received during my time under his wing. I would also like to thank the head of the Laboratory of gene expression regulation Doc. Petr Folk, CSc. and Petr Daněk for fruitful discussions, as well as other members of the Folk lab.

## Abstract

Oxidative stress represents a complex and intensely studied phenomenon tightly linked to a range of human diseases, and to aging in many organisms. A plethora of key cellular regulators, including the Notch signaling pathway, have been recently described to respond to the cellular redox status. We have characterized the role of CSL (CBF1/Su(H)/LAG-1) proteins, the effectors of Notch signaling pathway in metazoa, in oxidative stress response in fission yeast. *Schizosaccharomyces pombe* contains two CSL paralogs, Cbf11 and Cbf12, that have antagonistic functions in the regulation of cell cycle and cellular adhesion. Both proteins are able to bind the canonical CSL motif and activate transcription and, thus, function as genuine CSL transcription factors. We have determined that the strain lacking *cbf11* is resistant to hydrogen peroxide but not to menadione, a source of superoxide anion radical. Using double knock-outs to assess genetic interactions we have revealed that the resistance of *cbf11* knock-out is dependent on the antioxidants catalase and sulfiredoxin. Genes encoding these antioxidants are under transcriptional control of the Sty1 MAP kinase pathway and the Pap1 transcription factor which are also required for the resistance of *Δcbf11* cells. Cbf12 is believed to play only a minor role in oxidative stress response, nonetheless, it was shown to genetically interact with Sck1 during oxidative stress. Furthermore, cells lacking *cbf11* display nutrient-dependent respiration defect accompanied with differential regulation of genes required for respiration control and energy metabolism. Our findings contribute to the understanding of stress response in the fission yeast and propose a novel role for the CSL proteins in regulation of cell respiration and oxidative stress response.

**Key words:** oxidative stress, genetic interactions, *Schizosaccharomyces pombe*, CSL proteins, Cbf11, Cbf12, cell respiration

## Abstrakt

Oxidativní stres představuje komplexní a intenzivně studovaný fenomén, který je úzce spjat s řadou lidských onemocnění a procesem stárnutí u široké škály organismů. V nedávné době bylo popsáno velké množství klíčových buněčných regulátorů včetně signální dráhy Notch jako proteinů reagujících na redoxní stav buňky. V této práci jsme popsali roli proteinů CSL (CBF1/Su(H)/LAG-1), efektorů signální dráhy Notch u živočichů, v odpovědi na oxidativní stres u kvasinky *Schizosaccharomyces pombe*. *S. pombe* obsahuje dva paralogy proteinů CSL, Cbf11 a Cbf12, které fungují antagonisticky při regulaci buněčného cyklu a adheze. Oba proteiny jsou schopny vázat kanonický CSL element a aktivovat transkripci, takže fungují jako pravé transkripční faktory CSL. Zjistili jsme, že kmen postrádající gen *cbf11* je rezistentní vůči peroxidu vodíku ale ne vůči menadionu, zdroji superoxid anion radikálu. Analýzou genetických interakcí u dvojitéch deletantů jsme odhalili, že rezistence mutanta  $\Delta cbf11$  je závislá na přítomnosti antioxidantních enzymů katalázy a sulfiredoxinu. Geny kódující tyto enzymy jsou pod transkripční kontrolou signální dráhy MAP kinázy Sty1 a transkripčního faktoru Pap1, které jsou také nezbytné pro rezistenci buněk  $\Delta cbf11$ . Cbf12 pravděpodobně hraje pouze minoritní roli v odpovědi na oxidativní stres, nicméně byla prokázána jeho genetická interakce s kinázou Sck1 během oxidativního stresu. Buňky s delecí *cbf11* navíc v závislosti na dostupnosti živin vykazují defekt v buněčném dýchání doprovázený odlišnou regulací genů nutných pro respiraci a energetický metabolismus. Naše výsledky přispívají k pochopení stresové odpovědi u poltivé kvasinky a naznačují novou roli proteinů CSL v regulaci buněčného dýchání a odpovědi na oxidativní stres.

**Klíčová slova:** oxidativní stres, genetické interakce, *Schizosaccharomyces pombe*, proteiny CSL, Cbf11, Cbf12, buněčné dýchání

## Table of Contents

1	Introduction .....	9
1.1	Oxidative stress.....	9
1.1.1	Chemistry of oxidants.....	9
1.1.2	Overview of oxidative stress response across the kingdoms.....	14
1.1.3	Oxidative stress response of <i>Schizosaccharomyces pombe</i> .....	15
1.2	CSL proteins.....	23
1.2.1	CSL in <i>S. pombe</i> .....	24
1.3	The theory of genetic interactions .....	24
2	Thesis objectives .....	27
3	Materials and methods .....	28
3.1	Microorganismal strains and growth conditions.....	28
3.1.1	<i>Escherichia coli</i> strains and cultivation .....	28
3.1.2	<i>Schizosaccharomyces pombe</i> strains and cultivation .....	28
3.2	Transformation methods.....	29
3.2.1	Electroporation of <i>E. coli</i> .....	29
3.2.2	Transformation of <i>S. pombe</i> using lithium-acetate method.....	29
3.3	<i>Schizosaccharomyces pombe</i> genetic crosses.....	30
3.3.1	Mating type testing by iodine staining.....	31
3.4	Molecular cloning.....	32
3.4.1	Plasmid DNA isolation using the alkaline method.....	32
3.4.2	DNA isolation using Nucleospin® Plasmid and Nucleospin® Extract kits .....	33
3.4.3	Quick chromosomal DNA extraction from <i>S. pombe</i> .....	33
3.4.4	Polymerase chain reaction .....	33
3.4.5	Plasmids .....	35
3.4.6	DNA restriction with endonucleases.....	36
3.4.7	DNA ligation.....	37
3.4.8	Agarose gel electrophoresis.....	37
3.5	Phloxine staining.....	38
3.6	Flow cytometry .....	38
3.7	Microscopy of mitochondria.....	38
3.8	Respirometry .....	39
3.9	Spot tests.....	40

3.10	Gene expression analysis.....	41
4	Results .....	42
4.1	CSL proteins play a role in oxidative stress response.....	42
4.1.1	Sensitivity of CSL mutants varies with used ROS source .....	42
4.1.2	<i>cbf11</i> is crucial for cell respiration.....	43
4.1.3	Respiration of $\Delta cbf11$ depends on the carbon source .....	45
4.2	Upstream regulators of CSL.....	46
4.2.1	Construction of strains.....	47
4.2.2	CSL interact genetically with the Sty1 and Pap1 stress-response pathways .....	50
4.2.3	Cbf11 and Pka1 interact as negative regulators of oxidative stress response...	53
4.3	Downstream regulators of CSL.....	54
4.3.1	Construction of strains.....	54
4.3.2	Catalase and sulfiredoxin are responsible for the resistance of $\Delta cbf11$ .....	55
4.3.3	Cbf11 differentially regulates mitochondrial ATP synthesis coupled electron transport and glucose metabolism .....	58
5	Discussion .....	62
5.1	Cbf11 acts as a negative regulator of oxidative stress response .....	62
5.2	The regulatory network of CSL mutants during oxidative stress .....	64
5.3	The mitochondrial defect of $\Delta cbf11$ cells depends on the nutrients.....	67
5.4	The consequences of stress response activation in $\Delta cbf11$ cells.....	68
6	Conclusions.....	70
7	References.....	71
8	List of supplements.....	82

## List of abbreviations

ATP	adenosine triphosphate
bp	base pairs
bZIP	basic leucine zipper domain
CSL	CSL family proteins (C <u>B</u> F1/ <u>S</u> u(H), <u>L</u> AG-1)
ETC	mitochondrial electron transport chain
EDTA	ethylenediaminetetraacetic acid
dH <sub>2</sub> O	deionized water
DiOC <sub>6</sub> (3)	3,3'-dihexyloxacarbocyanine iodide
DMSO	dimethyl sulfoxide
dNTP	deoxynucleotide triphosphate
FSC	forward-scattered light intensity
GO	gene ontology
KO	knock-out
MAPK	mitogen-activated protein kinase
ME	malt extract
NADH	nicotinamide adenine dinucleotide
NADPH	nicotinamide adenine dinucleotide phosphate
ORF	open reading fram
PCR	polymerase chain reaction
PDI	protein disulfide isomerase
PEG	polyethylene glycol
PI	propidium iodide
PKA	protein kinase A
ROS	reactive oxygen species
RT	room temperature
RT-qPCR	reverse transcription and quantitative polymerase chain reaction
SAPK	stress-activated protein kinase
SGA	synthetic genetic array
SSC	side-scattered light intensity
TBH	<i>tert</i> -butyl hydroperoxide
TF	transcription factor
TOR	Target Of Rapamycin kinase
WT	wild type
YES	complex medium

# 1 Introduction

## 1.1 Oxidative stress

Historically, the free radicals were viewed as purely harmful to the human body. Denham Harman proposed in 1956 that free radicals, molecules or atoms with unpaired valence electrons, are the cause of aging and degenerative diseases (Harman, 1956). However, today we know that radicals are common intermediates of chemical reactions taking place in the living cells, they can act as signaling molecules or as defense mechanism in the immune response. Oxidative stress occurs when the equilibrium between the production and the detoxification of oxidants and their harmful effects is disturbed. Reactive oxygen species (ROS) are the most widely studied oxidants, but also reactive nitrogen species (RNS), reactive sulphur species (RSS), ionizing radiation, transition metals and other substances may cause oxidative stress (Finkel and Holbrook, 2000; Valko *et al.*, 2005; Nathan and Cunningham-Bussel, 2013; Poljšak and Fink, 2014).

Oxidative stress is associated with multiple cardiovascular and neurodegenerative diseases, diabetes, cancer, psychiatric disorders and aging (Balaban *et al.*, 2005; Valko *et al.*, 2007; Finkel, 2011; Rosini *et al.*, 2013; Aroor and DeMarco, 2014; Costa *et al.*, 2014; O'Donnell *et al.*, 2014). Oxidative damage and cellular ROS tend to accumulate in aging cells and in the case of above mentioned diseases. However, it remains controversial whether oxidative stress causes the disease or merely correlates with its occurrence. On the other hand, the role of reactive oxygen species and other oxidants in physiological functions is now well established even though not completely understood. Pathogen killing by phagocytes as a part of innate immunity was the first described physiological role of ROS in mammalian cells and since then ROS were discovered to regulate processes such as development, proliferation, migration, autophagy and inflammatory response (Nathan and Cunningham-Bussel, 2013; Rhee, 2013). The regulatory role of ROS is supported by the discovery of H<sub>2</sub>O<sub>2</sub> transporters across the plasma membrane and inner mitochondrial membrane (Bienert *et al.*, 2007; Miller *et al.*, 2010). Therefore, it has been suggested that not only the excess but also the lack of oxidants may lead to pathological responses (Finkel, 2011; Watson, 2014).

### 1.1.1 Chemistry of oxidants

Oxygen is undoubtedly one of the most important elements for the existence of life but its advantages come at the price of cellular damage or even death by reactive oxygen species if left uncontrolled. ROS comprise a family of molecules, such as hydrogen peroxide (H<sub>2</sub>O<sub>2</sub>), superoxide anion radical (O<sub>2</sub><sup>•-</sup>), hydroxyl radical (OH<sup>•</sup>), singlet oxygen (<sup>1</sup>O<sub>2</sub>), lipid peroxide (ROOH), ozone (O<sub>3</sub>) and hypochlorous acid (HOCl), whose reactivity and impact on cellular

compartments differ considerably (Murphy *et al.*, 2011). Superoxide, the principal precursor of hydrogen peroxide, is considered a poorly reactive oxidant unable to cross membranes. On the other hand, hydroxyl radical can be found on the opposite side of the reactivity spectrum, making it the most damaging ROS (Valko *et al.*, 2005; Dickinson and Chang, 2011; Forman *et al.*, 2014).

### 1.1.1.1 Sources of reactive oxygen species

Reactive oxidants naturally arise within the cells (Figure 1.1) but may also come from the environment. The major sources of intracellular ROS are the electron transport chain of active mitochondria, which accounts for 90% of cellular ROS production, NADPH-dependent oxidases and glycoprotein Ero1 in the endoplasmic reticulum. Other sources include cyclooxygenases, cytochromes P-450, lipoxygenases, xanthine oxidase, nitric oxide synthase,  $\beta$ -oxidation of long chain fatty acids in the peroxisomes, and free iron and copper ions released from metal-containing enzymes or storage proteins and chelators (Balaban *et al.*, 2005; Valko *et al.*, 2005; Nathan and Cunningham-Bussel, 2013; Holmström and Finkel, 2014).

Respiring mitochondria produce ROS mainly as by-products of the electron transport chain (ETC). Various sites in complexes I, II, and III of ETC are able to channel electrons from NADH and  $\text{FADH}_2$  to molecular oxygen not only to form water but also  $\text{O}_2^{\cdot-}$  and  $\text{H}_2\text{O}_2$ . However, production of ROS is not a mere undesired electron leakage but it is a process regulated by

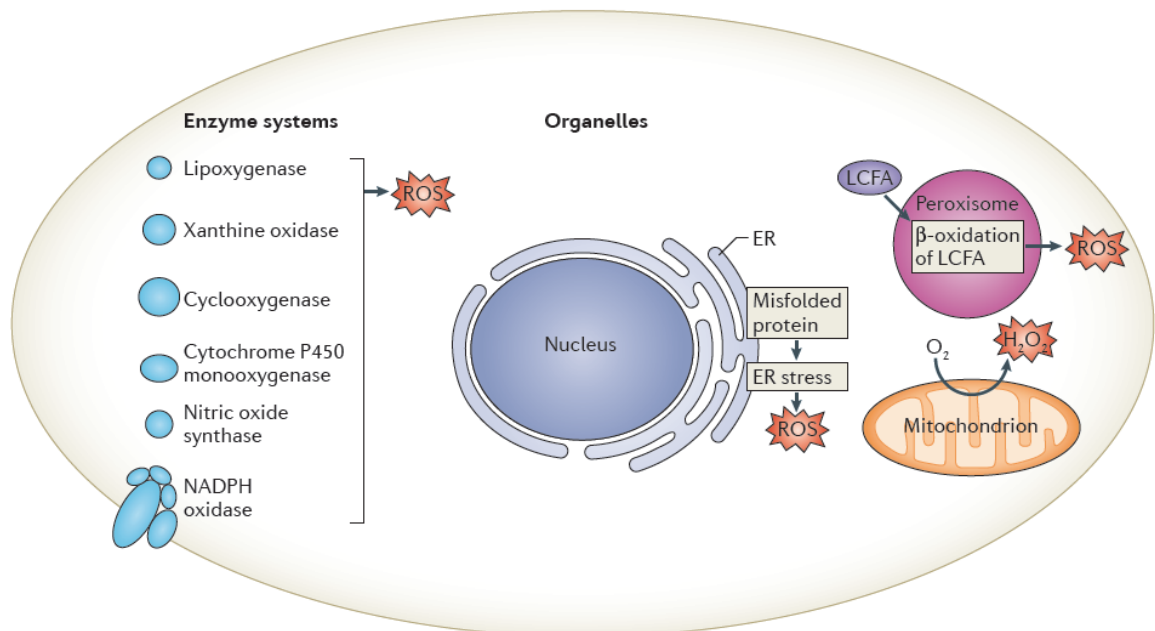


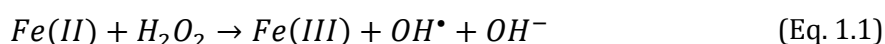
**Figure 1.1 Intracellular sources of reactive oxygen species.** Various enzyme systems and organelles can generate ROS. ER - endoplasmic reticulum, LCFA - long chain fatty acid. Adapted from (Holmström and Finkel, 2014).

inner membrane electrochemical potential, non-mitochondrial sources of ROS and electron transport chain substrates (Dickinson and Chang, 2011; Finkel, 2011; Nathan and Cunningham-Bussel, 2013; Quinlan *et al.*, 2013; Nickel *et al.*, 2014).

Endoplasmic reticulum is the site of oxidative protein folding which is necessary for proper function of many secreted proteins. The formation of a disulfide bond on the secreted protein is catalyzed by thioredoxin protein disulfide isomerase (PDI). The glycoprotein Ero1 is responsible for reoxidation of PDI and it uses molecular oxygen as the electron donor, forming H<sub>2</sub>O<sub>2</sub>. Since one molecule of H<sub>2</sub>O<sub>2</sub> is produced per disulfide bond formed, it is a significant source of intracellular ROS (Dickinson and Chang, 2011; Eletto *et al.*, 2014).

The NOX family of NAD(P)H oxidases is a group of transmembrane heme-containing enzymes that transport electrons across cellular membranes and their primary function is the regulated generation of O<sub>2</sub><sup>•-</sup> and H<sub>2</sub>O<sub>2</sub> (Dickinson and Chang, 2011; Finkel, 2011; Nathan and Cunningham-Bussel, 2013). The functional role of these enzymes is extremely context-dependent as they might have contrasting effects such as apoptosis, proliferation and protection against inflammation. This probably depends on the concentration and duration of the ROS burst, local concentration of the NOX enzyme and its interacting proteins (Bedard and Krause, 2007).

Enzymes are not the sole source of cellular ROS. Metals such as iron, copper, vanadium, chromium and cobalt produce the highly reactive hydroxyl radical via the Fenton reaction (Eq. 1.1):



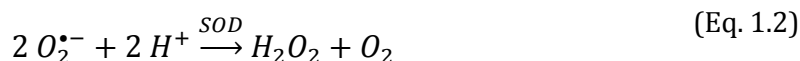
Intracellular concentration of iron is tightly regulated and majority of this metal is sequestered in iron-containing proteins such as hemoglobin, cytochromes, myoglobin, or in storage proteins, such as ferritin and hemosiderin. Iron homeostasis is also maintained by many chelating agents. These mechanisms together prevent the existence of large pools of free iron and, thus, undesired production of ROS (Valko *et al.*, 2005). Additionally, iron catalyzes the formation of lipid peroxides from polyunsaturated fatty acids which leads to production of peroxy radicals (ROO<sup>•</sup>). Once formed, lipid peroxidation proceeds as an autocatalytic radical reaction, causing significant alterations in membrane permeability (Valko *et al.*, 2007). Cyclization of lipo-peroxy radicals leads to formation of mutagenic and carcinogenic compounds such as malondialdehyde (Jomova and Valko, 2011).

### 1.1.1.2 The damaging effects of ROS and their detoxification

The toxicity of ROS is caused by disrupting physiological function of cellular enzymes, integrity of DNA and permeability of membranes, and also by inactivation of ROS-detoxifying mechanisms. Amino acid side chains, peptide backbone and metal-containing catalytic centers of enzymes are all vulnerable to oxidation by ROS. Interestingly, many enzymes maintaining redox homeostasis, DNA repair and replication are very susceptible to damage by ROS (Imlay, 2013; Jain *et al.*, 2013). DNA mutations may also arise from oxidation of nucleobases, especially guanine, or the sugar backbone. The most common product of DNA oxidation is 8-hydroxyguanine that has the ability to base pair with adenine, but also oxidation of other bases, abasic site formation or strand breaks may occur (Halliwell and Aruoma, 1991; Imlay, 2013). However, except for the telomeres, regions rich in guanine where the damage persists (Coluzzi *et al.*, 2014), mutations are usually promptly repaired by the cell. Whether DNA damage by ROS causes production of dysfunctional proteins and, thus, aging and cell death or damage directly to proteins leads to compromised repair mechanisms and DNA replication fidelity, leading to further protein coding errors is debated (Krisiko and Radman, 2013).

Enzymatic and non-enzymatic molecules cooperate to eliminate excessive reactive oxygen species via several mechanisms. Non-enzymatic antioxidants such as glutathione, ascorbate (Vitamin C), pyruvate, oxaloacetate,  $\alpha$ -ketoglutarate, flavonoids, carotenoids (Vitamin A) and  $\alpha$ -tocopherol (Vitamin E) have the capacity to scavenge less reactive oxidants and reduce oxidized molecules including other antioxidants (Chaudière and Ferrari-Iliou, 1999; Finkel and Holbrook, 2000; Balaban *et al.*, 2005; Valko *et al.*, 2007). Glutathione is the most abundant cellular antioxidant, present at 1-10 mM concentration predominantly in the reduced form (GSH). Its significance as a redox buffer is illustrated by massive mtDNA loss, iron and superoxide accumulation, and respiration incompetency when depleted (Ayer *et al.*, 2010). In addition to its ROS scavenging activity and antioxidant recycling, it is a common cofactor of enzymes such as glutathione peroxidase or glutathione S-transferase.

Enzymatic scavengers include superoxide dismutase, catalase, peroxidases, peroxiredoxins, thioredoxin, thioredoxin reductase and methionine sulfide reductase. Superoxide anion radical is enzymatically decomposed (Eq. 1.2) by superoxide dismutase (SOD).





The resulting H<sub>2</sub>O<sub>2</sub> may be detoxified by catalase (Eq. 1.3, page 12), glutathione peroxidase (Eq. 1.4) or peroxiredoxin. Glutathione and thioredoxin used as electron donors by glutathione peroxidase and peroxiredoxin, respectively, have to be regenerated by reductases at the expense of NADPH. Therefore, redox regulation of the cell and metabolic control must be tightly coupled (Chaudière and Ferrari-Iliou, 1999; Finkel and Holbrook, 2000; Nathan and Cunningham-Bussel, 2013).

### **1.1.1.3 ROS-dependent signal transduction**

ROS modulate protein function mainly through reversible oxidation of cysteine residues, a modification with the capability to alter the structural conformation of a protein and thus modulate its function. Cysteines may become oxidized to a sulfenic form (RSOH) which is unstable and can be further oxidized to a sulfinic (RSO<sub>2</sub>H) or even sulphonic (RSO<sub>3</sub>H) species. Other oxidative modifications include S-glutathionylation and S-nitrosylation (Forman *et al.*, 2014; Groitl and Jakob, 2014). Moreover, cysteine oxidation may be transferred from one protein to another which suggests that it may work as a signaling cascade by transducing signal via several protein-protein redox reactions. How the specificity of ROS-mediated redox signaling is achieved remains to be answered. Nevertheless, only a fraction of proteins contain cysteine residues sufficiently reactive towards ROS. Such cysteines need to be surface-exposed with low pK<sub>a</sub> in order to form nucleophilic thiolates. The specificity of this reaction is also promoted by localization of the ROS source close to the target molecule (Finkel, 2011; Forman *et al.*, 2014). Hence, cysteine oxidation is considered to be a post-translational modification not unlike phosphorylation.

In recent years, numerous intracellular pathways have been described to be affected by ROS and the cellular regulators directly oxidized by ROS have been identified. These molecular targets of ROS include tyrosine and serine/threonine phosphatases (e.g. PTEN), tyrosine and serine/threonine kinases (e.g. EGF receptor, protein kinase B, ATM kinase), peroxiredoxins, transcription factors (e.g. AP-1, p53), histone deacetylases, heat-shock proteins, metabolic enzymes, ion channels and even regulatory gene regions such as promoters (Valko *et al.*, 2007; Dickinson and Chang, 2011; Nathan and Cunningham-Bussel, 2013; Rhee, 2013). Surprisingly, even cytoskeletal proteins including actin and myosin seem to act as redox sensors (Smethurst *et al.*, 2013; Moen *et al.*, 2014).

The precise mechanism by which the oxidation signal is transmitted to the target protein is not yet fully understood, however, two models described below seem most feasible. The first

model, the redox relay (Figure 1.2A), suggests that scavenging enzymes act also as redox sensors and transmitters. In this mechanism, the scavenger enzymes are temporarily oxidized by ROS and mediate the oxidation of the target protein with concomitant reduction of itself or formation of intermolecular disulfide bond between the scavenger enzyme and the target protein. The second proposed mechanism, termed floodgate model (Figure 1.2B), involves inactivation of the scavenging enzymes, thus flooding the surroundings with ROS and allowing for ROS-mediated oxidation of the target protein (Reczek and Chandel, 2015). Furthermore, it is conceivable that the redox relay and the floodgate model take place simultaneously to achieve specificity of the signaling event through protein-protein interactions and a local pool of ROS.

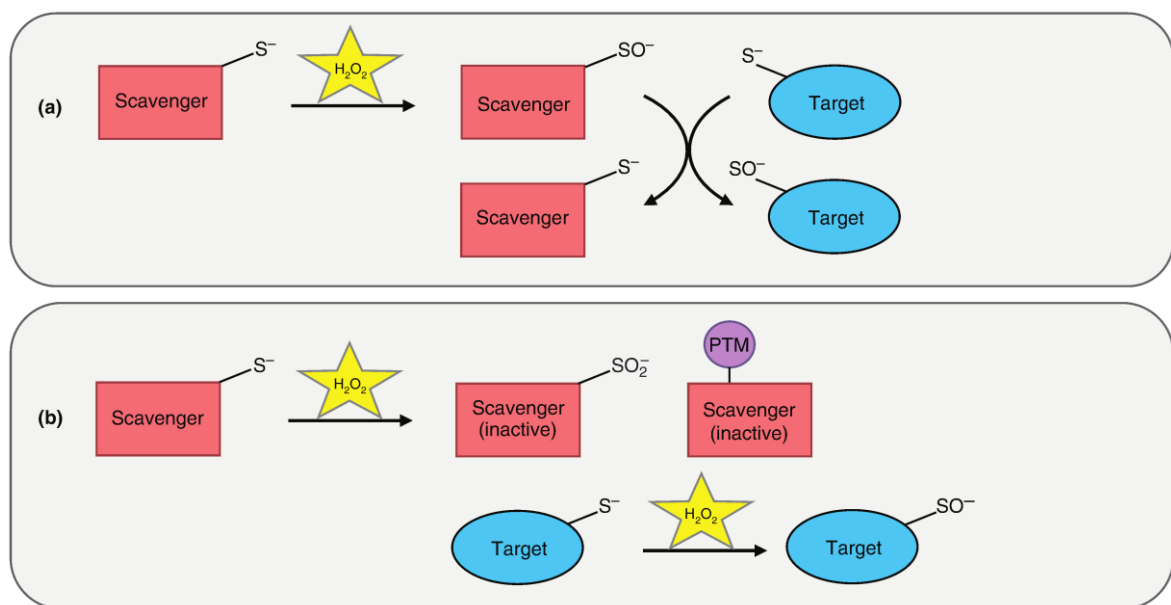


**Figure 1.2 Models of potential mechanisms for H<sub>2</sub>O<sub>2</sub>-dependent signal transduction. (A) The redox relay model. (B) The floodgate model. Adapted from (Reczek and Chandel, 2015).**

### 1.1.2 Overview of oxidative stress response across the kingdoms

Cells must sense and adapt to changes in their environment as well as disruption of intracellular homeostasis in order to survive. Different stress conditions, such as heat shock, osmotic stress, oxidative stress and DNA damage, induce a common response resulting in downregulation of glycolysis and the Krebs cycle, downregulation of general translation, reorganization of the cytoskeleton, upregulation of heat shock proteins, and induction of DNA repair processes and autophagy (Finkel and Holbrook, 2000; Nathan and Cunningham-Bussel, 2013; Smethurst *et al.*, 2013). Oxidative stress-specific responses take advantage of regulatory and metabolic proteins with susceptibility to oxidation by ROS. One example is the increase of pentose phosphate pathway flux to fulfill increasing demand for NADPH by ROS

scavengers. This is achieved by ROS-induced inactivation of pyruvate kinase, thus blocking glycolysis and diverting carbohydrate catabolism to the pentose phosphate pathway (Anastasiou *et al.*, 2011; Stincone *et al.*, 2014). Another interesting mechanism is the induction of DNA damage genes by translocation of tyrosyl-tRNA synthetase from cytoplasm to nucleus upon oxidative stress, leading to activation of E2F1 transcription factor known to promote expression of DNA repair and cell cycle progression genes (Wei *et al.*, 2014).

Three main signaling modules are used by organisms in response to oxidative stress – the MAPK signaling cascades, the multistep phosphorelay system and the redox relay. Mitogen-activated protein kinases (MAPK) constitute a large family of evolutionarily conserved signal transducing proteins, which control cell survival and adaptation in response to mitogenic stimuli. A subfamily of MAP kinases responds to diverse stress signals rather than mitogens and these proteins are, therefore, called stress-activated protein kinases (SAPK). The mammalian members of this family are the extracellular signal-regulated kinase (ERK), c-Jun amino-terminal kinase (JNK) and p38 mitogen-activated protein kinases (Papadakis and Workman, 2014).

The multistep phosphorelay systems, reminiscent of the two-component systems transducing environmental signals to MAPKs, were identified in fungi and plants, but not in animals. Unlike prokaryotic systems, where the sensor histidine kinase directly phosphorylates the response regulator, the eukaryotic systems include a third component, called His-containing phosphotransfer protein, that participates in the histidine to aspartate transfer of a phosphate group from the histidine sensor kinase to the response regulator (Ikner and Shiozaki, 2005).

The third pathway employs thiol-based redox signaling leading to modulation of activity of transcription factors such as bacterial OxyR, eukaryotic AP-1 family, Nrf2 and FoxO (Valko *et al.*, 2007; Veal *et al.*, 2007; Holmström and Finkel, 2014). Peroxiredoxins, enzymes detoxifying H<sub>2</sub>O<sub>2</sub> via cysteine oxidation in their active site, often act as sensors and regulate downstream effectors in this type of mechanism (Holmström and Finkel, 2014).

### **1.1.3 Oxidative stress response of *Schizosaccharomyces pombe***

The fission yeast, or *Schizosaccharomyces pombe*, is a unicellular organism belonging to the subphylum Archiascomycotina and it is evolutionarily distant from *Saccharomyces cerevisiae* (Heckman *et al.*, 2001). Genetic tractability, limited genome redundancy and inexpensive cultivation make this yeast a convenient model organism. Additionally, it shares some genes with humans that are missing from the budding yeast (Aravind *et al.*, 2000), including the CSL

proteins investigated in this thesis (Převorovský *et al.*, 2007). Due to the reasons mentioned above and others, the fission yeast is used extensively as a model organism for studies of stress response, cell cycle, DNA replication and repair, and RNA interference.

The cellular response of fission yeast to a variety of stresses, including heat shock, osmotic stress, oxidative stress, heavy metal stress and DNA damage, was termed the core environmental stress response (CESR). The induced CESR genes encode proteins that are involved mainly in carbohydrate and lipid metabolism, signaling and transcriptional regulation, and ROS scavenging. On the other hand, the repressed CESR genes are associated with protein synthesis, transcription, transport, cellular signaling and cytoskeletal organization (Chen *et al.*, 2003). In case of oxidative stress, the dose and chemical nature of the oxidative stress source affect the gene expression reprogramming. Low levels of H<sub>2</sub>O<sub>2</sub> affect the mRNA levels of relatively few genes compared to the higher doses and many CESR genes, including genes involved in ribosome biogenesis, that are normally repressed during stress are weakly induced and vice versa. In addition, the gene expression in response to *tert*-butyl hydroperoxide, a large organic peroxide, is similar to the one at medium dose of hydrogen peroxide (0.5 mM), whereas the response to menadione, a source of superoxide anion radical, is much weaker (Chen *et al.*, 2008). Additionally, *Schizosaccharomyces pombe* cells respond to H<sub>2</sub>O<sub>2</sub> or *tert*-butyl hydroperoxide, but not to menadione, by cell cycle arrest in G2-phase (Chen *et al.*, 2008).

Independently of the oxidative stress source and dose a set of genes, termed core oxidative stress response genes, is induced. They include catalase (*ctt1*), peroxiredoxin (*tpx1*), thioredoxin (*trx1*), thioredoxin reductase (*trr1*), sulfiredoxin (*srx1*), dehydrogenases and glutathione S-transferases (Chen *et al.*, 2008). Both catalase and the peroxiredoxin Tpx1 play crucial yet distinct role in detoxification of H<sub>2</sub>O<sub>2</sub>. Peroxiredoxin Tpx1 detoxifies basal oxidants that arise from normal cellular growth while catalase is the key scavenger upon oxidative stress, when the thioredoxin is inactivated (Paulo *et al.*, 2014). Interestingly, Tpx1 acts also as oxidative stress sensor and induces *ctt1* expression through redox-mediated activation of the transcription factor Pap1 (Bozonet *et al.*, 2005).

The differential expression in response to various types and doses of oxidants reflects the transcriptional regulation by multiple signaling cascades. Indeed, the transcription factor Pap1 is required for gene expression response to weak oxidative stress caused by menadione or low dose of hydrogen peroxide, while strong oxidative stress, i.e. high dose of H<sub>2</sub>O<sub>2</sub>, triggers SAPK Sty1-dependent transcriptional response (Quinn *et al.*, 2002; Chen *et al.*, 2008).

The *S. pombe* pathways regulating oxidative stress response will be reviewed in more detail in the following sections.

### 1.1.3.1 The players

#### 1.1.3.1.1 The stress-activated protein kinase (SAPK) pathway

The stress-activated protein kinase Sty1 (also known as Spc1 and Phh1), a homolog of the budding yeast Hog1 and mammalian p38 and JNK, plays a role in cell survival upon osmotic, heat, oxidative and heavy metal stress and controls several aspects of normal cell cycle (Millar *et al.*, 1995; Shiozaki and Russell, 1995; Degols *et al.*, 1996). The Sty1 MAP kinase is a part of canonical MAPK pathway activated by MAPKK Wis1 (Millar *et al.*, 1995; Shiozaki and Russell, 1995) and two upstream MAPKKs Win1 and Wis4 (Figure 1.3), also known as Wak1 (Samejima *et al.*, 1997, 1998; Shieh *et al.*, 1997). Activation of Sty1 upon oxidative stress leads to its relocalization from the cytoplasm to the nucleus (Gaits *et al.*, 1998) and gene

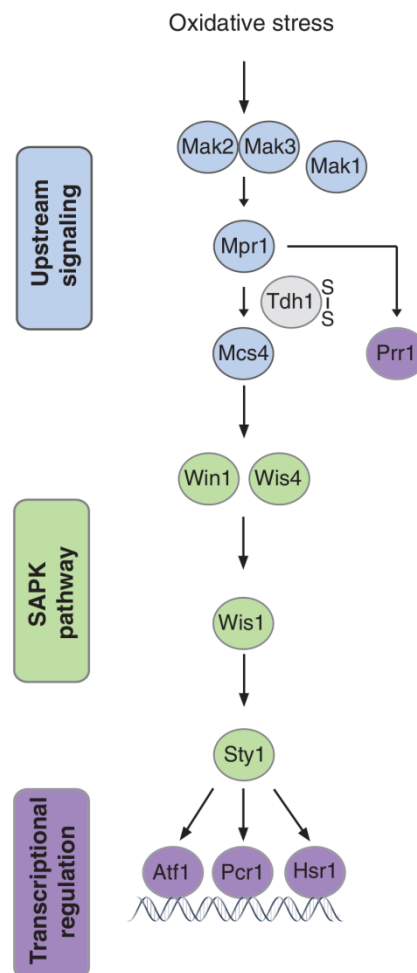


**Figure 1.3 Schematic representation of the stress-activated protein kinase signaling cascade and the multistep phosphorelay system.** Adapted from (Papadakis and Workman, 2014).

expression regulation dependent mainly on the bZIP transcription factor Atf1 (Shiozaki and Russell, 1996; Wilkinson *et al.*, 1996), homologous to mammalian ATF2 (Takeda *et al.*, 1995; Kanoh *et al.*, 1996). Atf1 binds to DNA even before stress in the form of a heterodimer with the bZIP transcription factor Pcr1, which stabilizes Atf1 (Lawrence *et al.*, 2007) and recruitment of Sty1 MAP kinase to these loci leads to high transcriptional response (Eshaghi *et al.*, 2010). Notably, not all Atf1-dependent genes are also Pcr1-dependent, which correlates with the phenotype of  $\Delta atf1$  cells being more severe than that of  $\Delta pcr1$  cells when exposed to hydrogen peroxide (Sansó *et al.*, 2008). In addition to the Atf1/Pcr1 heterodimer, Sty1 regulates transcription through several factors including Hsr1, Atf21 and Atf31 (Shiozaki and Russell, 1996; Chen *et al.*, 2008). The activity of Sty1 MAPK is kept in check to prevent the toxic effects of prolonged hyperactivation of the stress-response pathway (Millar *et al.*, 1995; Shieh *et al.*, 1997) by a handful of phosphatases – tyrosine phosphatases Pyp1 and Pyp2, and serine/threonine type 2C protein phosphatases Ptc1-Ptc4. Some of these phosphatase-encoding genes are constitutively expressed, such as *pyp1*, *ptc2* and *ptc3* (Millar *et al.*, 1995; Gaits *et al.*, 1997), whereas expression of *pyp2* is induced upon stress in Sty1-dependent manner (Millar *et al.*, 1995; Wilkinson *et al.*, 1996) and Ptc4 is post-translationally modified in response to oxidative stress (Di *et al.*, 2012).

#### 1.1.3.1.2 Redox relay of Pap1

Pap1 is an AP-1-like transcription factor, homologous to the mammalian c-Jun and the budding yeast Yap1 (Toda *et al.*, 1991), that regulates expression of genes required for adaptation to oxidative stress and for tolerance of toxic drugs (Toda *et al.*, 1991; Toone *et al.*, 1998; Nakagawa *et al.*, 2000; Chen *et al.*, 2008; Calvo *et al.*, 2009). In response to mild oxidative stress (Figure 1.4), Pap1 is activated in the cytoplasm by reversible thiol oxidation of four cysteine residues C278, C285, C501 and C532 (Vivancos *et al.*, 2004; Calvo *et al.*,

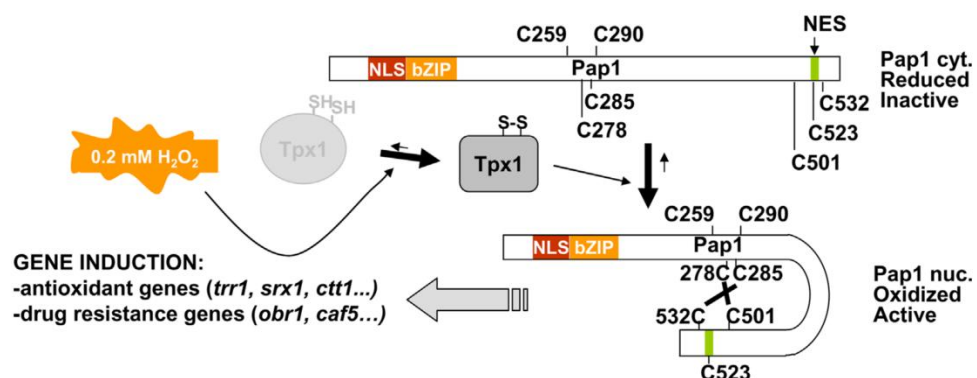


**Figure 1.4 Schematic depiction of Pap1 activation by oxidative stress.** Tpx1-dependent oxidation of Pap1 leads to hindrance of its NES, accumulation in the nucleus, and gene expression induction. NLS – nuclear localization signal, bZIP – basic leucine zipper domain, NES – nuclear export signal. Adapted from (Boronat *et al.*, 2014).

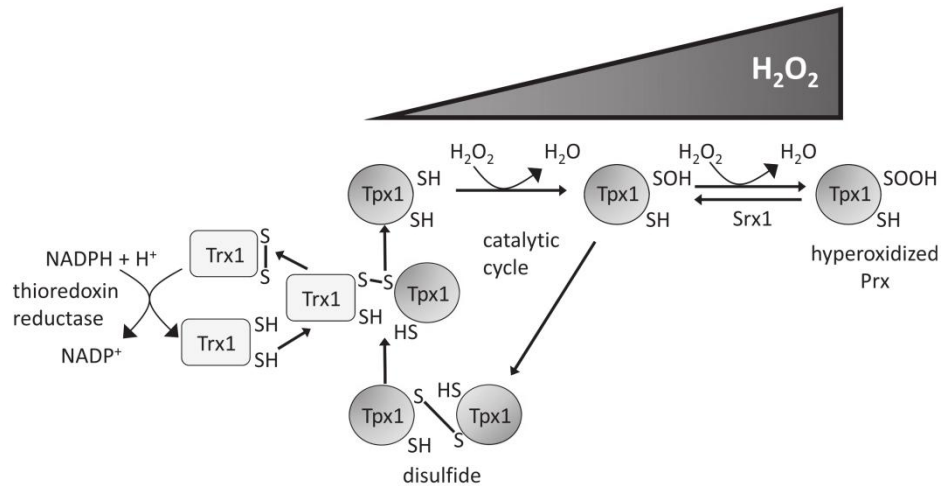


**Figure 1.5 A schematic representation of peroxiredoxin Tpx1 regulation.** In the catalytic breakdown of  $\text{H}_2\text{O}_2$  by Tpx1, the sulfenic form is stabilized by formation of an intermolecular disulfide bond. This disulfide bond is reduced by the thioredoxin Trx1, which is regenerated by thioredoxin reductase TrxR at the expense of NADPH. Upon increased concentration of  $\text{H}_2\text{O}_2$ , the sulfenic derivative of Tpx1 may be further oxidized to sulfinic acid. Sulfiredoxin Srx1 catalyzes the reduction of hyperoxidized Tpx1, thus restoring its thioredoxin peroxidase activity. Adapted from (Day *et al.*, 2012).

2013a) dependently on the 2-Cys peroxiredoxin Tpx1 (Bozonet *et al.*, 2005), leading to the nuclear import of Pap1 as a result of disruption of its association with the Crm1 nuclear exportin (Toone *et al.*, 1998; Calvo *et al.*, 2012). Redox-mediated activation of Pap1 is inhibited upon acute oxidative stress (Figure 1.5) which leads to inactivation of Tpx1 by hyperoxidation of its peroxidatic cysteine to sulfinic acid (Vivancos *et al.*, 2005). Interestingly, Tpx1 may be reduced and the Pap1 TF activated via Sty1-dependent induction of the sulfiredoxin *srx1* (Bozonet *et al.*, 2005; Vivancos *et al.*, 2005).

Two hypotheses have been proposed to describe the mechanism of Pap1 oxidation. The first hypothesis is based on the redox relay model (Chapter 1.1.1.3) and it states that thiol-disulfide exchange occurs between Tpx1 and Pap1, however, the Tpx1-Pap1 disulfide complex has been reported only upon depletion of the single cytoplasmic thioredoxin Trx1 (Calvo *et al.*, 2013b). Alternative hypothesis advocates that Tpx1 is important for preventing reduction of Pap1 by thioredoxin Trx1 and thioredoxin-like protein Tx11 rather than for direct oxidation of Pap1 and that Pap1 may be oxidized directly by  $\text{H}_2\text{O}_2$  or by another peroxidase (Brown *et al.*, 2013). This proposed mechanism is an example of the floodgate model described in Chapter 1.1.1.3.

#### 1.1.3.1.3 Multistep phosphorelay system

The multistep phosphorelay is a variation of the bacterial two-component system. The *Schizosaccharomyces pombe* genome encodes three sensor histidine kinases (*mak1*, *mak2* and

*mak3*) which transmit the signal through His-containing phosphotransfer protein Mpr1 to two response regulators Mcs4 and Prr1 (Shieh *et al.*, 1997; Ohmiya *et al.*, 1999; Buck *et al.*, 2001). The multistep phosphorelay system employing the Mcs4 response regulator has been implicated in activation of the SAPK pathway specifically upon oxidative stress. The histidine kinases Mak2 and Mak3 sense H<sub>2</sub>O<sub>2</sub> (Figure 1.3, page 17), which leads to autophosphorylation of the kinase and subsequent phosphorylation of Mpr1 and Mcs4. Phosphorylated response regulator Mcs4 associates with Wis4 and Win1 MAPKKs and promotes phosphorylation of Sty1 MAPK and Sty1-dependent gene expression (Shieh *et al.*, 1997; Buck *et al.*, 2001; Morigasaki *et al.*, 2008; Quinn *et al.*, 2011). A striking interacting partner of the response regulator Mcs4 and the MAPKKs Wis4 and Win1 is the glycolytic enzyme glyceraldehyde-3-phosphate dehydrogenase (GAPDH) Tdh1, which is transiently oxidized in its catalytic residue C152 upon oxidative stress and promotes association of Mpr1 with the complex of Mcs4, Wis4 and Win1, thus promoting activation of Sty1 MAPK (Morigasaki *et al.*, 2008).

The response regulator Prr1, homologous to *S. cerevisiae* Skn7p, is also implicated in oxidative stress response (Ohmiya *et al.*, 1999). Even though the role of Prr1 is minor for most genes, it contributes to gene expression regulation upon exposure to a wide range of H<sub>2</sub>O<sub>2</sub> concentrations (Chen *et al.*, 2008; Quinn *et al.*, 2011). Prr1 enhances recruitment of oxidized Pap1 transcription factor to the promoters of antioxidants such as *trr1*, *srx1* and *ctt1* and thus contributes to transcriptional upregulation of these genes (Chen *et al.*, 2008; Calvo *et al.*, 2012). Interestingly, the multistep phosphorelay system influences the activity of Prr1 only at high levels of H<sub>2</sub>O<sub>2</sub>, i.e. when it is not cooperating with Pap1, and phosphorylation of Prr1 by Mpr1 boosts the expression of genes such as *ctt1* and *trr1* (Quinn *et al.*, 2011).

#### **1.1.3.1.4 The cell integrity pathway**

Pmk1 is another fission yeast MAPK that is associated with oxidative stress response, however, its role has not been thoroughly mapped. The Pmk1 MAPK is involved in cell wall construction, morphogenesis, cytokinesis, and ion homeostasis (Toda *et al.*, 1996; Zaitsevskaya-Carter and Cooper, 1997), as a part of the cell integrity pathway together with Mkh1 MAPKK and Pek1 MAPK and it is activated upon multiple environmental stresses (Madrid *et al.*, 2006). Contrary to the Sty1 MAPK, it is not critical for cell viability in hydrogen peroxide but plays a dominant role during cell survival in other ROS sources such as *tert*-butyl hydroperoxide, paraquat or diethylmaleate (Madrid *et al.*, 2006; Chen *et al.*, 2008). Interestingly, the Pmk1 and Sty1 MAPK pathways show a certain degree of cross-talk: they are regulated by common phosphatases during osmotic stress (Madrid *et al.*, 2007) and Pmk1

positively regulates the activation of SAPK during transition from fermentative to respiratory metabolism (Madrid *et al.*, 2013).

#### **1.1.3.1.5 Nutrient sensing pathways**

Upon stress cells are challenged to balance two expression programs - growth and stress response, which are mutually exclusive. Nutrient sensing pathways, most notably TOR (target of rapamycin) and PKA, promote growth and negatively regulate stress-response genes, and thus counteract the effects of the SAPK pathway (López-Maury *et al.*, 2008; Rallis *et al.*, 2013a).

Fission yeast contains two TOR homologs, Tor1 and Tor2, which are mainly associated with TORC2 and TORC1 complexes, respectively. While TORC1 complex is the central growth regulator, TORC2 is implicated in DNA damage, telomere length maintenance, gene silencing and stress response (Weisman, 2010). The interplay between the TOR and SAPK signaling pathways is exemplified in the activation of Sty1 MAPK via Tor1-dependent downregulation of Pyp2 phosphatase following nutrient stress (Petersen, 2009).

The catalytic and regulatory subunits of cAMP-dependent protein kinase are encoded by *pka1* and *cgs1*, respectively, in the fission yeast (DeVoti *et al.*, 1991; Maeda *et al.*, 1994) and their expression is induced by multiple environmental stresses, including oxidative stress (Chen *et al.*, 2003). Pka1 and Sty1 have been shown to antagonistically regulate the expression of oxidative stress response genes such as *ctt1*, *gpx1*, *atf1* and *fbp1* (Neely and Hoffman, 2000; Zuin *et al.*, 2010b). In agreement with the increased expression of antioxidant genes, cells lacking Pka1 are resistant to hydrogen peroxide and display prolonged chronological lifespan (Roux *et al.*, 2006).

Protein kinases Sck1 and Sck2 have been identified as high-copy number suppressors of defects in the cAMP-dependent protein kinase pathway and they appear to function in a fashion redundant to Pka1 (Jin *et al.*, 1995; Fujita and Yamamoto, 1998). Indeed, the S6 kinase Sck2 has been shown to function within the TORC1 pathway as a positive regulator of global translation (Rallis *et al.*, 2013b). Additionally, Sck1 may also function as a negative regulator of the PKA activity (Mudge *et al.*, 2013).

#### **1.1.3.2 The interplay**

The stress response pathways cooperate to launch adaptive cellular response to a wide range of oxidative insults. The main stress-responsive signaling pathways of Sty1 and Pap1 are activated when the ROS concentration reaches certain threshold (Vivancos *et al.*, 2006; Veal *et al.*, 2007; Papadakis and Workman, 2014). However, even aerobic growth generates ROS

that need to be detoxified for cell survival. The main cellular peroxiredoxin, Tpx1, has been identified as the first line of defense against ROS due to its high cellular abundance and sensitivity towards peroxides, and it is essential for aerobic growth (Paulo *et al.*, 2014). Notably, transcription factors Pap1 and Prr1 control basal expression of the core oxidative stress response genes, including *tpx1*, during aerobic growth (Chen *et al.*, 2008), but unlike *tpx1* knock-out, cells lacking *pap1* or *prr1* do not show defects during aerobic growth.

Mild oxidative stress (Figure 1.6, left portion), simulated by less than 0.25 mM hydrogen peroxide in laboratory conditions, evokes Tpx1-dependent activation of Pap1, accumulation of the oxidized transcription factor in the nucleus where it regulates expression of up to 80 genes with the help of constitutively nuclear transcription factor Prr1 (Toone *et al.*, 1998; Bozonet *et al.*, 2005; Chen *et al.*, 2008). The transcription factor Atf1 is bound to promoters of its target genes even without activation by Sty1 MAPK (Eshaghi *et al.*, 2010), but is a target

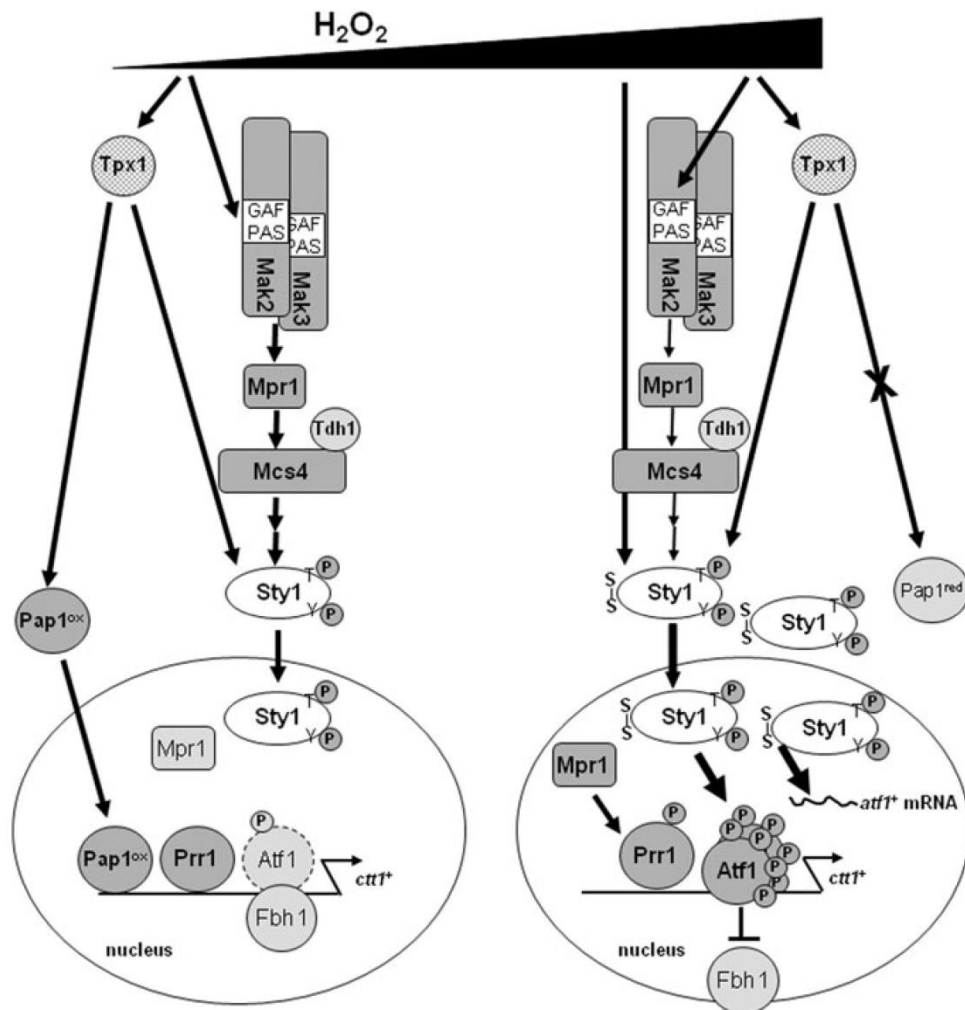


**Figure 1.6** Diagram summarizing concentration-dependent regulation of oxidative stress response. Adapted from (Quinn *et al.*, 2011).

for the ubiquitin-proteasome system and its degradation is dependent on an SCF E3 ligase Fbh1 (Lawrence *et al.*, 2009).

With mounting oxidative stress, the SAPK pathway centered on the MAP kinase Sty1 is activated (Figure 1.6, page 22). At least three modes of the SAPK pathway activation have been described until today. During intermediate oxidative stress, the Sty1 pathway is activated via the multistep phosphorelay system (Quinn *et al.*, 2002) and also by H<sub>2</sub>O<sub>2</sub>-induced formation of an intermolecular disulfide bond with Tpx1 (Veal *et al.*, 2004). Sty1-mediated phosphorylation of the transcription factor Atf1 stabilizes the protein by preventing its interaction with Fbh1 and thus promotes gene expression (Lawrence *et al.*, 2009). Transcription factors Atf1 and Pap1 regulate the expression of distinct genes, such as *trr1* for Pap1 and *gpx1* for Atf1 and common genes, such as *ctt1* or *srx1* (Bozonet *et al.*, 2005; Vivancos *et al.*, 2005; Chen *et al.*, 2008), which allows to tailor cellular functions according to the threat posed by increasing ROS concentration. High dose of hydrogen peroxide directly regulates Sty1 MAPK through formation of a disulfide bond between cysteines 153 and 158, which stabilizes *atf1* mRNA (Day and Veal, 2010). In response to high H<sub>2</sub>O<sub>2</sub> stress (6 mM) the response regulator Prr1 is activated by two-component signaling and it is important for induction of several genes such as *ctt1* or *trr1* in these conditions (Quinn *et al.*, 2011). Just as the higher oxidative stress activates the SAPK pathway, it hyperoxidizes Tpx1 and deactivates Pap1. The hyperoxidized Tpx is thought to allow thioredoxin Trx1 to reduce other oxidized proteins instead of Tpx1 and Pap1 and thus promote cell survival in acutely toxic levels of hydrogen peroxide (Day *et al.*, 2012).

## 1.2 CSL proteins

The CSL (C<sub>BF</sub>1, S<sub>uppressor of Hairless</sub>, L<sub>ag-1</sub>) family proteins are transcription factors conserved from fungi to human (Převorovský *et al.*, 2007). In metazoa, their best described function is the regulation of cell fates such as differentiation, proliferation and apoptosis as the effector components in the Notch signaling pathway (Hori *et al.*, 2012; Radtke *et al.*, 2013). The pathological impact of the Notch pathway deregulation is immense due to its prominent role in cell fate decisions, thus leading to oncological diseases (Ntziachristos *et al.*, 2014), and development, thus causing deformities in most body organs (Louvi and Artavanis-Tsakonas, 2012; Penton *et al.*, 2012).

The CSL proteins are comprised of three structurally integrated domains: the amino (NTD) and carboxy (CTD) terminal domains, which are highly similar to those of the Rel family transcription factors such as NF-κB, flank the central beta-trefoil domain (BTD) and together form a compact structure with many inter-domain interactions (Kovall and Hendrickson,

2004). Upon Notch pathway activation, the Notch intracellular domain (NICD) is released from the plasma membrane and translocated to the nucleus where it forms a transcriptional complex with DNA-bound CSL, Mastermind and other co-activators to drive the expression of Notch target genes. In the absence of the NICD, CSL associates with co-repressors to block the expression of Notch-dependent genes accompanied by chromatin remodeling (Hori *et al.*, 2012).

### **1.2.1 CSL in *S. pombe***

Despite lacking the metazoa-specific Notch signaling pathway the fission yeast *Schizosaccharomyces pombe* genome encodes two CSL homologs, named Cbf11 and Cbf12 (Převorovský *et al.*, 2007). The fission yeast CSL have been shown to regulate the cell cycle progression, DNA integrity maintenance, cell adhesion and flocculation, often in an antagonistic manner and dependent on the nutrients (Převorovský *et al.*, 2009; Převorovský, Tvarůžková *et al.*, manuscript submitted for publication).

Cbf11 and Cbf12 are non-essential nuclear proteins with transcription factor activity. Transcriptomic analysis of cells lacking or overexpressing the CSL paralogs under various growth conditions showed 524 differentially expressed genes, most notably enriched for the core environmental stress response (CESR) genes (Převorovský, Tvarůžková *et al.*, manuscript submitted for publication). Even though both proteins were shown to activate transcription from plasmid-derived expression system and bind the canonical metazoan CSL DNA motif *in vitro* and Cbf11 also *in vivo* (Oravcová *et al.*, 2013), the majority of promoters of the differentially expressed genes were not detected to be bound by the CSL proteins. Therefore, the CSL seem to regulate gene expression of many genes indirectly. However, Cbf11 is likely a direct activator of lipid metabolism genes since it binds their promoters and the  $\Delta cbf11$  mutant exhibits altered expression of these genes (Převorovský, Tvarůžková *et al.*, manuscript in preparation).

## **1.3 The theory of genetic interactions**

Genetic interaction is a phenomenon where the phenotype of a double mutant cannot be explained by combination of the single mutations' effects. The understanding how genes interact with one another to produce a given phenotype may be used to predict biochemical pathways and to identify functionally related genes. Genetic interactions are identified by detecting double mutants whose phenotype differs from the expected. Several models are used to calculate the expected phenotype and the multiplication of growth fitness of the single mutants is most commonly used for assessing genetic interactions in SGA assays

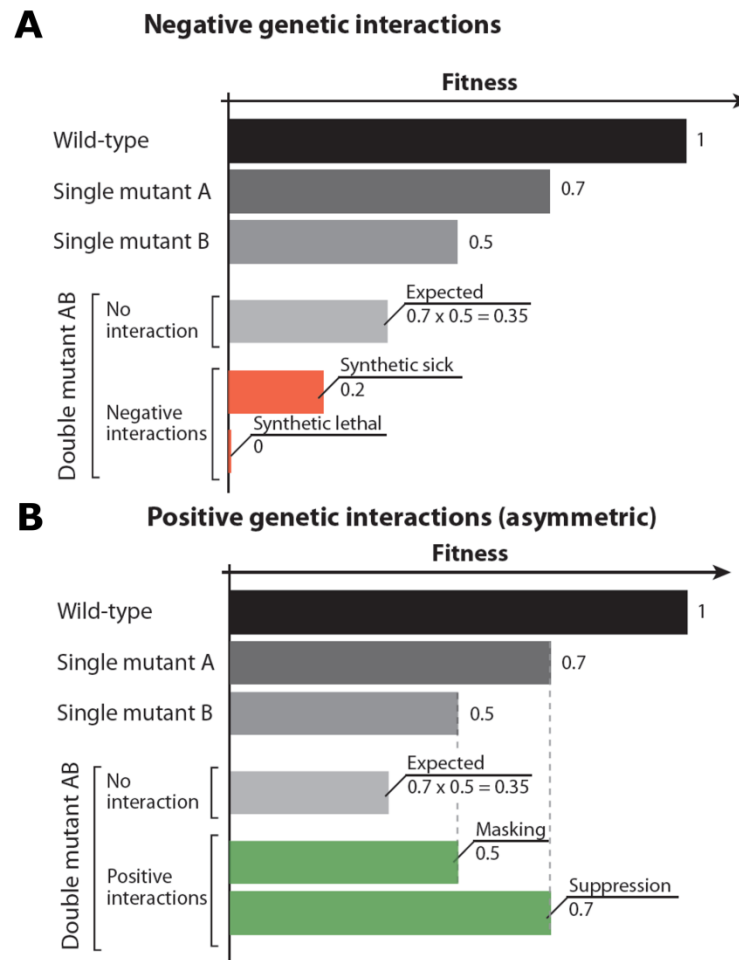


**Figure 1.7 A graphical representation of deducing genetic interactions from the observed phenotype. (A) Negative genetic interactions. (B) Positive genetic interactions. Adapted from (Dixon *et al.*, 2009).**

(Dixon *et al.*, 2009). However, traditional small-scale approaches such as spot tests are not readily quantifiable and are thus evaluated in a somewhat more subjective fashion.

Negative genetic interactions, double mutants whose fitness is worse than expected (Figure 1.7A), are usually interpreted as two genes operating in parallel pathways, so that they compensate for the other's function when only single mutation is present. Alternatively, the two genes may operate in the same pathway and the single mutations may cause decreased flux through the system which results in functionality failure only upon combining these mutations. Negative interaction is often referred to as synthetic sickness or synthetic lethality in the extreme case.

Positive genetic interactions are characterized by double mutants with phenotype less severe than that expected from the multiplicative model (Figure 1.7B). They are also termed alleviating or epistatic interactions and may result from various scenarios. Positive genetic interactions are frequently employed to explain the wiring within biological pathways as they

indicate participation of the two affected genes in one protein complex or pathway and the degree of defect rescue suggests which gene acts upstream and whether the connection between the two genes is activating or repressing (antagonistic).

## **2 Thesis objectives**

The purpose of the presented diploma thesis was to survey the oxidative stress-related phenotypes of the CSL (CBF1/Su(H)/Lag-1) mutants in fission yeast and to identify key upstream regulators as well as downstream effectors of CSL during oxidative stress response. The following tasks were necessary to achieve these objectives:

- Test sensitivity of the CSL single knock-outs and the double knock-out to various ROS sources.
- Describe potential aberrant mitochondrial activity of the CSL mutants.
- Construct strains bearing deletions of the CSL genes and genes known to be involved in oxidative stress response in order to identify genetic interactions.
- Screen the constructed double knock-outs for genetic interactions during oxidative stress.

### 3 Materials and methods

#### 3.1 Microorganismal strains and growth conditions

##### 3.1.1 *Escherichia coli* strains and cultivation

DH5 $\alpha$  bacterial strain was used for all cloning purposes in this study (see genotype below).

DH5 $\alpha$  strain F-  $\Phi$ 80*lacZ* $\Delta$ M15  $\Delta$ (*lacZYA-argF*) U169 *recA1 endA1 hsdR17* (rK-, mK+) *phoA supE44*  $\lambda$  - *thi-1gyrA96 relA1*

Bacterial cells were cultured in LB medium at 37°C on agar plates or in liquid medium with shaking (180 rpm).

LB medium 10 g/l peptone (Merck)  
5 g/l yeast extract (Formedium)  
10 g/l sodium chloride (Penta)

Solid medium was prepared by adding 20 g/l bacteriological agar (Oxoid) before autoclaving. Ampicillin was added to media (Table 3.1), where appropriate. Bacterial cells on solid media may be stored at 4-8°C for several weeks. For long-term storage, liquid cultures were mixed with sterile glycerol (10% final concentration), flash frozen in liquid nitrogen and stored in the freezer at -80°C.

**Table 3.1 List of antibiotics**

Antibiotic	Abbreviation	Stock concentration	Working concentration	Manufacturer
<b>G418 Geneticin</b>	G-418	100 mg/ml	100 $\mu$ g/ml	Sigma-Aldrich
<b>Nourseothricin</b>	clonNAT	100 mg/ml	100 $\mu$ g/ml	Werner BioAgents
<b>Hygromycin B</b>	hygB	100 mg/ml	200 $\mu$ g/ml	Invivogen
<b>Ampicillin</b>	Amp	100 mg/ml	100 $\mu$ g/ml	Biotika

##### 3.1.2 *Schizosaccharomyces pombe* strains and cultivation

Strains used in this study are listed in Supplementary Table 1. Yeast cells were cultured in complex medium (YES) or in Edinburgh minimal medium (EMM) at 32°C on agar plates or in liquid medium with shaking (180 rpm), unless stated otherwise. Growth of liquid cultures was monitored by measuring optical density (OD) using WPA Biowave C08000 Cell Density Meter (Biochrom).

YES medium 5 g/l yeast extract (Formedium)  
30 g/l glucose (Sigma-Aldrich)  
0.25 g/l SP supplements (Formedium)

EMM medium 12.3 g/l EMM Broth without dextrose (Formedium)  
20 g/l glucose (Sigma-Aldrich)

Glucose solution (200 g/l) was sterilized by autoclaving separately to prevent sugar browning. Solid medium was prepared by adding 20 g/l and 30 g/l bacteriological agar (Oxoid) to YES and EMM media, respectively, before autoclaving. Antibiotics (Table 3.1, page 28) were added to cooled media before pouring plates, where appropriate.

Yeast cells may be stored on solid media at room temperature or at 4-8°C for several weeks, unless specific mutations prevent to do so. Strains were normally stored at -80°C as glycerol stocks, which were prepared from cells in stationary phase (except for strains that lose viability in this growth phase) mixed with sterile glycerol (30% final concentration). Before freezing, cells were incubated 20 minutes on ice.

## **3.2 Transformation methods**

### **3.2.1 Electroporation of *E. coli***

To transform electrocompetent DH5 $\alpha$  cells, an aliquot (30-50  $\mu$ l cell suspension/transformation) was thawed on ice. Plasmid DNA or products of ligation reaction were added to the cells and the mixture was gently pipetted to pre-cooled electroporation cuvette with 2 mm gap size (Cell Projects). The electropulse was performed at 2.5 kV using the Gene Pulser Apparatus (Bio-Rad) and 1 ml pre-warmed LB medium with 0.5% glucose was added immediately. Cells were incubated 1 hour at 37°C, 180 rpm and spread on LB agar plates with ampicillin. Transformants were picked after overnight incubation at 37°C.

### **3.2.2 Transformation of *S. pombe* using lithium-acetate method**

Transformation of yeast cells was performed using the standard lithium-acetate method (Gregan *et al.*, 2006). Recipient strain was grown to exponential phase (corresponding to OD 0.3-1, where OD 1 is  $8 \cdot 10^6$  cells/ml for WT strain) and 10 ml of culture was collected by centrifugation (1000 *g*, 3 min, RT). Cells were washed with 10 ml sterile dH<sub>2</sub>O, resuspended in 1 ml sterile dH<sub>2</sub>O, transferred to a microcentrifuge tube and collected (1000 *g*, 3 min, RT). Cells were washed with 1 ml LiAc/TE solution (1000 *g*, 3 min, RT) and resuspended in 100  $\mu$ l LiAc/TE solution. Transforming DNA (plasmid or linearized DNA) was added to washed cells together with 2  $\mu$ l denatured salmon sperm DNA (10 mg/ml; Sigma-Aldrich) and the mixture was incubated at room temperature 10 min. Next, 260  $\mu$ l 40% PEG/LiAc/TE solution was added, the cell suspension was mixed gently and incubated 1-3 hours at 30°C without

shaking. Then, 43  $\mu$ l DMSO was added and incubated 5 min at 42°C, cooled to room temperature and centrifuged (1000 *g*, 3 min, RT). Cells were resuspended in small volume (up to 100  $\mu$ l) of supernatant, spread on appropriate plates and incubated at 32°C until monoclonies formed. In case of DNA integration into genomic locus, cells were spread on nonselective YES plates, incubated 1 day at 32°C, replica plated on selective plate and incubated at 32°C until monoclonies formed.

10x LiAc	1 M lithium acetate; pH 7.5
10x TE	0.1 M Tris-HCl, 10 mM EDTA; pH 7.5
LiAc/TE	150 $\mu$ l 10X LiAc, 150 $\mu$ l 10X TE, 1200 $\mu$ l dH <sub>2</sub> O
40% PEG/LiAc/TE	400 $\mu$ l 50% PEG 4000, 50 $\mu$ l 10x LiAc, 50 $\mu$ l 10x TE

### 3.3 *Schizosaccharomyces pombe* genetic crosses

Fission yeast has two mating types: h<sup>+</sup> and h<sup>-</sup> corresponding to alleles of the *mat1* locus. Laboratory strains are usually unable to switch mating types (called heterothallic) and are, therefore, stably h<sup>+</sup> or h<sup>-</sup>. To induce mating, cells of opposite mating types have to be mixed and starved for nitrogen. Once conjugated, cells proceed through sporulation and formation of a curved ascus containing four spores on a nitrogen-poor medium. Strains to be mated have to have the property to select for the desired genotype of the resulting genetic cross. This is usually done by using antibiotic resistance cassettes or auxotrophies (Hentges *et al.*, 2005; Sabatinos and Forsburg, 2010).

A small amount of biomass was removed from a glycerol stock with a sterile toothpick, placed on a YES plate and incubated at 32°C 2-3 days until sufficient amount of biomass formed. A small amount of fresh biomass from both strains to be mated was added to 30  $\mu$ l sterile dH<sub>2</sub>O in a microcentrifuge tube using separate sterile toothpicks. Contents were mixed by pipetting and suspension was placed on a malt extract (ME) plate that was allowed to dry before inverting. The plate was incubated at 25°C for 2 days or until mature asci with spores formed. The presence of asci was visualized using Nomarski microscopy (Inverted microscope Olympus CK2). Using a sterile pipette tip a tiny amount of biomass was added to 300  $\mu$ l  $\beta$ -glucuronidase solution (Sigma-Aldrich, G7017, stock diluted 100x and 0.22  $\mu$ m filter sterilized for working solution) in a microcentrifuge tube and incubated at 37°C overnight. Spores may be stored at this stage for several weeks at 4°C. Digestion of ascus wall, liberation of spores and killing of vegetative cells was confirmed using Nomarski microscopy and concentration of spores in the suspension was estimated. Suspension corresponding to approximately 50 spores with desired genotype (genetic linkage has to be considered) was

spread onto a selective plate and incubated at 32°C until monoclonies of sufficient size formed. Monoclonies were picked, streaked on a fresh selective plate and incubated at 32°C 1-2 days. The mating type was determined using PCR (Chapter 3.4.4), or mating with reference h<sup>+</sup> and h<sup>-</sup> strains followed by evaluation using microscopy or iodine staining (Chapter 3.3.1). Genotype of the resulting clones was verified by PCR (Chapter 3.4.4).

Malt extract (ME) plates	30 g/l malt extract
	20 g/l agar
	200 µg/ml adenine (stock 10 mg/ml)
	200 µg/ml uracil (stock 5 mg/ml)
	200 µg/ml leucine (stock 20 mg/ml)
	100 µg/ml ampicillin (stock 100 mg/ml)

pH of malt extract solution was adjusted to 5.5 before adding agar. Sterile adenine, uracil, leucine and ampicillin solutions were added after autoclaving.

### 3.3.1 Mating type testing by iodine staining

The mating type of a strain may be tested by crossing with reference h<sup>+</sup> and h<sup>-</sup> strains and determining which combination successfully conjugated and sporulated. Formation of spores may be visualized by Nomarski microscopy, however, this may be time consuming if testing many strains. A quick method for assessing sporulation employs staining of starch in ascus wall with iodine vapors (Sabatinos and Forsburg, 2010). Well characterized reference h<sup>+</sup> and h<sup>-</sup> strains without defects in conjugation or sporulation were streaked parallel to each other on malt extract plates. Tested clones were streaked perpendicular to reference strains as seen in Figure 3.1 using separate sterile toothpicks for each tested clone and reference strain, plates were incubated at 25°C 2-3 days. To spore asci, the plate was inverted over several

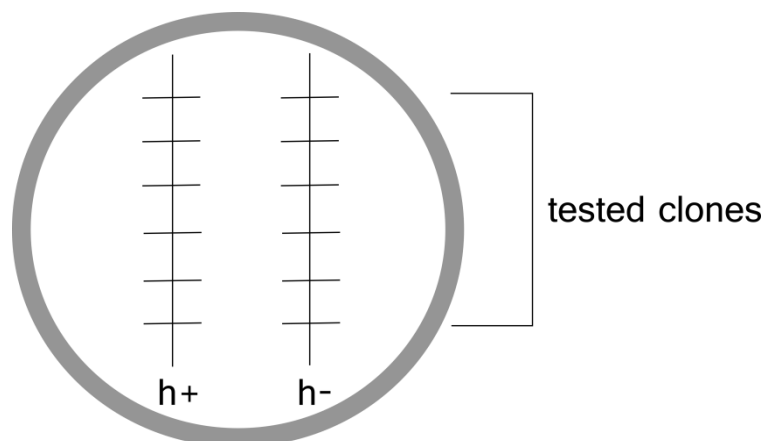


**Figure 3.1** A schematic representation of mating type testing by crossing uncharacterized clones with reference strains and iodine staining. Reference h<sup>+</sup> and h<sup>-</sup> strains are streaked parallel to each other on ME plate. The tested clones are streaked perpendicular to reference strains and the plate is incubated at 25°C 2-3 days. Spore formation is visualized by placing the plate upside down over several iodine crystals.

iodine crystals for 5-10 min in a fume hood as iodine is volatile and toxic. Patches containing spores turned purple to black, unsporulated yeast was colored orange. Leftover iodine crystals may be recycled, iodine in plates was allowed to sublime in the fume hood and plates were discarded as usual.

### 3.4 Molecular cloning

#### 3.4.1 Plasmid DNA isolation using the alkaline method

Adapted from method described elsewhere (Birnboim and Doly, 1979), *E. coli* strain with appropriate plasmid was spread onto LB plate with ampicillin and incubated at 37°C overnight. One monoclonal colony was used to inoculate 10-50 ml LB media with ampicillin and incubated at 37°C, 180 rpm overnight. Cell culture was cooled on ice 5-10 min and cells were collected by centrifugation (3000 *g*, 10 min, 4°C). Pellet was resuspended in one volume of ice-cold solution I (volume depends on original cell culture volume, 1 ml for 10 ml culture, 3 ml for 50 ml culture), two volumes of solution II were added, mixed by inverting the tube and incubated 5-10 min at room temperature to lyse cells, accompanied by increase in viscosity. Cell lysate was returned to ice bath and 1.5 volumes of solution III were added. The tube contents were mixed by inverting and incubated 15 min on ice. The precipitate was centrifuged (20 000 *g*, 20 min, 4°C), the supernatant was transferred to a clean tube and mixed with isopropanol (0.6 volumes of the supernatant). The mixture was immediately centrifuged (3000 *g*, 6 min, 4°C), the sediment was dissolved in 300 µl dH<sub>2</sub>O and the same volume of 10 M LiCl was added. RNA precipitate was formed by incubation at -80°C 10 min and collected by centrifugation (16 000 *g*, 5 min, 4°C). The supernatant was transferred to a clean tube and DNA was precipitated using incubation with 96% ethanol (1 volume of the supernatant) at -80°C 10 min. The precipitate was collected by centrifugation (16 000 *g*, 5 min, 4°C), washed with 1 ml 70% ethanol and dried at room temperature or 37°C to remove residual ethanol. The isolated plasmid DNA was dissolved in 50-100 µl dH<sub>2</sub>O and quality was evaluated by agarose gel electrophoresis (Chapter 3.4.8).

Solution I	25 mM Tris-HCl (pH 8.0) 10 mM EDTA-NaOH 10 g/l glucose
Solution II	10 g/l SDS 0.2 M NaOH
Solution III (pH 5.4)	3 M potassium acetate 2 M acetic acid

### 3.4.2 DNA isolation using Nucleospin® Plasmid and Nucleospin® Extract kits

Isolation of plasmid DNA from transformed *E. coli* was performed with Nucleospin® Plasmid Kit (Macherey-Nagel) as described by the manufacturer. The Nucleospin® Extract Kit (Macherey-Nagel) was used to purify DNA fragments from PCR reaction mixture or agarose gel according to the manufacturer's guidelines. The purity and concentration of DNA was measured spectrophotometrically (NanoDrop 2000, ThermoScientific).

### 3.4.3 Quick chromosomal DNA extraction from *S. pombe*

Genomic DNA for routine PCR genotyping may be isolated from *S. pombe* using heat, SDS and lithium acetate to lyse the cells and denature the proteins, yielding a solution of DNA and RNA after alcohol precipitation (Looke *et al.*, 2011). Biomass from fresh patch of cells on a plate was picked using a sterile pipette tip, resuspended in 100 µl 0.2 M lithium acetate, 10 g/l SDS and incubated at 70°C 5 min. Then, 300 µl 96% ethanol was added, the tube contents were vortexed and centrifuged (14 000 *g*, 3 min, RT). The supernatant was removed, pellet was washed with 70% ethanol, vortexed and centrifuged (14 000 *g*, 1 min, RT). The supernatant was removed, pellet was dissolved in 100 µl dH<sub>2</sub>O and centrifuged (14 000 *g*, 30 s, RT). Supernatant (1-5 µl) was used for PCR (Chapter 3.4.4).

### 3.4.4 Polymerase chain reaction

The polymerase chain reaction (PCR) was used to amplify DNA fragments for cloning purposes or to verify plasmid constructs and strain genotypes. The typical reaction components for both purposes are summarized in Table 3.2.

**Table 3.2 Typical components of PCR reaction**

Reaction components	High-fidelity PCR for cloning	Routine analytical PCR
<b>dNTPs, each</b>	0.2 mM	0.25 mM
<b>Mg<sup>2+</sup></b>	2 mM	3 mM
<b>Primers, each</b>	0.5 µM	0.5 µM
<b>Template</b>	phenol-chloroform extracted genomic DNA (1 ng-1 µg)	yeast or bacterial biomass, plasmid DNA, genomic DNA (10 pg-1 µg)
<b>Polymerase</b>	Q5® High-Fidelity Polymerase (0.02 units/µl)	BIOTAQ, Taq DNA Polymerase (0.025 units/µl)
<b>Buffer</b>	1X Q5® Reaction Buffer	1X NH <sub>4</sub> -based buffer or 1X KCl buffer
<b>dH<sub>2</sub>O</b>	up to 25 µl	up to 20 µl

The most common application was colony PCR where biomass from *S. pombe* or *E. coli* is used as a source of DNA template. Small amount of fresh biomass is picked from a plate using a sterile pipette tip and resuspended in the PCR mixture. Especially for yeast cells, it is critical to use 2 days old biomass at the most. The cells are disrupted in the initial 5 min incubation at 94°C in the thermal cycler.

**Table 3.3 List of primers used in this study**

<b>Name</b>	<b>Application</b>	<b>Sequence</b>
MM	mating locus, h <sup>-</sup>	TACGTTTCAGTAGACGTAGTG
MP	mating locus, h <sup>+</sup>	GGTAGTCATCGGTCTTCC
MT1	mating locus, outer genomic sequence	AGAAGAGAGAGTAGTTGAAG
MP31	genotyping of <i>cbf12</i> locus, ORF	TGTGCAGATTTGGATGGC
MP32	genotyping of <i>cbf12</i> locus, outer genomic sequence	AAATCAATCCCCTCCACG
MP33	genotyping of <i>cbf12</i> , <i>cbf11</i> and <i>ctt1</i> loci, kanMX6/natMX6 cassette	GCGCACGTCAAGACTGTC
kan-rev	genotyping of <i>cbf11</i> locus, kanMX6 cassette	AATGCTGGTCGCTATACTGC
MP27	genotyping of <i>cbf11</i> locus, ORF	TATGCTGGACTATAGTGGGC
MP28	genotyping of <i>cbf11</i> locus, outer genomic sequence	GATACAGCAACTCCTCCCG
MP144	genotyping of <i>cbf11</i> and <i>ctt1</i> loci, outer genomic sequence	GTCGTTAGAACGCGGCTACA
MP150	genotyping of <i>cbf11</i> locus, upstream junction	AGGGATCGAAAGACATCCGC
MP151	genotyping of <i>cbf11</i> locus, downstream junction	GCTTGTACACACGGCCTTCAA
MP171	<i>ctt1</i> deletion plasmid, upstream flanking region	AAAAGGGCCCTCCAAAGGGTGCATGTCCAGC
MP172	<i>ctt1</i> deletion plasmid, upstream flanking region	AAAACGAGTGGAATTAGTTGAACGACGA GCAAATG
MP173	<i>ctt1</i> deletion plasmid, downstream flanking region	AAAAGGGCCCCGGCCAAACCTCAACTGGC
MP174	<i>ctt1</i> deletion plasmid, downstream flanking region	AAAAAGATCTGAATGCGAGACATGTGTAAT GCCG
MP175	genotyping of <i>ctt1</i> locus, upstream junction	CCGCATGAATACAGGCCAAA
MP176	genotyping of <i>ctt1</i> locus, downstream junction	CTGATTGCCACGTCAAAGC

The polymerase chain reaction proceeded in the PTC-200 Peltier Thermal Cycler (MJ Research) or in Veriti 96-Well Thermal Cycler (Life Technologies). The cycling parameters for high-fidelity PCR using Q5® High-Fidelity Polymerase were as follows:

1. 98°C 2 min
2. 3x (98°C 10 s  
52°C 20 s  
72°C 20 s)
3. 22x (98°C 10 s  
64°C 20 s  
72°C 20 s)
4. 72°C 2 min
5. 4°C ∞

The cycling parameters for routine PCR using BIOTAQ or Taq DNA polymerases varied according to the primers used (Table 3.3, page 34), length of amplified region and the template:

1. 94°C 1-5 min
2. 30-35x (94°C 30 s  
54°C or 56°C 30-40 s  
72°C 1 min-2 min)
3. 72°C 5 min
4. 4°C ∞

Enzymes and buffers:

- Q5® High-Fidelity Polymerase, 2 units/μl  
5X Q5® Reaction Buffer (NEB)
- BIOTAQ DNA Polymerase, 5 units/μl  
10X NH<sub>4</sub> Reaction Buffer  
50 mM MgCl<sub>2</sub> Solution (Bioline)
- *Taq* DNA Polymerase, recombinant, 5 units/μl  
10X *Taq* Buffer with KCl  
10X *Taq* Buffer with (NH<sub>4</sub>)<sub>2</sub>SO<sub>4</sub>  
25 mM MgCl<sub>2</sub> (ThermoScientific/Life Technologies)

#### 3.4.5 Plasmids

Plasmids used in this study are listed in

Table 3.4 (page 36) and the empty targeting vector is depicted in Figure 3.2 (page 36).

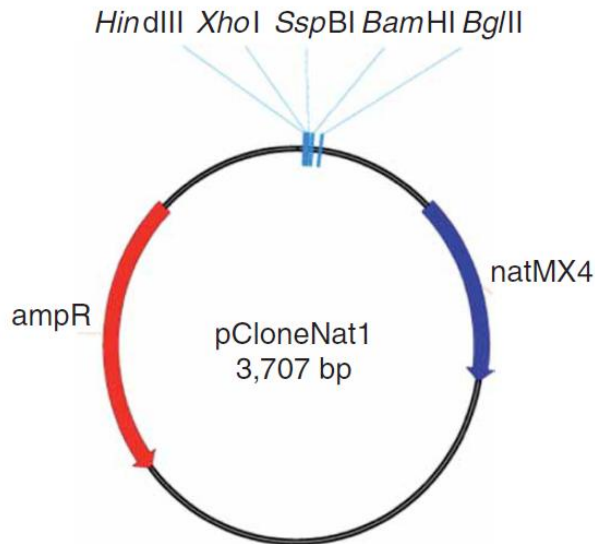


**Figure 3.2** Map of targeting vector pCloneNat1. Adapted from (Gregan *et al.*, 2006).

**Table 3.4** List of plasmids used in this study

Name	Vector	Description
pMP45	pCloneNat1	knock-out plasmid for <i>cbf12</i>
pMP91	pCloneNat1	knock-out plasmid for <i>cbf11</i>
pMP126	pCloneNat1	knock-out plasmid for <i>ctt1</i>

#### 3.4.6 DNA restriction with endonucleases

The DNA restriction reaction was prepared in 1.5 ml microcentrifuge tubes as follows:

0.1-4 µg	DNA
1X or 2X	restriction buffer*
0.05-1 U/µl	restriction endonuclease (Table 3.5)*
up to 20 µl-40 µl	dH <sub>2</sub> O

\*as recommended by the manufacturer

The reaction mixture was incubated at 37°C 1-16 hours. The enzyme was inactivated by incubating 20 min at 65°C, where applicable, or by adding DNA loading dye containing EDTA. The successful DNA digestion was verified using agarose gel electrophoresis (Chapter 3.4.8).

**Table 3.5** Restriction endonucleases used in this study

Enzyme	Manufacturer
ApaI (10 U/µl)	ThermoScientific
BglII (10 U/µl)	ThermoScientific
XbaI (10 U/µl)	ThermoScientific
XhoI (10 U/µl)	ThermoScientific

### 3.4.7 DNA ligation

Reactions set up to ligate digested DNA fragments contained:

0.25-2 µg	DNA with cohesive ends (vector:insert in molar ratio 1:3)
1X	T4 DNA ligase buffer (ThermoScientific)
0.25-0.375 units/µl	T4 DNA ligase (5 units/µl; ThermoScientific)
up to 20-40 µl	dH <sub>2</sub> O

The ligation reaction proceeded at 4°C 16 hours and was stopped by incubation at 65°C 10 min.

### 3.4.8 Agarose gel electrophoresis

Agarose gel electrophoresis was used to separate DNA fragments according to their size. Electrophoresis was performed in horizontal arrangement using Blue Marine 100 or 200 apparatus (Serva). Agarose gel was prepared using 1-1.5% agarose (SeaKem LE Agarose, Lonza) in 1X TAE buffer. DNA samples were mixed with 6X DNA Loading Dye or 6X Orange DNA Loading Dye (both ThermoScientific) to final concentration of 1X and loaded onto the gel. DNA ladder (Figure 3.3) was used to estimate the size of fragments. DNA fragments were separated by applied electrical field with constant voltage 40-100 V. Gel was stained by 10 min incubation in ethidium bromide solution (0.5 µg/ml) and DNA was visualized with the use of ultraviolet transilluminator.

50X TAE	2 M Tris, pH 8.5
	0.1 M EDTA (Na <sub>2</sub> EDTA·2 H <sub>2</sub> O)
	1 M acetic acid

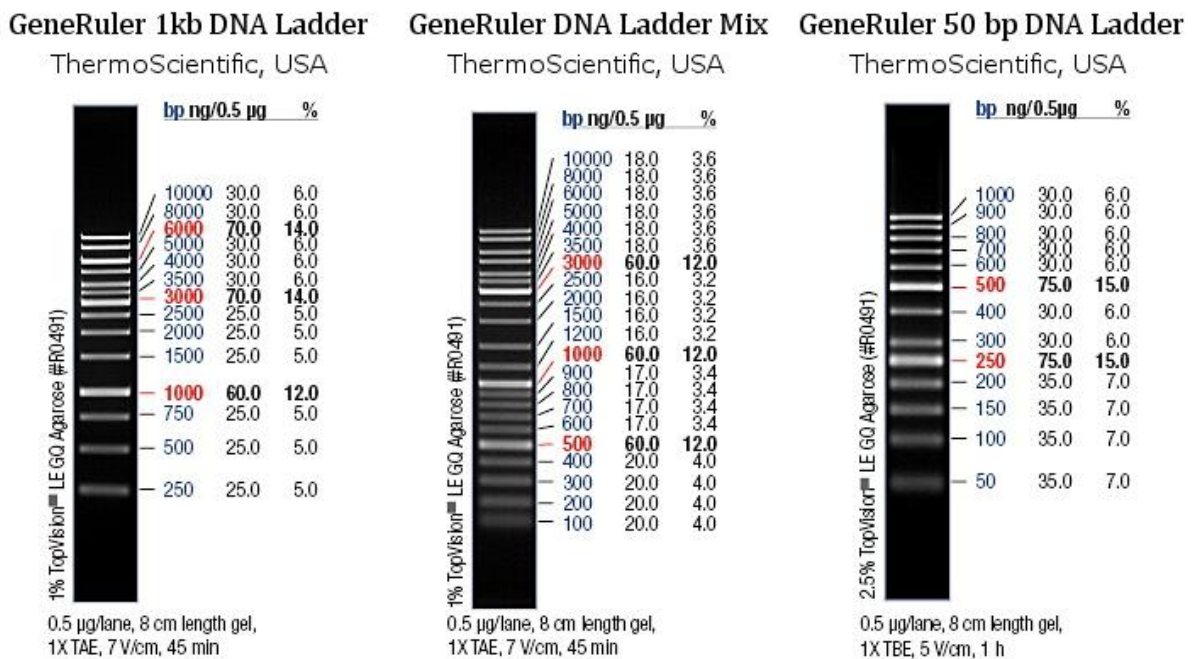


Figure 3.3 Overview of DNA Ladders. Adapted from the manufacturer's website.

### 3.5 Phloxine staining

Phloxine B is a vital dye that is transported out of metabolically active cells, whereas it stains dead cells dark red. Phloxine staining was used to assess ploidy of constructed strains since diploid colonies contain larger fraction of dead cells and thus are stained darker compared to haploid colonies. A small amount of fresh biomass was streaked on YES plate containing 5 mg/l phloxine B (diluted from 5g/l stock, Sigma-Aldrich) and incubated 2 days at 32°C. Control haploid and diploid strains need to be streaked on the same plate as tested clones for comparison.

### 3.6 Flow cytometry

Cell ploidy was assessed by staining DNA with propidium iodide (PI) and flow cytometry analysis. Cells from liquid culture or scraped from a fresh plate were fixed with 70% (v/v) ethanol, cells may be stored for several months at 4°C at this stage. For flow cytometry, 300 µl ethanol-fixed cells (originating from 1 ml culture of OD 0.5,  $\sim 4 \cdot 10^6$  cells/ml, if different, adjust cell suspension volume) were rehydrated by adding 3 ml 50 mM sodium citrate. Cells were collected (1000 g, 5 min, RT), resuspended in 500 µl 50 mM sodium citrate containing 0.1 mg/ml RNase A (10 mg/ml; ThermoScientific) and incubated 2-16 hours at 37°C. This step is necessary, as RNA may also be stained by propidium iodide. DNA was stained by adding 500 µl 50 mM sodium citrate containing 8 µg/ml propidium iodide. Stained cells were analyzed right away or stored in dark at 4°C overnight. The DNA content was measured using LSR II flow cytometer (BD Biosciences). Propidium iodide was excited with yellow-green laser (561 nm) and fluorescence was detected in red channel (610/20). Data was collected for FSC-A, SSC-A, PI-A and PI-W, where A stands for area and W for width of the fluorescence signal. Gating in SSC-A vs. FSC-A dot plot was employed to select for single cells, thus removing signal from cell debris and large aggregates. Doublets, two cells stuck together, as well as G<sub>1</sub> and S-phase cells were gated out using PI-A vs. PI-W dot plot (Knutsen *et al.*, 2011). After applying both gates, at least 10 000 events were recorded. Data were analyzed in FlowJo software (FlowJo, LLC).

### 3.7 Microscopy of mitochondria

Mitochondria were visualized by DiOC<sub>6</sub>(3), a lipophilic charged dye that is selective for mitochondria at low concentration but stains also other internal membranes at high concentration. *S. pombe* WT and  $\Delta cbf11$  strains carrying chromosomally encoded fluorescently labeled nucleolar protein Gar2 (MP326 and MP344, respectively) were grown to exponential phase of growth (OD $\sim$ 0.5, corresponding to  $\sim 4 \cdot 10^6$  cells/ml) and 500 µl of each culture was mixed in 2 ml microcentrifuge tube. DiOC<sub>6</sub>(3) (Life Technologies) stock solution (17.5 mM in ethanol) was diluted to 17.5 µM working solution with ethanol and 10

$\mu\text{l}$  were added to 1 ml of prepared cell culture mix. Cells were incubated 20 min at 32°C, 180 rpm in dark, gently centrifuged (1000 *g*, 3 min, RT), supernatant was removed and 1  $\mu\text{l}$  of cell paste was spread on microscopy slide, covered with a slip and immediately observed using Olympus CellR microscope in GFP channel.

### 3.8 Respirometry

Oxygen consumption of intact cells as a measure of cellular respiration was assessed using the Oroboros Oxygraph 2-k (Oroboros Instruments). Both chambers of the respirometer were rinsed thoroughly with dH<sub>2</sub>O and ethanol. Stoppers were washed by inserting into the chamber with dH<sub>2</sub>O or ethanol. The respirometer temperature was set to 32°C, measurement frequency to 2 s and stirring rate to 750 rpm. Electrode functionality was checked by pipetting 2.5 ml media, e.g. YES, into both chambers and measuring equilibrium solubility of oxygen in the medium (without inserted stoppers). Stable signal and rate of oxygen consumption (first derivative of oxygen concentration with respect to time) approaching 0 corresponds to a well functioning electrode, otherwise electrode membrane or other parts may require service. The stoppers were fully inserted into the chambers, overflow of media was removed using the integrated suction system and oxygen concentration in the chamber was measured over time. Since no cells were present, the oxygen concentration should remain constant, if it is not the case, the chamber may be contaminated. All liquid was removed from the chambers with the integrated suction system and 2.1 ml exponentially growing culture of OD 0.50 (corresponding to  $4 \cdot 10^6$  cells/ml for WT strain) was pipetted into the chamber. If OD was not exactly 0.50, it was diluted accordingly with medium in the chamber. It is critical that cells are transported from the incubator to the respirometer as quickly as possible, keeping the culture in polystyrene box to prevent cooling. Equilibrium oxygen solubility in the yeast culture was measured in open chamber until oxygen consumption rate stayed close to 0 for 2-5 minutes. The chamber was closed, culture overflow was removed with the integrated suction system and oxygen concentration was measured until 10 minutes of constant oxygen consumption were recorded. Electron transport chain was blocked with addition of 2.5  $\mu\text{M}$  antimycin A and oxygen consumption was measured for several minutes (2-10 min). After the measurement, chambers were rinsed thoroughly with dH<sub>2</sub>O and ethanol. The chambers were filled with dH<sub>2</sub>O for storage. Data was analyzed using the Oroboros Datlab software (Oroboros Instruments). Due to unknown oxygen solubility factor of the *S. pombe* cultivation media, the rate of respiration was measured in % O<sub>2</sub> consumed/(min·ml·OD). The oxygen solubility factor was set to an arbitrary value, but the same for all experiments performed (set to 0.93). Respiration rate was calculated using the formula in (Eq. 3.5, where the variables correspond to:

average(closed chamber)	average rate of cellular O <sub>2</sub> consumption, instrument output in pmol/(s·ml)
average(open chamber)	correction for average background O <sub>2</sub> consumption of the respirometer, instrument output in pmol/(s·ml)
O <sub>2</sub> concentration (open chamber)	equilibrium O <sub>2</sub> solubility in cultivation medium, instrument output in nmol/ml

The coefficient 12 in (Eq. 3.5) is derived from adjusting the units of the instrument output units to % O<sub>2</sub> consumed/(min·ml·OD).

$$rate = \frac{(average(closed\ chamber) - average(open\ chamber)) * 12}{O_2\ concentration(open\ chamber)} \quad (Eq. 3.5)$$

### 3.9 Spot tests

The spot tests were used to assess cell viability and growth defects upon exogenous oxidative stress and growth on non-fermentable carbon source. This assay employs spotting an array of serial dilutions of culture onto a plate. Cells exponentially growing in YES medium (OD 0.3-1, where OD 1 is  $8 \cdot 10^6$  cells/ml for WT strain) were harvested by centrifugation (1000 *g*, 3 min, RT) in the amount corresponding to 0.7 OD. The cell pellet was resuspended in 350 µl YES and 300 µl were transferred to 96-well plate where they were 10-fold serially diluted (4 steps) with YES medium. The cells were spotted onto plates using the 48-pin spotting tool (Sigma-Aldrich) which was sterilized by washing in 70% ethanol and flaming after spotting each plate. The plates were allowed to dry and were incubated 5 days at 32°C. Photographs were taken at days 3 and 5, or as necessary.

To test sensitivity to ROS, the plates contained either hydrogen peroxide (Sigma-Aldrich) or menadione sodium bisulfite (Sigma-Aldrich) as a source of superoxide. Due to potentially unstable nature of the used drugs, the plates were poured on the day of spotting and the drug was added to YES agar cooled to 45°C.

The ability of the cells to respire was tested by growth on plates containing non-fermentable carbon source, in this case, glycerol. The plates consisted of YES + 3% glucose medium (standard YES) or YES + 3% glycerol + 0.1% glucose. The plates were poured the day before spotting.

### 3.10 Gene expression analysis

The expression of genes annotated in the PomBase database to GO categories (Wood *et al.*, 2012) mitochondrial ATP synthesis coupled electron transport (GO: 0042775), canonical glycolysis (GO: 0061621) and gluconeogenesis (GO: 0006094) was analyzed using the data set from microarray-based transcriptome profiling of exponentially growing WT and  $\Delta cbf11$  cells in YES medium (Převorovský, Tvarůžková *et al.*, manuscript submitted for publication). The average expression levels of four independent biological repeats were visualized using the box plot in R and the statistical significance of differential regulation of the GO categories was determined using the one-tailed Mann-Whitney *U* test (0.05 significance level). For clustering analysis, *pyk1* (encoding pyruvate kinase) expression data was removed from analysis due to missing values preventing the algorithm to proceed. Clustering was performed based on Euclidean distances using the 'complete linkage' method in R. The occurrence of iron metal in proteins encoded by the analyzed genes was inferred from PomBase annotation and literature search (Wood *et al.*, 2012).

## 4 Results

Oxidative stress represents a complex and still widely unexplored phenomenon implied in multiple human diseases, pathogen virulence and aging. The fission yeast *Schizosaccharomyces pombe* is a popular unicellular eukaryotic model for stress studies and the major pathways of oxidative stress response have been described in detail. The *S. pombe* CSL proteins, homologous to mammalian CSL transcription factors involved in the Notch signaling pathway, have been identified and scrutinized in our laboratory. Transcriptome profiling revealed that cells lacking *cbf11* overexpress a range of oxidative stress response genes such as catalase, sulfiredoxin or glutathione S-transferases (Převorovský, Tvarůžková *et al.*, manuscript submitted for publication) and that the CSL transcript levels respond to hydrogen peroxide treatment (Chen *et al.*, 2003). These preliminary results led us to further explore the role of fission yeast CSL proteins in oxidative stress response.

### 4.1 CSL proteins play a role in oxidative stress response

#### 4.1.1 Sensitivity of CSL mutants varies with used ROS source

Oxidative stress occurs naturally in cells without exogenous intervention and may also arise from environmental factors. The latter is often employed to screen for genes and proteins involved in oxidative stress response and to elucidate the cellular defense mechanisms. In this study, the sensitivity of *S. pombe* CSL mutants was determined by observing cell viability and growth defects upon chronic exposure of cells to hydrogen peroxide and menadione, a superoxide anion radical generator. A third ROS source, iron ions in the form of iron (II) chloride and Mohr's salt, was utilized but did not give reproducible results (data not shown).

The resistance of  $\Delta cbf11$  strain to hydrogen peroxide (Figure 4.1A, page 43) indicates that Cbf11 is truly involved in oxidative stress response. The deletion of *cbf12* does not affect the sensitivity of WT or  $\Delta cbf11$  cells towards H<sub>2</sub>O<sub>2</sub> (Figure 4.1A, page 43). The observation that the resistance of the double knock-out  $\Delta cbf11 \Delta cbf12$  is indistinguishable from that of  $\Delta cbf11$  suggests that *cbf12* is not required for the role of Cbf11 in oxidative stress response.

Various ROS sources induce the oxidative stress response via different signaling pathways which results in induction of a differential gene expression program (Chen *et al.*, 2008). The involvement of CSL proteins in oxidative stress response also seems to be selective for the ROS source, as the CSL mutant strains display sensitivity comparable to WT cells when exposed to menadione (Figure 4.1B, page 43).

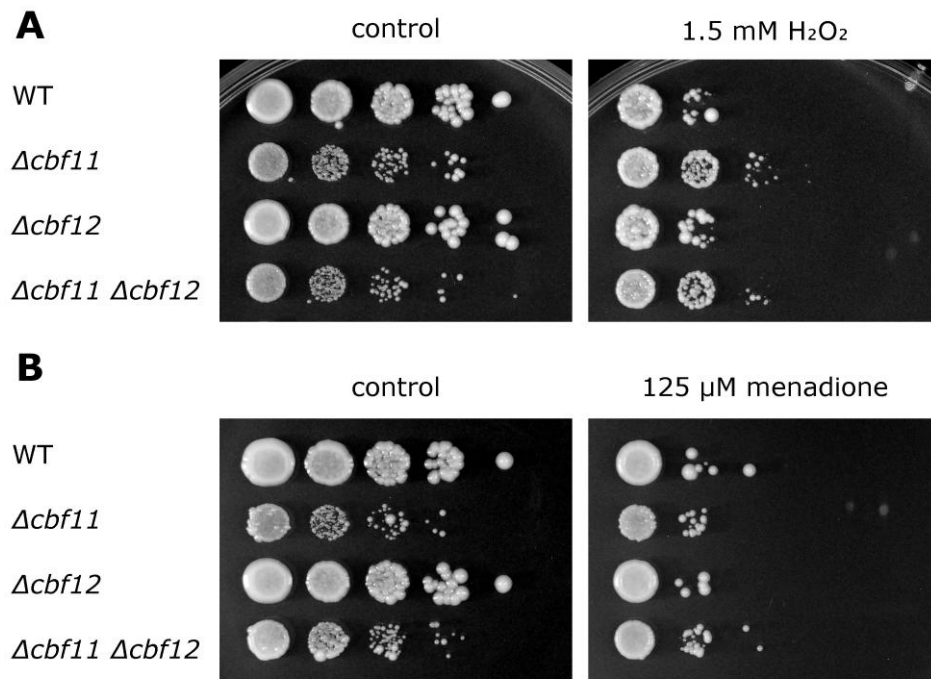


**Figure 4.1  $\Delta cbf11$  and  $\Delta cbf11 \Delta cbf12$  cells are resistant to H<sub>2</sub>O<sub>2</sub> but not to menadione.** 10-fold serial dilutions of cultures with the indicated genotypes were spotted on control YES plates or plates containing an ROS source and grown for 3 days. **(A)** The  $\Delta cbf11$  and  $\Delta cbf11 \Delta cbf12$  strains are resistant to 1.5 mM H<sub>2</sub>O<sub>2</sub>,  $\Delta cbf12$  shows the same sensitivity as WT. **(B)** The CSL mutants do not show significant difference in sensitivity to 125  $\mu$ M menadione compared to WT. This sensitivity experiment was performed 3 times, and a representative experiment is shown.

#### 4.1.2 *cbf11* is crucial for cell respiration

The electron transport chain in mitochondria is considered the largest producer of intracellular ROS (Quinlan *et al.*, 2013) and, consequently, mitochondria have evolved elaborate antioxidant mechanisms. The respiratory complexes are hence a hub of oxidative stress management since they produce ROS but are also vulnerable to oxidative damage, often causing even higher ROS production (Valko *et al.*, 2005; Gomez *et al.*, 2014). Since CSL proteins are involved in oxidative stress response we tested whether they affect mitochondrial function. Oxygen consumption, an indicator of respiratory rates, of CSL mutants exponentially growing in complex media was measured using the Oroboros Oxygraph. As observed in Figure 4.2A (page 44),  $\Delta cbf11$  and  $\Delta cbf11 \Delta cbf12$  strains have decreased oxygen consumption compared to WT or  $\Delta cbf12$ . Although this result correlates with the sensitivity of CSL mutants to H<sub>2</sub>O<sub>2</sub> in the sense that *cbf11* is the dominant regulator in both experiments and *cbf12* is not concerned, it was not expected. Mitochondrial dysfunction caused either genetically or by antimycin A-mediated respiration inhibition is associated with increased intrinsic oxidative stress and sensitivity to extracellularly supplied

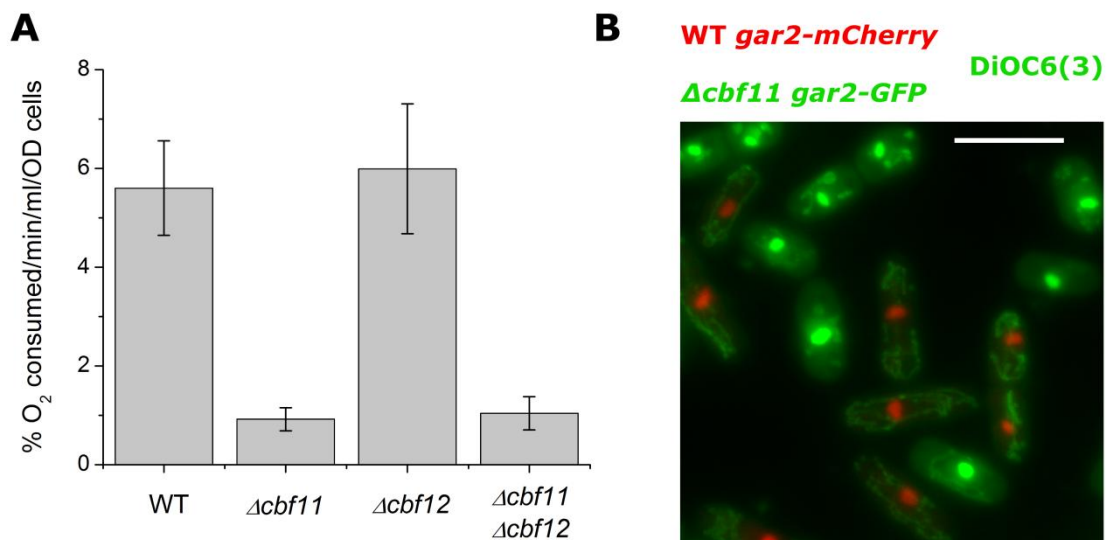


**Figure 4.2 Cbf11 regulates respiratory activity and mitochondrial morphology.** **(A)** Oxygen consumption of exponentially growing cultures with the indicated genotypes in complex medium (YES + 3% glucose) was measured using the Oroboros Oxygraph. Error bars represent the standard deviation of three independent biological replicates. **(B)** DiOC<sub>6</sub>(3) staining of mitochondria in WT and  $\Delta cbf11$  cells expressing fluorescently labeled nucleolar protein Gar2 reveals prominent morphological changes and a decrease in staining of  $\Delta cbf11$  cells. The signal from red and green channels were overlaid. Scale bar 10  $\mu$ m.

H<sub>2</sub>O<sub>2</sub> (Zuin *et al.*, 2008). This finding led us to observe the mitochondrial morphology of cells lacking *cbf11*. Mitochondria are dynamic structures perpetually undergoing fusion and fission depending on the cell cycle, nutrient availability or growth phase. Unlike in the budding yeast where the mitochondria are aligned along the mother-daughter cell axis and accumulate on cell poles during bud formation in actin cable-dependent manner (Boldogh and Pon, 2006), *S. pombe* mitochondria are aligned parallel to the cell axis and their motility relies on the microtubules (Jourdain *et al.*, 2009). WT and  $\Delta cbf11$  cells expressing mCherry- or GFP-fused nucleolar protein Gar2, respectively, were grown to exponential phase in complex medium and mitochondria were visualized by green-fluorescent stain DiOC<sub>6</sub>(3). Independent cultures of strains with WT *cbf11* allele and deletion of *cbf11* were mixed prior to staining. As expected for mitochondria in WT cells, DiOC<sub>6</sub>(3) stains tubular network aligned along the cell axis (Figure 4.2B). The DiOC<sub>6</sub>(3) staining of  $\Delta cbf11$  strain revealed diversity of phenotypes ranging from lack of any observable structures, aggregates with intense staining, fragments throughout the cell to fiber-like structures. The interpretation of this phenotype is not trivial. DiOC<sub>6</sub>(3) is a charged lipophilic dye which preferentially stains mitochondria due to their membrane potential but in the case of aberrant mitochondrial potential and size or at high concentrations of the dye it also permeates other cellular membranes, producing non-specific

staining. Nevertheless, it can be concluded that deletion of *cbf11* leads to anomalous mitochondrial morphology and membrane potential.

#### 4.1.3 Respiration of $\Delta cbf11$ depends on the carbon source

The low cellular respiration in glucose-containing complex medium and aberrant mitochondrial morphology of  $\Delta cbf11$  cells indicate deregulation of energy metabolism in this mutant or defects in mitochondria and thus inability to respire sufficiently. The latter was tested by viability and respiratory activity of the  $\Delta cbf11$  strain grown on nonfermentable carbon source.

Glycerol is utilized solely through oxidation by the respiratory chain and the ability of the  $\Delta cbf11$  and  $\Delta cbf11 \Delta cbf12$  mutants to grow in complex medium (YES) containing 3% glycerol and 0.1% glucose (Figure 4.3A) implies the functionality of their respiratory complexes in

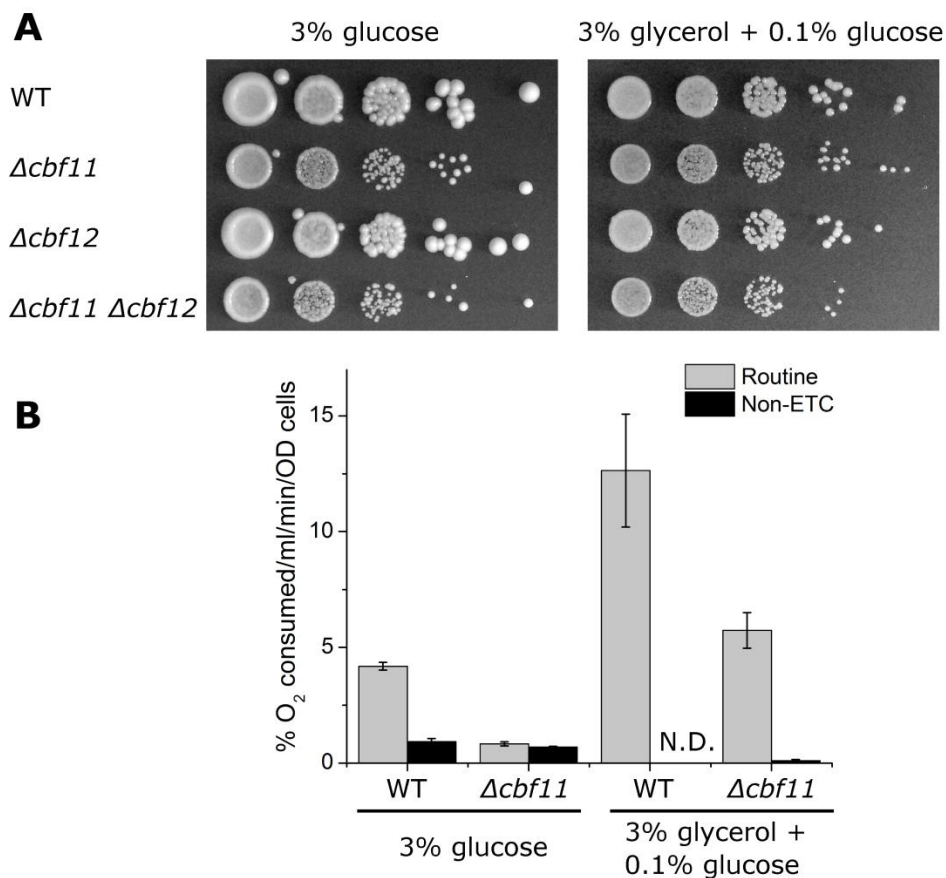


**Figure 4.3 Respiration of  $\Delta cbf11$  is induced by nonfermentable carbon source. (A)** 10-fold serial dilutions of exponentially growing cultures with the indicated genotypes were spotted on YES plates containing 3% glucose or 3% glycerol and 0.1% glucose and incubated for 3 days. **(B)** Routine and non-ETC respiration of exponentially growing WT and  $\Delta cbf11$  cultures in YES + 3% glucose or YES + 3% glycerol + 0.1% glucose was measured using the Oroboros Oxygraph. Non-ETC respiration was determined by adding antimycin A, except for WT grown in glycerol (not determined, N.D.). Error bars represent the standard deviation/range of at least two independent biological replicates.

mitochondria. Low concentration of glucose was used to boost growth of cells during transition from fermentation to respiration and it is not sufficient to sustain growth without active respiration. Anyhow, the CSL mutants are viable when grown in complex media containing only glycerol as a carbon source (data not shown). Notably, the growth defect of  $\Delta cbf11$  and  $\Delta cbf11 \Delta cbf12$  in YES + 3% glucose is preserved in YES + 3% glycerol + 0.1% glucose as observed by smaller colony sizes compared to WT.

As suggested by the viability of  $\Delta cbf11$  on glycerol-containing medium, respiration is induced in this strain under these conditions (Figure 4.3B, page 45). The rule out other potential explanations for increased oxygen consumption in the  $cbf11$  knock-out, the flow of electrons through electron transport chain (ETC) was blocked by addition of antimycin A, an inhibitor of complex III. Clearly, the increased oxygen consumption of  $\Delta cbf11$  cells grown in 3% glycerol + 0.1% glucose compared to 3% glucose is due to increased ETC activity. Respiration of WT cells in nonfermentable media is higher compared to glucose-containing media, as described previously (Heslot *et al.*, 1970a; Zuin *et al.*, 2008). Strikingly, the respiration of  $\Delta cbf11$  grown in YES + 3% glucose is extremely low as can be deduced from the small difference between routine and non-ETC oxygen consumption. Moreover, the non-ETC oxygen consumption of the  $\Delta cbf11$  mutant grown in complex medium containing glycerol is markedly lower than when containing only glucose. This discrepancy has likely arisen from small number of biological replicates but may also have a biological background, such as deregulation of the NADPH oxidases.

## 4.2 Upstream regulators of CSL

The cellular response to oxidative stress is complex, with various sensor systems, signaling pathways regulating both common and specific target molecules. The wiring of signaling pathways is usually decoded by studying genetic interactions (Chapter 1.3). This approach requires construction of double (or multiple) mutants (Chapter 4.2.1). To identify the upstream regulators of CSL proteins nine factors already known to participate in the regulation of oxidative stress response were selected. These included the mitogen-activated protein kinase Sty1 and its main downstream transcription factor Atf1, transcription factor Pap1, transcription factor Prr1, protein kinase A (Pka1), two protein kinases acting in the TOR signaling pathway (Sck1 and Sck2), mitogen-activated protein kinase Pmk1 and the transcription factor Hsr1. The selected factors span the spectrum of described regulators of response to various sources of ROS and the molecular mechanism of some of them, such as Sty1 MAPK and Pap1 TF, has been thoroughly mapped, allowing better understanding of the role of the CSL proteins during oxidative stress.

#### 4.2.1 Construction of strains

Double knock-outs of CSL and the regulators of oxidative stress response were prepared by strain crossing or by CSL gene deletion via linearized plasmid-mediated homologous recombination in a strain bearing a deletion of the oxidative stress response regulator, as previously described (Gregan *et al.*, 2006). Knock-outs of *atf1* and *pap1* were crossed with  $\Delta cbf11$  (MP83) or  $\Delta cbf12$  (MP73) and the desired double mutants were selected on EMM medium containing nourseothricin. The CSL genotypes and the mating type were determined by 3-primer system PCR. The 3-primer system PCR distinguishes between the existence of endogenous CSL genomic locus and its deletion in the case of CSL genotyping and between the h+ and h- alleles in the case of *mat1* locus by providing a product of different size in either case (Figure 4.4A, page 48). The primers MP27, MP28 and kan-rev were used to genotype the *cbf11* locus and primers MP31, MP32 and MP33 were used to genotype the *cbf12* locus. The mating type was determined using primers MM, MP, MT1. Genotyping of  $\Delta cbf11 \Delta atf1$  (MP367, labeled 1) and  $\Delta cbf12 \Delta atf1$  (MP365, labeled 2) is shown for illustration (Figure 4.4B, page 48). Knock-outs of *pka1*, *sck1*, *sck2* and *hsr1* were crossed with  $\Delta cbf11$  (MP114) or  $\Delta cbf12$  (MP21) and the desired double mutants were selected for with nourseothricin and geneticin ( $\Delta pka1$ ,  $\Delta sck1$ ,  $\Delta sck2$ ) or nourseothricin and hygromycin B ( $\Delta hsr1$ ). The resulting strains were genotyped as described above. The double deletion mutants of CSL and *pmk1*, *prp1* and *sty1* were prepared by linearized plasmid-mediated homologous recombination due to potential problems with strain crossing, such as mating or sporulation defects of the single mutants and the lack of selection marker for the resultant double mutant. XbaI-linearized plasmids pMP91 and pMP45 were used to delete *cbf11* and *cbf12*, respectively, and nourseothricin-resistant clones were selected. The genotype of  $\Delta cbf11$  was confirmed with MP150 and MP144 primers at the upstream junction site and with MP33 and MP151 at the downstream junction site (Figure 4.4C, page 48). The genotype of  $\Delta cbf12$  was verified using the 3-primer system (MP31, MP32, MP33) described above for crossing strains (Figure 4.4A, page 48). Genotyping of  $\Delta cbf11 \Delta prp1$  (MP354, labeled 1) and  $\Delta cbf12 \Delta prp1$  (MP355, labeled 2) is shown for illustration (Figure 4.4D, page 48).

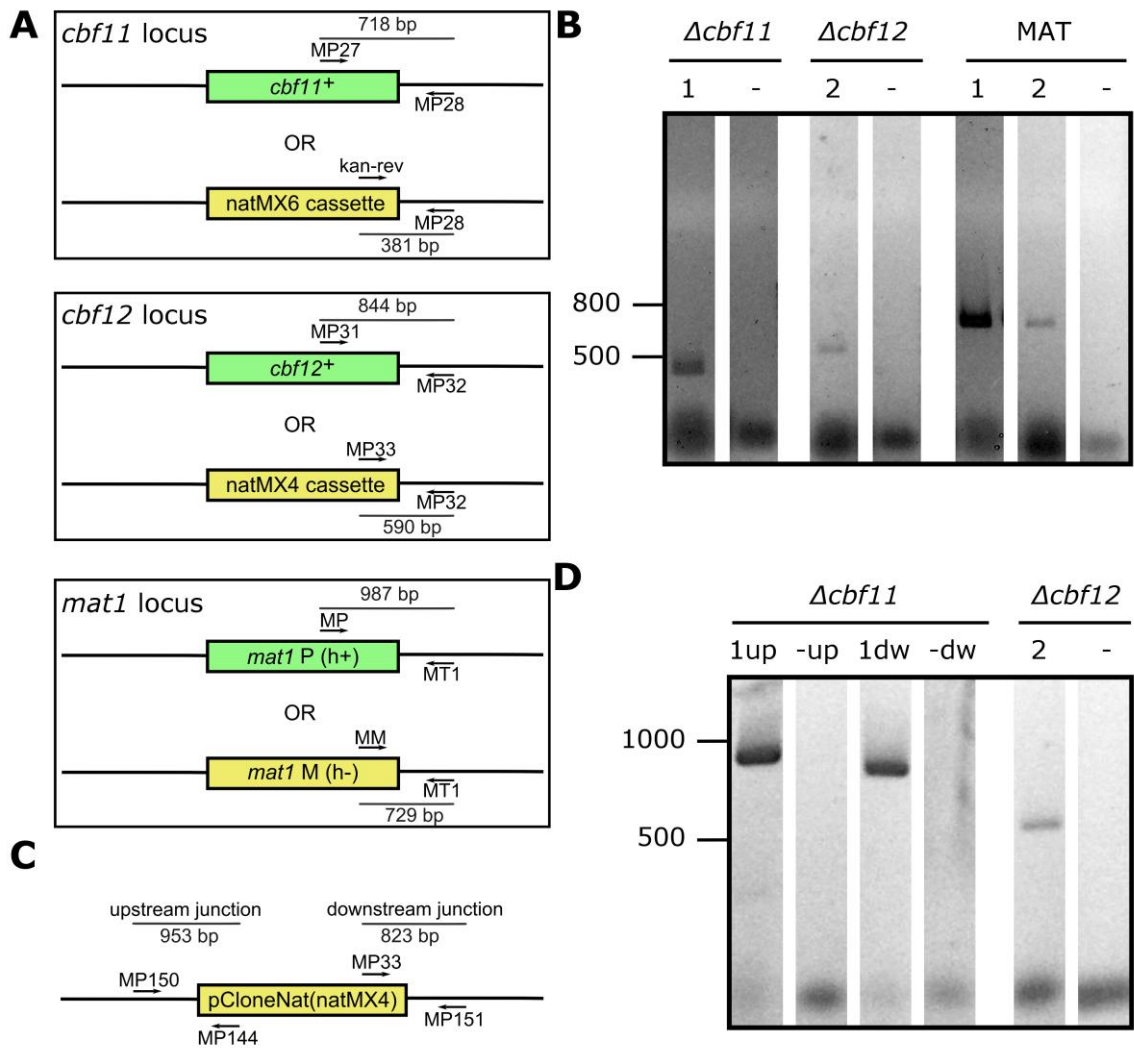


**Figure 4.4 Construction of double deletion mutants. (A)** A schematic representation of the 3-primer systems used to verify the genotype of *cbf11*, *cbf12* and the mating loci. Primer names and PCR product sizes are indicated for each locus. **(B)** Genotyping of  $\Delta cbf11$ ,  $\Delta cbf12$  and the mating loci (labeled MAT) in  $\Delta cbf11 \Delta atf1$  (MP367, labeled 1) and  $\Delta cbf12 \Delta atf1$  (MP365, labeled 2). The expected PCR product sizes (381 bp for  $\Delta cbf11$  and 590 bp for  $\Delta cbf12$ ) were acquired. Both tested strains are h<sup>-</sup> (729 bp). Negative control (-) was performed without DNA template. PCR products were separated in 1.5% agarose gel. **(C)** A schematic representation of  $\Delta cbf11::natMX4$  genotyping performed after linearized plasmid-mediated homologous recombination. Primer names and PCR product sizes are indicated for upstream and downstream junctions. **(D)** Genotyping of  $\Delta cbf11$  and  $\Delta cbf12$  in  $\Delta cbf11 \Delta prr1$  (MP354, labeled 1up and 1dw for upstream and downstream junction verification, respectively) and  $\Delta cbf12 \Delta prr1$  (MP355, labeled 2). The expected PCR product sizes (985 bp for  $\Delta cbf11$  upstream, 823 bp for  $\Delta cbf11$  downstream and 590 bp for  $\Delta cbf12$ ) were acquired. Negative control (-) was performed without DNA template. PCR products were separated in 1.5% agarose gel.

*Schizosaccharomyces pombe* cells are generally haploid and mating is normally followed by meiosis. However, diploids do occur during strain crossing and they need to be avoided for most applications as their properties tend to differ from haploid strains due to presence of homologous chromosomes. All strains were observed in Nomarski microscopy to detect possible diploids or morphological changes compared to the parental strains. Notably, the microscopic observation of  $\Delta sty1 \Delta cbf11$  and  $\Delta pka1 \Delta cbf11$  mutants revealed that the phenotype of the parent *sty1/pka1* knock-outs is recapitulated in these double knock-outs. Deletion of *cbf11* causes a decrease in cell length (Převorovský, Tvarůžková *et al.*, manuscript submitted for publication), called the 'wee' phenotype (Hayles *et al.*, 2013). The mitogen-activating kinase Sty1 and protein kinase A (Pka1) are prominent cell cycle regulators and their disruption causes cell elongation (Shiozaki and Russell, 1995) and shortening (Jin *et al.*, 1995), respectively. The morphology of  $\Delta sty1$  is preserved in  $\Delta cbf11 \Delta sty1$  and the 'wee' phenotype of  $\Delta cbf11$  and  $\Delta pka1$  is even more pronounced in the double mutant (Převorovský, Tvarůžková *et al.*, manuscript submitted for publication). Moreover, microscopic observation of several  $\Delta cbf11 \Delta sty1$  isolates (data not shown) indicated presence of diploid cell fraction. Since the mutant  $\Delta cbf11 \Delta sty1$  was prepared by deleting *cbf11* in a sterile  $\Delta sty1$  strain, the diploid cells which are heterozygous for the *cbf11* allele may occur and cannot be selected against using nourseothricin. Candidate haploid clones were selected based on Nomarski microscopy and phloxine B staining in YES agar plates. Phloxine B is a vital dye which stains diploid colonies darker color than haploid colonies due to higher fraction of dead cells in diploid strains (data not shown). Selected clones of  $\Delta cbf11 \Delta sty1$  grown on YES agar plates containing nourseothricin were subjected to DNA content analysis by flow cytometry. Using gating on cells with single nuclei, which correspond to late S-phase and G2-phase cells in the fission yeast, we measured essentially only particles with 2C DNA content in WT cells (Knutsen *et al.*, 2011). The single mutants  $\Delta sty1$  and  $\Delta cbf11$  display predominantly 2C DNA content (Figure 4.5A, page 50), while all independent  $\Delta cbf11 \Delta sty1$  isolates tested show a wide range of DNA content (Figure 4.5B, page 50), suggesting presence of diploid cells or cells with disrupted coordination of cell and nuclear division in the  $\Delta cbf11 \Delta sty1$  strain. It has to be noted that cells lacking *cbf11* exhibit abnormal DNA content distribution, such as >2C cell population (Figure 4.5, page 50), and cytokinesis defects (Převorovský *et al.*, 2009) and thus the double knock of of *cbf11* and *sty1*, an important cell cycle regulator, is expected to have cell cycle-related defects. Isolate #2 was selected for further experiments. Interestingly, later cultivation of  $\Delta cbf11 \Delta sty1$  isolate #2 in liquid YES medium to exponential phase yielded normal DNA content distribution comparable to  $\Delta sty1$ , even without the defects observed in the  $\Delta cbf11$  single mutant (Figure 4.5C, page 50), which shows that deletion of *sty1* suppresses

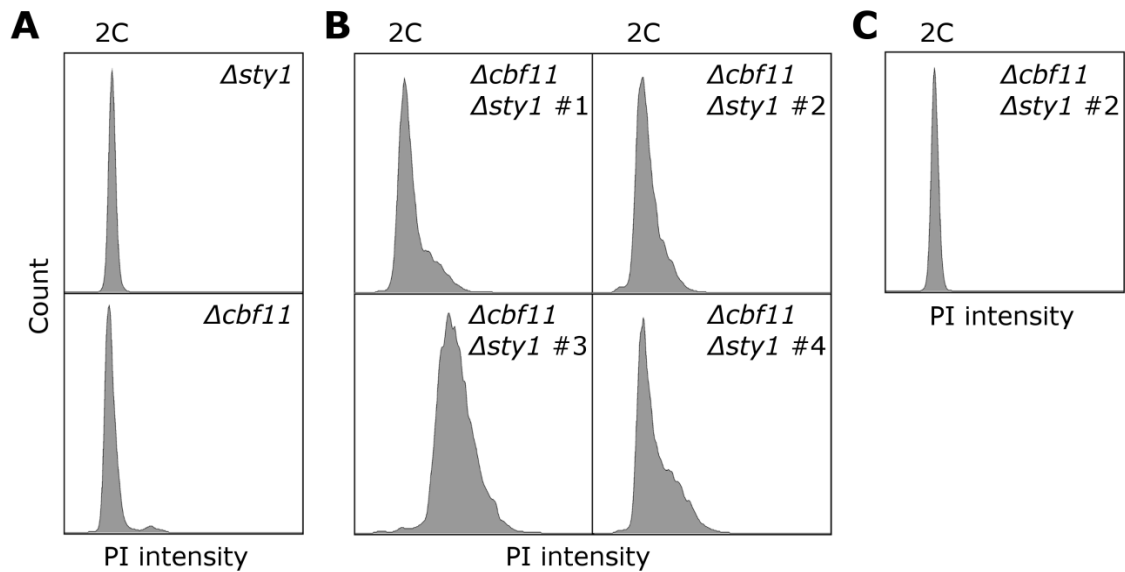


**Figure 4.5 DNA profiles of  $\Delta cbf11 \Delta sty1$  isolates.** Flow cytometry analysis of DNA content in fixed, propidium iodide-stained cells grown to exponential phase in YES (A,C) or cells grown for 3 days on YES agar plates (B). **(A)** Parent strains  $\Delta sty1$  and  $\Delta cbf11$  have predominantly 2C DNA content, even though the latter shows aberrant DNA distribution. **(B)** Four isolates of  $\Delta cbf11 \Delta sty1$  prepared by deletion of *cbf11* in  $\Delta sty1$  show various amount of >2C DNA content. **(C)**  $\Delta cbf11 \Delta sty1$  #2 isolate grown to exponential phase shows normal DNA content distribution unlike in (B).

the DNA content defect of  $\Delta cbf11$  (Převorovský, Tvarůžková *et al.*, manuscript submitted for publication). This discrepancy was probably caused by different cultivation methods and the aberrant DNA content of  $\Delta cbf11 \Delta sty1$  strain grown on agar plates is an artifact caused by presence of nourseothricin antibiotic or uneven cell growth and cell differentiation in the yeast colony.

#### 4.2.2 CSL interact genetically with the Sty1 and Pap1 stress-response pathways

Mitogen-activated protein kinase (MAPK) Sty1 is a member of the central stress-response pathway which is activated upon heat shock, osmotic stress, oxidative stress and other cellular insults. One of its main targets is transcription factor Atf1, which induces the expression of oxidative stress response genes and the cell becomes adept at destroying excess ROS and repairing damage to proteins, lipids and DNA. Consequently, cells lacking either *sty1* or *atf1* are sensitive to  $H_2O_2$  (Figure 4.6, page 51; Degols *et al.*, 1996; Wilkinson *et al.*, 1996; Calvo *et al.*, 2009). We sought whether the Sty1 pathway is involved in the resistance of  $\Delta cbf11$  cells (Figure 4.1A, page 43) by serial dilution of double mutants of *cbf11* and *sty1* or *atf1* on complex medium plates containing hydrogen peroxide as a source of ROS. Intriguingly, while  $\Delta cbf11$  does not suppress the sensitivity of  $\Delta sty1$  at all (Figure 4.6A, page 51), the sensitivity of  $\Delta atf1$  is partially suppressed by *cbf11* knock-out (Figure 4.6B, page 51). This observation demonstrates the indispensable role of Sty1 in maintaining the resistance of

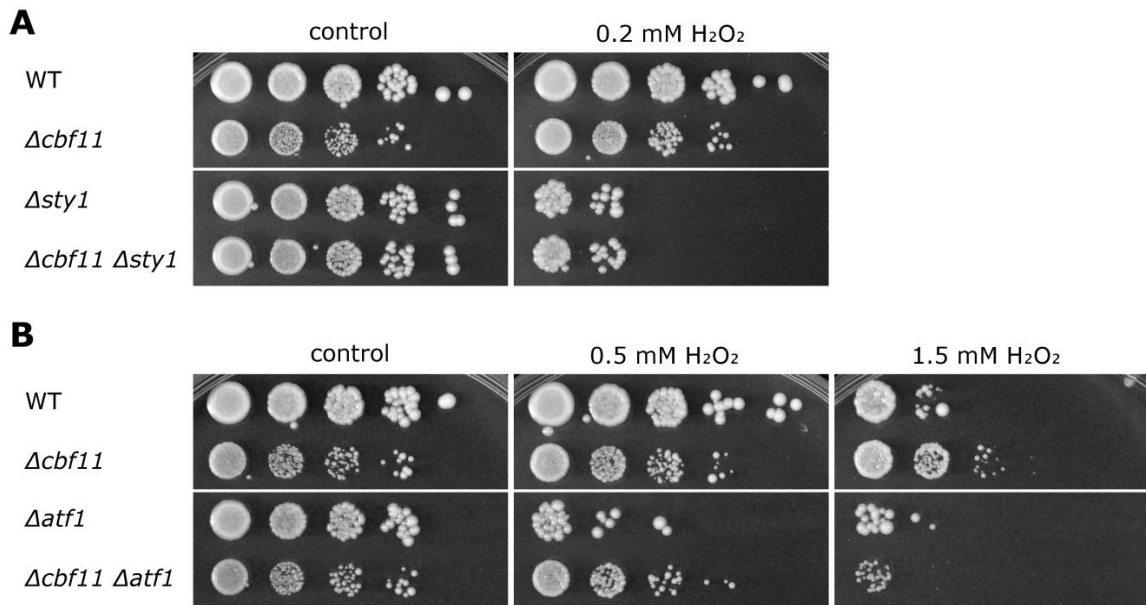


**Figure 4.6 Sty1 and partially Atf1 are required for resistance of  $\Delta cbf11$  cells.** 10-fold serial dilutions of cultures with the indicated genotypes were spotted on YES plates with or without H<sub>2</sub>O<sub>2</sub> at the indicated concentrations and grown for 3 days. **(A)** While *sty1* is required for resistance of  $\Delta cbf11$ , **(B)** *atf1* deletion affects the sensitivity of  $\Delta cbf11$  only at high concentration of H<sub>2</sub>O<sub>2</sub>.

$\Delta cbf11$  mutant to oxidative stress. The mechanism of the  $\Delta cbf11$  strain resistance is not known, perhaps through expression of oxidative stress response genes in Sty1-dependent manner. However, the main effector of Sty1, the transcription factor Atf1, is required for survival and resistance of the  $\Delta cbf11$  strain only at high levels of oxidative stress, which suggests involvement of other Sty1-dependent regulatory proteins under low stress conditions.

The main regulator of oxidative stress response at low stress conditions (menadione treatment or low concentration of H<sub>2</sub>O<sub>2</sub>) is the redox-sensitive transcription factor Pap1 (Quinn *et al.*, 2002; Chen *et al.*, 2008) which collaborates with the transcription factor Prr1 to activate a subset of oxidative stress response genes (Calvo *et al.*, 2012). As described previously (Toone *et al.*, 1998; Ohmiya *et al.*, 1999), mutants in *pap1* and *prr1* are sensitive to H<sub>2</sub>O<sub>2</sub> (Figure 4.7, page 52). Similarly to Sty1, Pap1 is essential for the resistance of  $\Delta cbf11$  even though minor suppression of the  $\Delta pap1$  sensitivity by deletion of *cbf11* is visible upon low H<sub>2</sub>O<sub>2</sub> treatment (Figure 4.7A, page 52). Prr1 is also an important factor for the exhibition of  $\Delta cbf11$  strain resistance to hydrogen peroxide (Figure 4.7B, Day 5, page 52). Remarkably, the  $\Delta cbf11 \Delta prr1$  mutant displays improved viability over  $\Delta prr1$  on complex medium containing 0.5 mM H<sub>2</sub>O<sub>2</sub>, but the growth rate is severely reduced (Figure 4.7B, page 52). Note that  $\Delta pap1$  is more sensitive to H<sub>2</sub>O<sub>2</sub> than  $\Delta prr1$  (0.25 mM H<sub>2</sub>O<sub>2</sub> in Figure 4.7A compared to

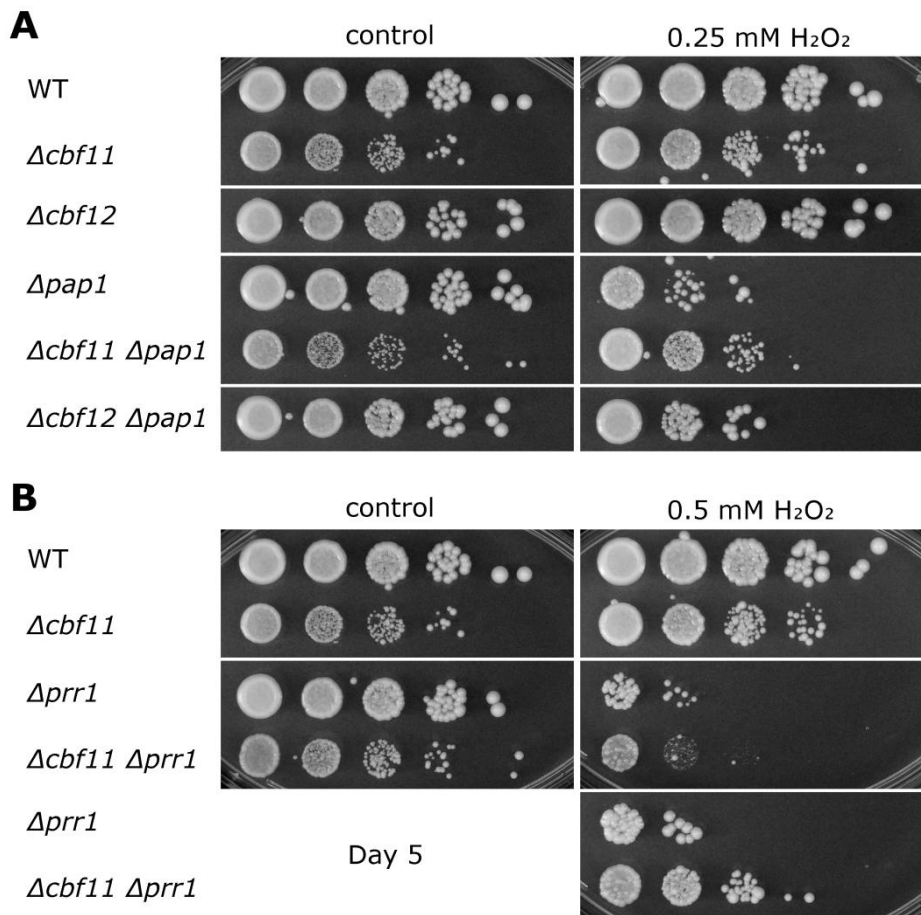


**Figure 4.7 Pap1 and Prr1 transcription factors are needed for  $\Delta cbf11$  strain resistance.** 10-fold serial dilutions of cultures with the indicated genotypes were spotted on YES plates with or without H<sub>2</sub>O<sub>2</sub> at the indicated concentration and grown for 3 days unless stated otherwise. **(A)** Both *cbf11* and *cbf12* deletions partially suppress the strong sensitivity of  $\Delta pap1$ . **(B)** The sensitivity of  $\Delta prr1$  is moderately suppressed by deletion of *cbf11*.

0.5 mM H<sub>2</sub>O<sub>2</sub> in Figure 4.7B). The deletion of *cbf12* in WT background does not have an effect on sensitivity to oxidative stress (Figure 4.1, page 43) and it does not impact the sensitivity of most oxidative stress response mutants either (data not shown). Exceptionally, the sensitivity of  $\Delta pap1$  is marginally suppressed in the  $\Delta cbf12 \Delta pap1$  double mutant (Figure 4.7A). The effect of *cbf12* deletion on the  $\Delta pap1$  strain resistance to H<sub>2</sub>O<sub>2</sub> is subtle, but consistent in three independent experiments and it suppresses both the growth defect and reduced viability of the *pap1* knock-out upon oxidative stress. Therefore, it is tempting to speculate that both CSL paralogs in *S. pombe* are involved in oxidative stress response.

Mitogen-activated protein kinase Pmk1 of the cell integrity pathway and zinc-finger transcription factor Hsr1 are alternative regulators of oxidative stress response and their mutants have only a mild phenotype upon H<sub>2</sub>O<sub>2</sub> treatment (Madrid *et al.*, 2006; Barba *et al.*,

2008; Chen *et al.*, 2008). The sensitivity of double deletion mutants of *pmk1* and *hsr1* with CSL to H<sub>2</sub>O<sub>2</sub> was studied by spot testing and did not reveal any interactions (data not shown).

#### 4.2.3 Cbf11 and Pka1 interact as negative regulators of oxidative stress response

Protein kinase A, also known as the cAMP-dependent protein kinase, is a hub of cellular signaling. It is a prominent regulator of the cell cycle (Jin *et al.*, 1995), sexual development (Maeda *et al.*, 1994), glucose metabolism (Byrne and Hoffman, 1993), cell respiration and aging (Roux *et al.*, 2006; Zuin *et al.*, 2010a). Cells lacking *pka1* were found to be resistant to H<sub>2</sub>O<sub>2</sub> (Figure 4.8). Strikingly, the level of  $\Delta pka1$  resistance is indistinguishable from that of  $\Delta cbf11$  and the double mutant  $\Delta cbf11 \Delta pka1$ , suggesting that Pka1 and Cbf11 act as negative regulators of oxidative stress response via a shared mechanism.

TOR kinase targets Sck1 and Sck2 protein kinases were identified as high copy number suppressors of  $\Delta pka1$  defects (Jin *et al.*, 1995; Fujita and Yamamoto, 1998). The *sck1* and *sck2* mutants mimic some phenotypes of  $\Delta pka1$ , however, the manifestation is usually more modest. Contrary to  $\Delta pka1$ , the  $\Delta sck1$  and  $\Delta sck2$  mutants are not resistant to H<sub>2</sub>O<sub>2</sub>, the former is even mildly sensitive (Figure 4.8). The resistance of  $\Delta cbf11$  to H<sub>2</sub>O<sub>2</sub> is retained in the  $\Delta cbf11 \Delta sck1$  and  $\Delta cbf11 \Delta sck2$  double mutants. The sensitivity of  $\Delta sck1$  to H<sub>2</sub>O<sub>2</sub> is alleviated by the

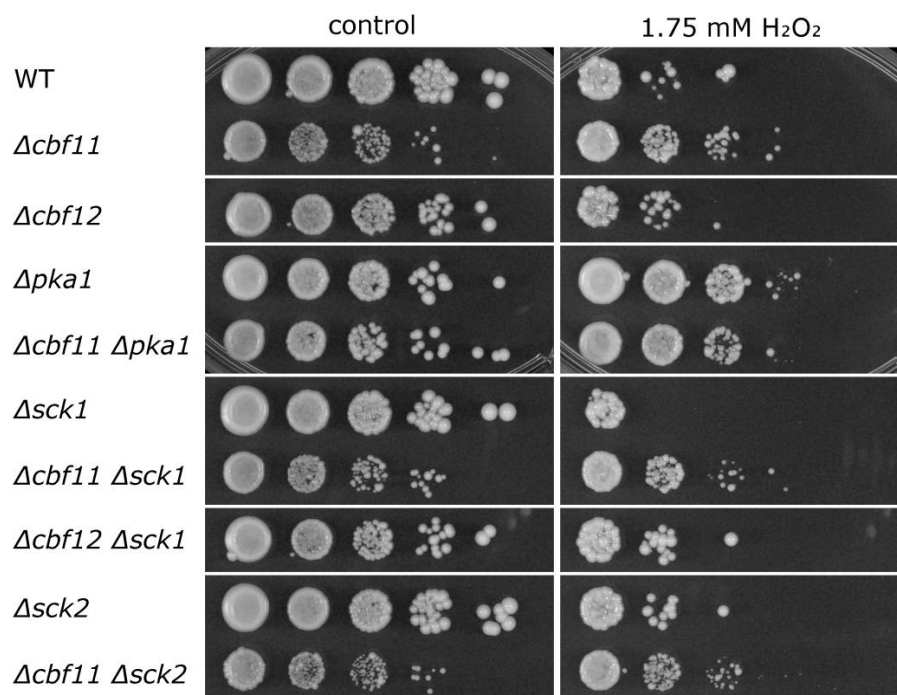


**Figure 4.8 Cbf11 and Pka1 probably act as negative regulators of oxidative stress response via common mechanism.** 10-fold serial dilutions of cultures with the indicated genotypes were spotted on YES plates with or without 1.75 mM H<sub>2</sub>O<sub>2</sub> and grown for 3 days. Viability of  $\Delta pka1$  and  $\Delta cbf11 \Delta pka1$  is indistinguishable from that of  $\Delta cbf11$  upon H<sub>2</sub>O<sub>2</sub> treatment. Unlike  $\Delta pka1$ , the  $\Delta sck1$  and  $\Delta sck2$  mutants are not resistant to H<sub>2</sub>O<sub>2</sub> and do not affect the resistance of  $\Delta cbf11$ .

deletion of *cbf12*, designating it the second case of involvement of Cbf12 in oxidative stress response. None of the other 7 double mutants of CSL and regulators of oxidative stress response gave similar results. Based on the observations described above, Sck1 and Sck2 are not markedly involved in the oxidative stress response and do not affect the fitness of CSL knock-outs upon H<sub>2</sub>O<sub>2</sub> treatment.

### 4.3 Downstream regulators of CSL

The cell employs a collection of executive molecules to battle the increased ROS concentration and oxidative damage to cell components. Our goal was to determine which antioxidant proteins are responsible for the resistance of  $\Delta cbf11$  cells. The transcriptome profiling of  $\Delta cbf11$  mutant revealed that genes coding for antioxidants and oxidative stress response signaling proteins have induced expression level in the  $\Delta cbf11$  strain (Převorovský, Tvarůžková *et al.*, manuscript submitted for publication). We have selected four antioxidant enzymes with the highest fold expression induction in  $\Delta cbf11$  compared to WT control cells, namely glutathione S-transferase (*gst2*, 9.6x), sulfiredoxin (*srx1*, 7.8x), catalase (*ctt1*, 6x) and glutathione peroxidase (*gpx1*, 2.9x) for genetic interaction testing using the double mutants of  $\Delta cbf11$  with deletions of the above mentioned genes.

#### 4.3.1 Construction of strains

The strains  $\Delta srx1$ ,  $\Delta gpx1$  and  $\Delta gst2$  were kindly provided by Elizabeth Veal and double mutants with  $\Delta cbf11$  were acquired by linearized plasmid-mediated (pMP91) deletion of *cbf11* as described in Chapter 4.2.1. To construct the  $\Delta ctt1$  strain, a plasmid bearing sequences homologous to upstream and downstream regions of *ctt1* open reading frame, and nourseothricin resistance cassette (*natMX4*) was prepared as described in (Gregan *et al.*, 2006). The upstream and downstream homology regions were cloned by Q5<sup>®</sup> High-Fidelity Polymerase (NEB) using the primer pairs MP171+MP172 and MP173+MP174, respectively (Figure 4.9A, page 55). Column-purified PCR products were digested with *Apa*I, ligated, column-purified and digested with *Xho*I and *Bgl*II endonucleases. The plasmid backbone containing *natMX4* was used from pMP91 by *Xho*I and *Bgl*II digestion. The digested plasmid and homology regions were separated in 1% agarose gel, the appropriate bands were purified, ligated and transformed into DH5 $\alpha$  strain of *E. coli*. Eight clones were tested by colony PCR using MP33 and MP144 primers for the presence of the correct plasmid, yielding PCR products of expected size for all clones tested (data not shown). Plasmids were extracted from 2 positive clones and verified by restriction digestion using *Apa*I, *Xho*I and *Bgl*II (Figure 4.9B, page 55). The plasmid, named pMP126, was verified by sequencing using MP33 and MP144 primers, which correspond to the plasmid section containing *ctt1* ORF upstream and downstream flanking regions designed for homologous recombination. Strains  $\Delta ctt1$  and

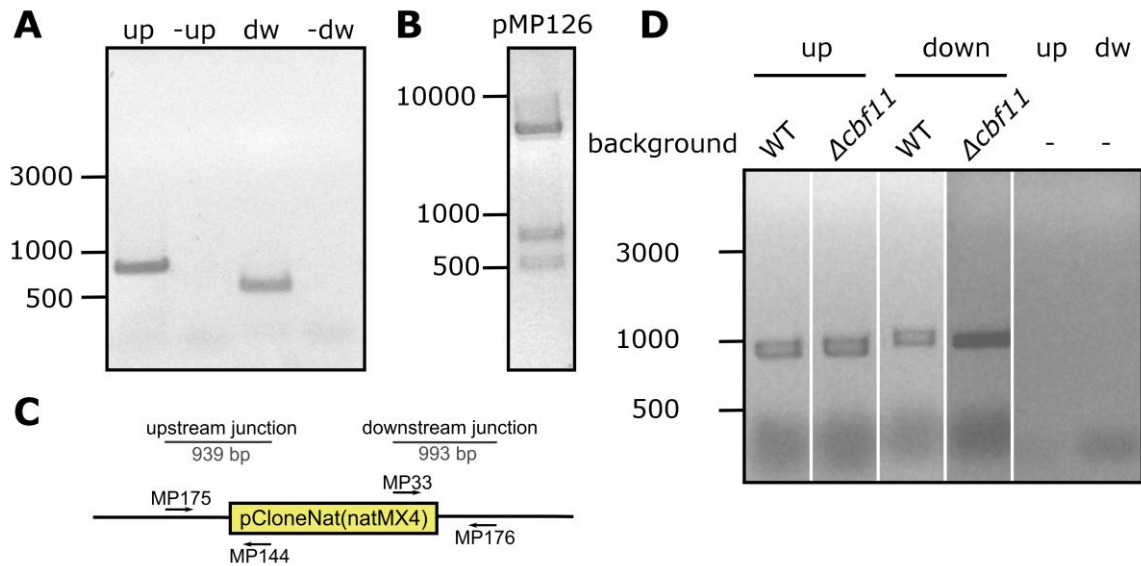


**Figure 4.9 Construction of *ctt1* knock-out strain.** (A) Amplification of upstream (up, 733 bp) and downstream (dw, 471 bp) flanking regions of *ctt1* ORF. Negative control (-) was performed without DNA template. PCR products were separated in 1% agarose gel. (B) Restriction digestion of *ctt1* knock-out plasmid pMP126 by *Apal*, *XhoI* and *BglII* yielding fragments of expected sizes 471 bp, 733 bp and ~4 kb was separated in 1.5% agarose gel. (C) A schematic representation of  $\Delta ctt1::natMX4$  genotyping performed after linearized plasmid-mediated homologous recombination. Primer names and PCR product sizes are indicated for upstream and downstream junctions. (D) Genotyping of  $\Delta ctt1$  after deletion of *ctt1* in WT and  $\Delta cbf11$  background. The expected PCR product sizes (939 bp for upstream junction, 993 bp for downstream junction) were acquired. Negative control (-) was performed without DNA template. PCR products were separated in 1% agarose gel.

$\Delta cbf11 \Delta ctt1$  were prepared by transforming WT (JB32) and  $\Delta cbf11$  (MP44), respectively, with the *Apal*-linearized pMP126 plasmid. Nourseothricin-resistant clones were verified by colony PCR using primers MP175+MP144 and MP176+MP33 annealing to upstream and downstream junction site, respectively (Figure 4.9C,D).

#### 4.3.2 Catalase and sulfiredoxin are responsible for the resistance of $\Delta cbf11$

Catalase is encoded by a single gene *ctt1* in *S. pombe* and it is the major hydrogen peroxide scavenger in the cell (Mutoh *et al.*, 1999; Paulo *et al.*, 2014), therefore, the deletion of *ctt1* causes a substantial increase in cell sensitivity to  $H_2O_2$  compared to WT cells. When the yeast cells lack both *cbf11* and *ctt1* they are also very sensitive to  $H_2O_2$ , although less than  $\Delta ctt1$  alone (Figure 4.10A, page 56, note the low  $H_2O_2$  concentration). This indicates that catalase is very important for the resistance of  $\Delta cbf11$  cells but also additional factors participate.

Another strongly induced antioxidant in  $\Delta cbf11$  cells (Převorovský, Tvarůžková *et al.*, manuscript submitted for publication) is the sulfiredoxin *srx1*. The enzyme encoded by the *srx1* gene is responsible for reduction of peroxiredoxin Tpx1 when overoxidized during severe oxidative stress, thus allowing the activation of transcription factor Pap1 and

induction of transcriptional response (Bozonet *et al.*, 2005). The deletion of *srx1* leads to severe impairment of antioxidant defense mechanisms (Zuin *et al.*, 2008), represented by increased sensitivity to H<sub>2</sub>O<sub>2</sub> (Figure 4.10B). As in the case of *ctt1*, the resistance of  $\Delta cbf11$  is debased by deletion of *srx1* and the sensitivity of the double mutant  $\Delta cbf11 \Delta srx1$  is slightly decreased compared to  $\Delta srx1$  (Figure 4.10B). Therefore, both *ctt1* and *srx1* are critical for increased fitness of  $\Delta cbf11$  cells upon H<sub>2</sub>O<sub>2</sub> treatment.

Other potential candidates to be responsible for the resistance of  $\Delta cbf11$  to H<sub>2</sub>O<sub>2</sub> were the glutathione peroxidase Gpx1 and glutathione S-transferase Gst2, both of which are transcriptionally upregulated in the  $\Delta cbf11$  mutant (Převorovský, Tvarůžková *et al.*, manuscript submitted for publication). The glutathione peroxidase Gpx1, or more precisely thioredoxin peroxidase since it does not use glutathione but thioredoxin as the electron donor (Lee *et al.*, 2007), is responsible for H<sub>2</sub>O<sub>2</sub> detoxification and may play a role in oxidative stress response signaling. As shown in Figure 4.11A (page 57), the  $\Delta gpx1$  mutant is not sensitive to H<sub>2</sub>O<sub>2</sub> and it does not affect the resistance of  $\Delta cbf11$  considerably. Therefore, the glutathione/thioredoxin peroxidase Gpx1 is likely not the enzyme conferring resistance on the  $\Delta cbf11$  mutant. Our results that the  $\Delta gpx1$  cells are not sensitive to hydrogen peroxide differ from those published in a study by the Hidalgo group (Paulo *et al.*, 2014), where the

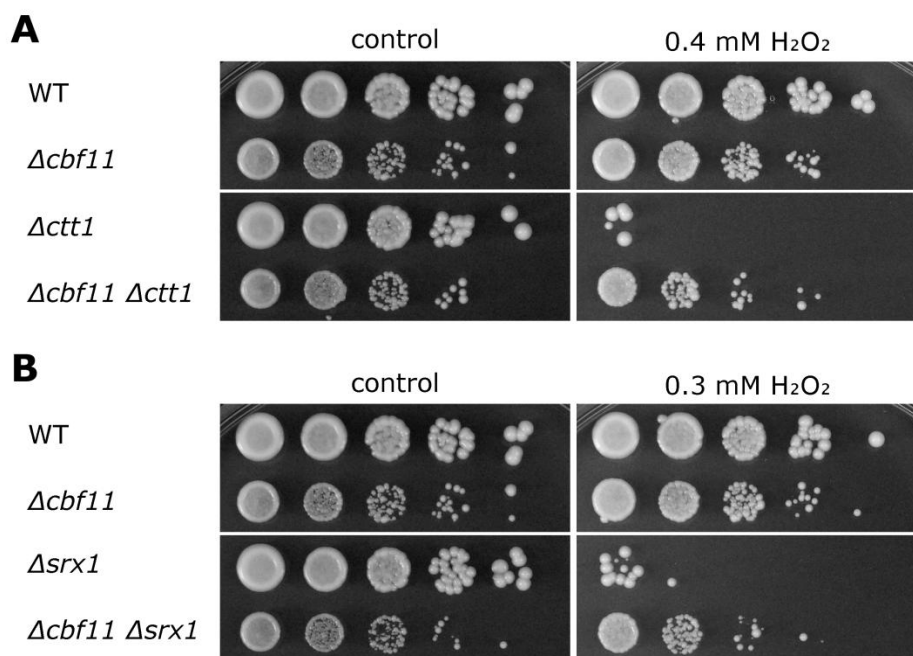


**Figure 4.10** *ctt1* and *srx1* are required for full resistance of  $\Delta cbf11$  cells. 10-fold serial dilutions of cultures with the indicated genotypes were spotted on YES plates with or without H<sub>2</sub>O<sub>2</sub> at the indicated concentration and grown for 3 days. Both *ctt1* (**A**) and *srx1* (**B**) are required for the resistance of  $\Delta cbf11$  cells. This sensitivity experiment was performed twice, and a representative experiment is shown.

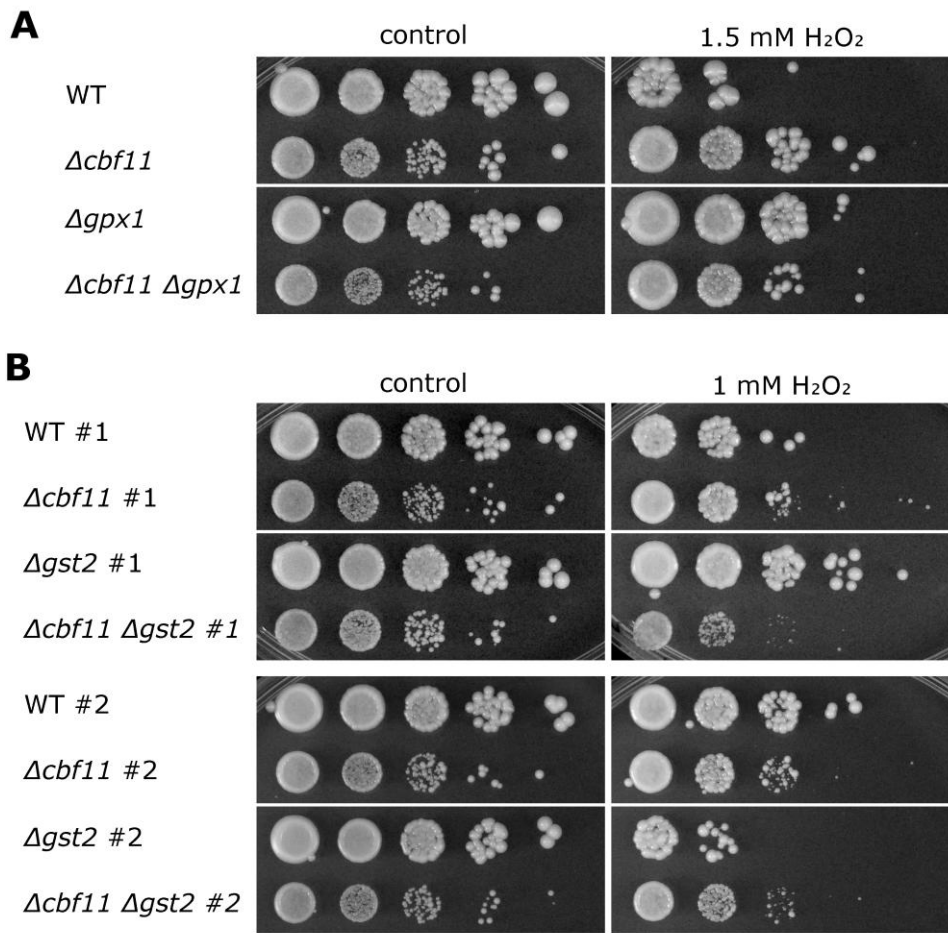


**Figure 4.11 Gpx1 and Gst2 are not major players in the resistance of  $\Delta cbf11$  cells.** 10-fold serial dilutions of cultures with the indicated genotypes were spotted on YES plates with or without H<sub>2</sub>O<sub>2</sub> at the indicated concentration and grown for 5 (A) or 3 (B) days. **(A)** The viability of  $\Delta cbf11$  is not affected by  $\Delta gpx1$  mutation in the presence of H<sub>2</sub>O<sub>2</sub>. **(B)** Although two independent experiments (labeled #1 and #2) yielded inconsistent results for the sensitivity of  $\Delta gst2$ , the resistance of  $\Delta cbf11$  cells to H<sub>2</sub>O<sub>2</sub> is not influenced by  $gst2$  deletion.

$\Delta gpx1$  mutant is described to be mildly sensitive. This discrepancy may have arisen from different genetic background and cultivation conditions such as temperature of growth, presence of supplements in the media or the yeast extract batch, all of which differed between our and Hidalgo's group study.

The *S. pombe* genome encodes three glutathione S-transferases, all of which are induced upon oxidative stress. Except for their role in detoxification of xenobiotics, they may also function to detoxify H<sub>2</sub>O<sub>2</sub> and act as signaling molecules in the oxidative stress response (Veal *et al.*, 2002). Although *gst2* is one of the most upregulated transcripts in the  $\Delta cbf11$  mutant (Převorovský, Tvarůžková *et al.*, manuscript submitted for publication), the *gst2* gene deletion does not impact the viability of  $\Delta cbf11$  when grown in the presence of H<sub>2</sub>O<sub>2</sub> (Figure 4.11B). However, the  $\Delta cbf11 \Delta gst2$  double mutant displays slower growth compared to the parent strains when grown on YES + H<sub>2</sub>O<sub>2</sub> (Figure 4.11B). It has to be noted that the

sensitivity of WT and  $\Delta gst2$  strains was inconsistent in two independent experiments (compare #1 and #2 in Figure 4.11B, page 57). Nevertheless, we did not pursue additional experiments to explain this inconsistency because the aim of this experiment was to compare the sensitivity of the  $\Delta cbf11$  mutant and the  $\Delta cbf11 \Delta gst2$  double knock-out, not to characterize the  $\Delta gst2$  mutant which was described by others (Veal *et al.*, 2002).

#### 4.3.3 Cbf11 differentially regulates mitochondrial ATP synthesis coupled electron transport and glucose metabolism

We have shown that the exponentially growing  $\Delta cbf11$  cells in complex medium fail to maintain cellular respiration. Therefore, we have explored whether the genes encoding proteins required for electron transport chain mediated respiration are downregulated accordingly. In addition, the electron transport chain is a major ATP source and to maintain the energetic balance in the cell, other means of ATP production such as glycolysis need to be

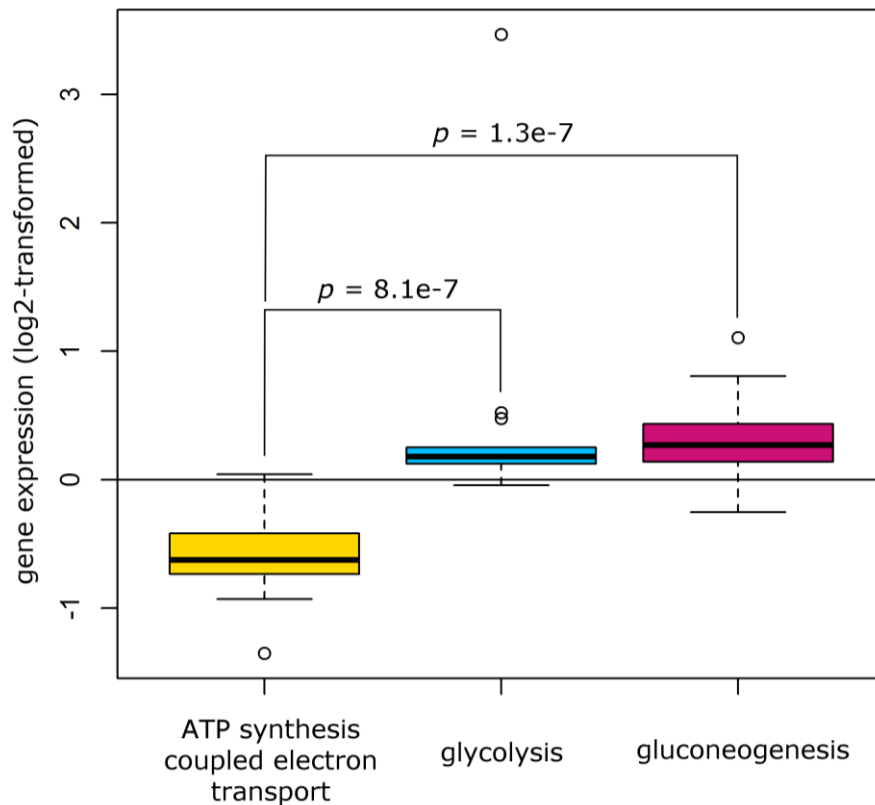


**Figure 4.12 Mitochondrial ATP synthesis coupled electron transport and glucose metabolism are differentially regulated by Cbf11.** Boxplot representation of expression ratios of ATP synthesis coupled electron transport genes (GO: 0042775, n = 22, yellow), glycolysis genes (GO: 0061621, n =14, blue) and gluconeogenesis genes (GO: 0006094, n = 18, purple) in  $\Delta cbf11$  strain compared to the WT strain. The log2 of average values of four independent experiments was used for analysis. The statistical significance was determined using the one-tailed Mann-Whitney *U* test and shows that respiratory genes are differentially regulated compared to either glycolysis or gluconeogenesis genes in the *cbf11* knock-out.

induced. To test this hypothesis, we have analyzed the expression level of genes belonging to three GO annotations (Wood *et al.*, 2012) – mitochondrial ATP synthesis coupled electron transport, canonical glycolysis and gluconeogenesis, in the  $\Delta cbf11$  cells. As shown in Figure 4.12 (page 58), ATP synthesis coupled electron transport genes are repressed ( $p = 3.3e-5$ , calculated with one tailed Mann-Whitney  $U$  test) while the glycolytic and gluconeogenic genes are induced ( $p=0.001$  and  $p = 0.0006$ , respectively, calculated with one tailed Mann-Whitney  $U$  test). It may seem contradictory, that both glycolysis and gluconeogenesis genes

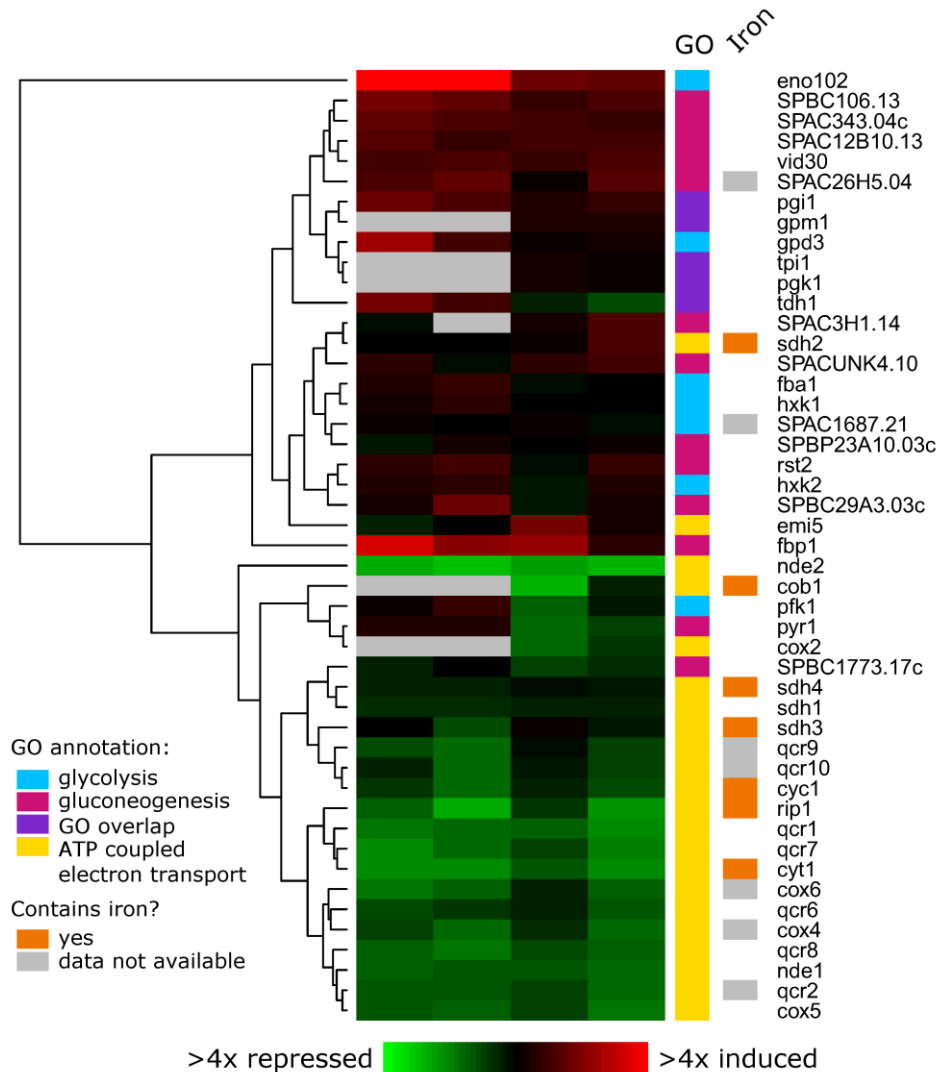


**Figure 4.13 Cbf11 regulates the cell energy metabolism.** Heatmap of expression profiles of genes with GO annotation: mitochondrial ATP synthesis coupled electron transport, glycolysis and gluconeogenesis in the  $\Delta cbf11$  strain. The four columns represent independent biological repeats. The mRNA levels in  $\Delta cbf11$  strain relative to the levels in WT strain are color-coded as indicated at bottom, with missing data in gray. The GO annotations are color-coded as in Figure 4.12 and as indicated at the bottom left, violet denotes genes common for GO annotations glycolysis and gluconeogenesis. Occurrence of iron metal in proteins encoded by the depicted transcripts is shown in orange, with missing data in gray.

are upregulated because these two processes have opposing function, however, these pathways share common enzymes and their function is modulated mostly at the post-translational level. As a result, transcriptome analysis does not answer whether glycolysis or gluconeogenesis is taking place. To gain more insight into the differential regulation of respiratory and glucose metabolism genes, hierarchical clustering of genes based on their expression profiles was performed. Two major clusters formed, clearly distinguishing the expression pattern of glucose metabolism genes and ATP synthesis coupled electron transport genes (Figure 4.13, page 59).

The gene *eno102* is induced on average 11-fold in the  $\Delta cbf11$  cells and belongs to top 10 overexpressed genes in the *cbf11* knock-out transcriptome (Převorovský, Tvarůžková *et al.*, manuscript submitted for publication). It encodes a putative enolase, magnesium ion-containing enzyme catalyzing the reversible dehydration of 2-phospho-D-glycerate to phosphoenolpyruvate (Nelson *et al.*, 2008). Even though the *eno102* gene does not possess gluconeogenesis GO annotation, the encoded protein should function in both glycolysis and gluconeogenesis if the predicted enolase enzymatic activity is correct. The expression level of its paralog, *eno101*, was not measured using this microarray.

Fructose-1,6-bisphosphatase, encoded by *fbp1*, is a strictly gluconeogenic enzyme which catalyzes the hydrolysis of C-1 phosphate on fructose-1,6-bisphosphate and thus yields fructose-6-phosphate (Nelson *et al.*, 2008). The *fbp1* transcription is induced on average 2.2-fold in the *cbf11* knock-out (Převorovský, Tvarůžková *et al.*, manuscript submitted for publication). Remarkably, it is known to be antagonistically regulated by Sty1 and Pka1 pathways (Neely and Hoffman, 2000), which were both shown to genetically interact with *cbf11*. Whether the transcriptional induction of *eno102* and *fbp1* in  $\Delta cbf11$  has any physiological effect such as activation of glycolysis or gluconeogenesis remains elusive and will be discussed in the following chapter.

The most repressed gene with mitochondrial ATP synthesis coupled electron transport GO annotation, *nde2*, encodes a putative NADH:ubiquinone oxidoreductase. The *nde2* mRNA is on average downregulated 2.6-fold and belongs to top 10 downregulated mRNAs in the  $\Delta cbf11$  transcriptome (Převorovský, Tvarůžková *et al.*, manuscript submitted for publication). In most prokaryotic and eukaryotic organisms this enzyme is a part of a large polypeptide assembly, called complex I of the electron transport chain (ETC), however, the yeasts *Schizosaccharomyces pombe* and *Saccharomyces cerevisiae* have lost most complex I subunits during evolution (Gabaldón *et al.*, 2005) and therefore only form complexes II-V of the electron transport chain. Genes *nde2* and its paralog *nde1*, whose expression is also repressed

in the *cbf11* knock-out (1.6x), are homologous to *S. cerevisiae* *NDI1* and *NDI2*. The internal (Ndi1p) and external (Ndi2p) NADH dehydrogenases in the budding yeast have been described to channel electrons from NADH to the respiratory chain (Joseph-Horne *et al.*, 2001).

Iron in the form of iron-sulfur clusters or heme is a common constituent of electron transport chain proteins and it is critical for proper respiration. As you can see in Figure 4.13 (page 59), genes belonging to ATP synthesis coupled electron transport GO annotation are enriched for genes encoding iron-containing proteins compared to glucose metabolism genes. The transcript levels of six out of seven iron-containing proteins that appear in the three analyzed GOs are downregulated. An example of such gene is *cyt1*, which encodes putative heme-containing cytochrome c1, and it is 1.9-fold downregulated in cells lacking *cbf11* (Převorovský, Tvarůžková *et al.*, manuscript submitted for publication).

## 5 Discussion

The opinion that ROS and oxidative stress are merely an undesired consequence of aerobic growth leading to cell damage has changed within the last 15 years (Magalhaes and Church, 2006). Intracellular ROS have been proposed to function as a universal stress signal seeing that numerous pathways and well known regulators of key cellular processes have been described to be modulated by the cellular redox state (Finkel and Holbrook, 2000). Cells deliberately produce ROS to locally induce necessary signaling cascades to regulate stress adaptation, differentiation, proliferation or stem cell biology (Magalhaes and Church, 2006; Holmström and Finkel, 2014).

There is evidence, that NADPH-oxidase-derived ROS and mitochondrial ROS play an important role in modulating the Notch signaling. ROS promote Notch activity and upregulation of the CSL-target genes of the HES/HEY protein family during proliferation and cell fate regulation of colon progenitor cells as well as during keratinocyte differentiation. The mechanism of ROS-mediated activation of the Notch pathway has not been unraveled but redox regulation of several of its components seems plausible (Coant *et al.*, 2010; Hamanaka and Glasauer, 2013). The potential role of CSL transcription factors in redox signaling may be studied in the fission yeast, which lacks most components of the Notch pathway except for two CSL paralogs, Cbf11 and Cbf12, without the confounding effects of the upstream regulator Notch (Převorovský *et al.*, 2007; Gazave *et al.*, 2009).

### 5.1 Cbf11 acts as a negative regulator of oxidative stress response

One of the early cues for investigating the role of CSL proteins during oxidative stress came from a transcriptomic analysis of *S. pombe* cells exposed to a variety of noxious conditions, which revealed that mRNA levels of *cbf12* changes upon stress (Chen *et al.*, 2003). However, we have later contradicted these results using RT-qPCR, a more targeted and sensitive approach compared to microarrays employed in the genome-wide analysis, which showed that neither *cbf11* nor *cbf12* transcript levels are affected by hydrogen peroxide treatment (Petr Daněk, personal communication). Nevertheless, cells lacking *cbf11* are resistant to H<sub>2</sub>O<sub>2</sub> and not to menadione, a source of superoxide (Chapter 4.1.1, Figure 4.1, page 43). This finding led us to propose that Cbf11 is involved in oxidative stress response, possibly as a transcriptional regulator since the CSL proteins are evolutionarily conserved transcription factors and Cbf11 has been shown to activate transcription (Oravcová *et al.*, 2013). An alternative hypothesis is that the deletion of *cbf11* blocks entry of H<sub>2</sub>O<sub>2</sub> into the cell. Hydrogen peroxide is a small uncharged molecule with a dipole moment similar to that of water and so it is expected to partially diffuse through the lipid bilayer. The similarity of H<sub>2</sub>O<sub>2</sub>

with water points to aquaporins as channels for not only water but also H<sub>2</sub>O<sub>2</sub> (Bienert *et al.*, 2007) and their expression may be modified in the *cbf11* knock-out. In addition, diffusibility of H<sub>2</sub>O<sub>2</sub> through the membrane may be affected by its composition and several lipid metabolism genes are downregulated in the  $\Delta cbf11$  mutant (Převorovský, Tvarůžková *et al.*, manuscript submitted for publication). Despite the theoretical plausibility of the proposed hypothesis our follow-up experiments showed that the resistance of cells lacking *cbf11* is dependent on the SAPK pathway and several antioxidant enzymes and thus the alternative hypothesis was rejected.

In agreement with resistance to H<sub>2</sub>O<sub>2</sub>, the transcriptome of exponentially growing  $\Delta cbf11$  cells contains upregulated genes encoding antioxidants such as catalase (*ctt1*, ~6-fold), sulfiredoxin (*srx1*, ~8-fold) or glutathione S-transferases (*gst2*, ~10-fold; *gst1*, ~2-fold; *gst3*, ~2-fold) (Převorovský, Tvarůžková *et al.*, manuscript submitted for publication; Petr Daněk, personal communication). The resistance of *cbf11* knock-out originates indeed from upregulation of catalase and sulfiredoxin since the double mutants  $\Delta cbf11 \Delta ctt1$  and  $\Delta cbf11 \Delta srx1$  are very sensitive to hydrogen peroxide (Chapter 4.3.2, Figure 4.10, page 56). Whether *ctt1* and *srx1* are the only antioxidants responsible for resistance of  $\Delta cbf11$  remains to be tested by constructing the triple mutant  $\Delta cbf11 \Delta ctt1 \Delta srx1$ . Other investigated genes encoding antioxidants induced in the *cbf11* knock-out, *gpx1* and *gst2* were found not to play a role in the resistance of  $\Delta cbf11$  to hydrogen peroxide (Chapter 4.3.2, Figure 4.11, page 57). Therefore, Cbf11 acts as a negative regulator of oxidative stress response. The mechanism is not understood, but Cbf11 probably does not regulate expression of antioxidant genes directly because it was not detected to bind promoters of these genes using the ChIP-qPCR method (Petr Daněk, personal communication).

The antagonistic properties of Cbf11 and Cbf12 in the regulation of cell adhesion, coordination of cell and nuclear division (Převorovský *et al.*, 2008) as well as affecting expression of numerous transcripts in an antagonistic manner (Převorovský, Tvarůžková *et al.*, manuscript submitted for publication) suggest that upon depletion of *cbf11*, *cbf12* may accumulate and evoke upregulation of antioxidant genes. Surprisingly, the deletion of *cbf12* does not affect the sensitivity of WT or  $\Delta cbf11$  towards H<sub>2</sub>O<sub>2</sub> (Chapter 4.1.1, Figure 4.1A, page 43). Consequently, the observed resistance of  $\Delta cbf11$  cannot be explained by accumulation of *cbf12*.

Cells lacking *cbf11* are not resistant to menadione, as mentioned earlier. Menadione is a synthetic compound with systematic name 2-methyl-1,4-naphtoquinone that is believed to exert its cytotoxicity through ETC-mediated formation of superoxide anion radicals (Castro *et*

*al.*, 2008). In the fission yeast menadione is known to induce weak transcriptional response reminiscent of mild hydrogen peroxide treatment, but unlike intermediate hydrogen peroxide or TBH treatment (Chen *et al.*, 2008). Therefore, it is not surprising that cells lacking *cbf11*, though they have upregulated several antioxidant enzymes, are not resistant to menadione. Accordingly, the mRNA level of superoxide dismutase, encoded by *sod1* and *sod2* (SPAC1486.01), is not altered in the *cbf11* knock-out (Převorovský, Tvarůžková *et al.*, manuscript submitted for publication). A study in the budding yeast revealed that menadione is activated in the cell by conjugation with glutathione and when glutathione is depleted, the sensitivity of the cells to menadione is decreased (Zadzinski *et al.*, 1998). We have found that a gene encoding glutathione S-transferase is highly upregulated (~10-fold based on microarray analysis, 46-fold based on RT-qPCR) in the *cbf11* knock-out (Převorovský, Tvarůžková *et al.*, manuscript submitted for publication; Petr Daněk, personal communication). Large amounts of glutathione S-transferase in the  $\Delta cbf11$  strain may lead to high concentration of activated menadione and thus severe oxidative stress unlike in WT cells. Even though the  $\Delta cbf11$  cells have induced stress response, it may not be sufficient to counteract the severe oxidative stress in this mutant and the cells are thus neither resistant nor sensitive to this drug compared to WT cells.

## 5.2 The regulatory network of CSL mutants during oxidative stress

Mitogen-activated protein kinase Sty1 is indispensable for cell survival during multiple environmental stresses. Indeed, cells lacking *sty1* are very sensitive to H<sub>2</sub>O<sub>2</sub> (Millar *et al.*, 1995; Degols *et al.*, 1996). The H<sub>2</sub>O<sub>2</sub> sensitivity test of  $\Delta cbf11 \Delta sty1$  showed that Sty1 MAPK is essential for the resistance of  $\Delta cbf11$  cells since the sensitivity of the double mutant is indistinguishable from that of  $\Delta sty1$  (Chapter 4.2.2, Figure 4.6, page 51). Strikingly, transcription factor Atf1, the main target of Sty1 during oxidative stress response, is dispensable for maintaining resistance of the *cbf11* knock-out under intermediate stress (0.5 mM H<sub>2</sub>O<sub>2</sub>). These results indicate that Sty1 mediates expression of genes required for survival under intermediate H<sub>2</sub>O<sub>2</sub> stress via other transcription factors, such as Pap1, Hsr1 or Pcr1. Nonetheless, Atf1 is required for  $\Delta cbf11$  resistance to higher H<sub>2</sub>O<sub>2</sub> dose (Chapter 4.2.2, Figure 4.6B, page 51). The recruitment of alternative transcription factors in  $\Delta cbf11 \Delta atf1$  strain is likely for that reason concentration-dependent.

The transcription factor Pap1 is thought to regulate gene expression with the help of Prr1 mostly in response to mild oxidative stress when the SAPK is not activated (Quinn *et al.*, 2002; Chen *et al.*, 2008). The higher importance of Pap1 compared to Prr1 in gene expression regulation is reflected in their respective sensitivities to peroxide, the former being more

sensitive than the latter (Chapter 4.2.2, Figure 4.7, page 52). Deletion of *pap1* or *prp1* in  $\Delta cbf11$  background leads to reduction of the observed resistance of the *cbf11* knock-out strain. The genetic interaction between *cbf11* and *prp1* is questionable, though. One might argue that the effect of  $\Delta cbf11$  resistance and  $\Delta prp1$  sensitivity is additive in the double knock-out pointing to the conclusion that Prr1 and Cbf11 affect the sensitivity to ROS independently of each other. Nevertheless, spot tests are not a very sensitive method for precise quantitative evaluation of fitness and from a visual assessment of growth of the double knock-out  $\Delta cbf11 \Delta prp1$  on agar plates containing a range of H<sub>2</sub>O<sub>2</sub> concentrations (data not shown) we concluded that there is a genetic interaction between *cbf11* and *prp1*. We thus believe that the Pap1/Prr1 heterodimer is important for the resistance of  $\Delta cbf11$  strain to H<sub>2</sub>O<sub>2</sub>. Even though deletion of *cbf12* was not detected to affect sensitivity of WT cells and most oxidative stress mutants, it marginally suppresses the sensitivity of  $\Delta pap1$  (Chapter 4.2.2, Figure 4.7A, page 52). Interestingly, cells lacking *cbf12* are mildly resistant to acute dose of H<sub>2</sub>O<sub>2</sub> compared to WT cells (Martin Přeborovský, personal communication). Therefore, it is tempting to speculate that both CSL paralogs in *S. pombe* are involved in oxidative stress response. Moreover, we have indications that Pap1 physically interacts with Cbf12, and Prr1 with both CSL paralogs in *S. pombe* (Pancaldi *et al.*, 2012; Martin Přeborovský, personal communication).

The role of nutrient sensing pathways in oxidative stress response is not well established in the fission yeast. The cAMP-dependent protein kinase Pka1 is thought to function as a negative regulator of oxidative stress response indirectly affecting Sty1 activation by regulating mitochondrial ROS production depending on nutrient conditions (Zuin *et al.*, 2010a). Cells lacking *pka1* or *cbf11* are resistant to H<sub>2</sub>O<sub>2</sub> and the resistance of the double knockout  $\Delta cbf11 \Delta pka1$  does not differ from that of either parent strain (Chapter 4.2.3, Figure 4.8, page 53). This observation suggests that the mechanisms how  $\Delta cbf11$  and  $\Delta pka1$  strains establish their resistance to peroxide are not completely independent, i.e. there is a genetic interaction. Depletion of Pka1 genetically or by glucose starvation leads to phosphorylation of Sty1 MAPK and upregulation of Sty1-dependent genes. The mechanism is not yet clear, but cells with depleted Pka1 have increased respiration rates and ROS levels compared to WT cells growing in complex media, which are thought to activate the SAPK pathway (Zuin *et al.*, 2010a). Contrary to the increased respiration of the  $\Delta pka1$  strain, cells lacking *cbf11* have diminished electron transport chain activity (Chapter 4.1.2, Figure 4.2, page 44). Nonetheless, there is no clear correlation between the rate of respiration and ROS production (Nickel *et al.*, 2014), thus *pka1* and *cbf11* knock-outs may promote Sty1-dependent expression of stress response genes via increased ROS production. Alternatively, depletion of Pka1 or Cbf11

mediates cellular resistance to hydrogen peroxide through a different Sty1-dependent mechanism. Measurements of ROS levels and Sty1 phosphorylation in the  $\Delta cbf11$  strain in cooperation with Petr Daněk are underway to elucidate the molecular mechanism of Sty1-dependent antioxidant activation in the *cbf11* knock-out.

The role of Sck1 and Sck2 kinases, homologs of mammalian AKT and budding yeast Sch9, in oxidative stress response is quite vague. Both kinases negatively regulate cell longevity, though independently of each other and Pka1 (Roux *et al.*, 2006; Chen and Runge, 2009). Sck1 has only a minor role in affecting cellular lifespan and the mechanism is not understood, while depletion of *sck2* leads to considerable Sty1-dependent lifespan extension (Zuin *et al.*, 2010a). The transcript levels of *sck1* and *sck2* are differentially regulated during H<sub>2</sub>O<sub>2</sub> stress, the former being mildly upregulated while the latter downregulated (Chen *et al.*, 2003, 2008). Although, *sck1* and *sck2* knock-outs tend to mimic  $\Delta pka1$  phenotypes (Jin *et al.*, 1995; Fujita and Yamamoto, 1998), it is not the case during oxidative stress. Cells lacking *sck1* and *sck2* are mildly sensitive and not sensitive to hydrogen peroxide, respectively, compared to the WT strain (Chapter 4.2.3, Figure 4.8, page 53). Moreover, deletion of *sck1* or *sck2* does not affect the resistance of  $\Delta cbf11$  strain. The positive genetic interaction between *sck1* and *cbf11* implicates that they may act antagonistically upon a common regulator of oxidative stress response. The sensitivity of  $\Delta sck1$  to H<sub>2</sub>O<sub>2</sub> is relieved to the WT/ $\Delta cbf12$  level also by deletion of *cbf12* (Chapter 4.2.3, Figure 4.8, page 53). It is rather curious that deletion of *cbf12* was observed to suppress sensitivity of only two mutants,  $\Delta pap1$  and  $\Delta sck1$ , out of nine tested. A possible explanation for this phenomenon is that the contribution of Cbf12 to oxidative stress response is so subtle that it is under the detection limit using the spot tests. Consequently, it seems that Cbf12 plays a role either in affecting the level/activity of Cbf11 or sensitivity to H<sub>2</sub>O<sub>2</sub> is decreased in  $\Delta cbf12$   $\Delta pap1$  and  $\Delta cbf12$   $\Delta sck1$  mutants independently of Cbf11. We have indications, that the *cbf12* mRNA level is altered in  $\Delta cbf11$  strain (Petr Daněk, personal communication) and that the level and isoform of Cbf12 is affected by deletion of *cbf11* when expressed as TAP-fusion from its endogenous locus (data not shown) Unfortunately, the fusion proteins may not be expressed at physiological levels since we know that *cbf12* mRNA stability is negatively regulated by RNA-binding protein Zfs1 which binds to the region of mRNA that is disrupted by the TAP-fusion (Wells *et al.*, 2012). It is likely that the relationship between Cbf11 and Cbf12 is mutual in regulating their respective levels but has not been thoroughly studied yet. Whether Cbf12 affects function of Cbf11 during oxidative stress remains to be tested by preparing triple knock-out of *cbf11*, *cbf12* and *pap1* or *sck1*.

### 5.3 The mitochondrial defect of $\Delta cbf11$ cells depends on the nutrients

Mitochondrial dysfunction and oxidative stress are associated with a similar set of diseases and aging, and many kinases known to play role in oxidative stress response have been detected in mitochondria, including SAPK, PKA or AKT (Di *et al.*, 2012; Boland *et al.*, 2013; Pulliam *et al.*, 2013). The CSL proteins have a nuclear localization when visualized as chromosomally or plasmid-encoded GFP fusions (Převorovský *et al.*, 2009). However, during our pilot study of Cbf11 interacting proteins several mitochondrial proteins were pulled down (Martin Převorovský, personal communication), which suggests that a fraction of Cbf11 protein may possibly reside in mitochondria and, similarly to Sty1 (Di *et al.*, 2012), can shuttle between mitochondria and nucleus.

Unlike *Saccharomyces cerevisiae* and other yeasts, *Schizosaccharomyces pombe* is considered “petite-negative” yeast (Heslot *et al.*, 1970b). The cytoplasmic petite mutants, also called vegetative petites, have lost their mitochondrial DNA and are thus unable to grow on nonfermentable carbon sources. Yeast species in which cytoplasmic petite mutants were difficult to isolate were termed “petite-negative”. The typical characteristics of “petite negative” yeasts are the absence of anaerobic growth and glucose-mediated repression of respiration, however, *S. pombe* is capable of growing anaerobically for several generations and regulate respiration activity based on the carbon source (Heslot *et al.*, 1970a). We have shown that cells lacking *cbf11* have negligible respiration rate and anomalous mitochondrial morphology during exponential growth in complex medium (Chapter 4.1.2, Figure 4.2, page 44). Remarkably, our preliminary results on mammalian cells indicated that the role of CSL in the regulation of cellular respiration is evolutionary conserved (Ondřej Tolde, personal communication).

Regulation of respiratory function has a profound effect on chromatin structure through controlling availability of acetyl-CoA and thus histone acetylation (Friis *et al.*, 2014). Our results show that the  $\Delta cbf11$  strain does not only have severely decreased respiration level but its heterochromatin seems perturbed (Martin Převorovský, personal communication). Interestingly, both respiration and histone deacetylases are regulated by the NAD<sup>+</sup>/NADH ratio. Since the pools of cytosolic and mitochondrial reducing equivalents (NADH and NADPH) are equilibrated by the malate-aspartate shuttle and several enzymatic reactions, the depletion of NADPH during oxidative stress as a result of protein repair will likely lead to a decrease in the mitochondrial stock of NADH, which in turn downregulates respiration, and the increase in NAD<sup>+</sup> boosts the activity of histone deacetylases. Nonetheless, experiments need to be performed to determine whether cells lacking *cbf11* display increased NADPH-

dependent thioredoxin reductase activity or disrupted NAD(P)<sup>+</sup>/NADH ratio and histone acetylation.

The respiratory defect of  $\Delta cbf11$  strain is modulated by nutrients and largely dependent on the PKA and SAPK pathways. During calorie restriction, i.e. depletion of fermentable carbon source, which normally occurs in early stationary phase, the activity of respiratory enzymes and oxygen consumption are increased (Poole and Lloyd, 1973). *S. pombe* cells grown in complex medium with glycerol instead of glucose as a carbon source have also increased oxygen consumption (Zuin *et al.*, 2008 and Chapter 4.1.3, Figure 4.3, page 45). Moreover, the *cbf11* knock-out is able to respire, even though less than WT cells, when forced to do so by the absence of glucose. This observation and the rescue of  $\Delta cbf11$  respiratory defect by disruption of the PKA or SAPK pathways (data not shown) point to the conclusion, that mitochondria in the *cbf11* knock-out are not permanently damaged but their function is downregulated based on the cellular nutrient and stress level. Mitochondrial morphology is very dynamic and fluctuates based on the cell cycle, nutrients and stress. Drugs known to inhibit protein synthesis, such as mTOR inhibitors cause dramatic changes to the mitochondria (Boland *et al.*, 2013). A possible explanation for the nutrient-dependent respiration defect of  $\Delta cbf11$  is that nutrient-sensing pathways such as PKA and TORC1 are deregulated in this mutant, which is supported by the fact that Cbf11 genetically interacts with Pka1 and Sck1.

#### **5.4 The consequences of stress response activation in $\Delta cbf11$ cells**

Deletion of *cbf11* leads to compromised growth accompanied by defects in nuclear integrity and septum formation when grown in complex medium (Převorovský *et al.*, 2009). We have recently discovered that deletion of *sty1* suppresses the growth defects of the *cbf11* knock-out (Převorovský, Tvarůžková *et al.*, manuscript submitted for publication), but can the hyperactivation of Sty1 stand behind the defects of  $\Delta cbf11$  strain?

Chronic activation of the stress-response Sty1 pathway is lethal (Millar *et al.*, 1995; Shieh *et al.*, 1997). Since Sty1 kinase regulates not only stress response but also meiosis and cell cycle progression (Shiozaki and Russell, 1995, 1996), it is not straight-forward which process deregulation is incompatible with cell survival. The lethality of Sty1 hyperactivation is partially suppressed by deletion of one its targets, kinase *Srk1*, which functions as an inhibitor of Cdc25 phosphatase and thus blocks entry into mitosis (Smith *et al.*, 2002; López-Avilés *et al.*, 2005). Intriguingly, CSL proteins antagonistically regulate expression of 81 periodically expressed genes, including *srk1*, which is 2.4-fold upregulated in  $\Delta cbf11$  cells

and 1.9-fold in *cbf12* overexpressing cells, and its promoter is bound by Cbf12 (Převorovský, Tvarůžková *et al.*, manuscript submitted for publication).

Furthermore, it was proposed that constitutive activation of catalase, whose expression is under the control of Sty1/Atf1 and Pap1 regulators, induces iron starvation response through sequestering available iron for its heme group. During iron starvation transcription of many genes encoding iron-containing proteins is repressed, leading to compromised growth (Labbé *et al.*, 2007). It has to be noted, however, that the authors of this study did not include any evidence supporting the role of catalase overexpression in inducing iron starvation response (Paulo *et al.*, 2014). Despite the vagueness of this report, we have observed that the gene encoding catalase, *ctt1*, and iron starvation response genes, such as *shu1*, *fip1* and *frp1*, are upregulated in exponentially growing  $\Delta cbf11$  cells (Převorovský, Tvarůžková *et al.*, manuscript submitted for publication; Petr Daněk, personal communication). Shu1 is involved in heme assimilation (Mourer *et al.*, 2015) and its transcript is the second most overexpressed gene (22-fold) in *cbf11* knock-out transcriptome (Převorovský, Tvarůžková *et al.*, manuscript submitted for publication). On the other hand, genes required for ATP synthesis coupled electron transport are downregulated in the *cbf11* knock-out (Chapter 4.3.3, Figure 4.12, page 58). Most notably many proteins encoded by respiratory genes contain iron (Chapter 4.3.3, Figure 4.13, page 59) and are also downregulated during iron starvation response (Labbé *et al.*, 2007). Clearly, cells lacking *cbf11* mimic iron starvation response but it remains to be answered whether this mutant is truly starved for iron by sequestering it into catalase or Cbf11 participates in regulating iron metabolism.

The energetic metabolism is disrupted in the  $\Delta cbf11$  strain. As mentioned earlier, the respiratory genes are downregulated while the glycolytic and gluconeogenic genes are upregulated in this mutant. Chronically activated stress response, as judged by upregulation of antioxidant genes in the *cbf11* knock-out without exogenous ROS source, is energetically demanding. Therefore, with the respiration defect in the  $\Delta cbf11$  strain, the cells must induce other energy-producing pathways such as glycolysis or  $\beta$ -oxidation of fatty acids. Glycolysis is usually blocked during oxidative stress by glyceraldehyde 3-phosphate dehydrogenase Tdh1 oxidation (Grant *et al.*, 1999), thus fatty acid catabolism seems as a more likely means of energy production in  $\Delta cbf11$  strain. This hypothesis is supported by our preliminary results, that the lipid content is indeed decreased in cells lacking *cbf11* compared to WT cells (Róbert Zach, personal communication).

## 6 Conclusions

The presented thesis addressed oxidative stress-related properties of the CSL mutants including sensitivity to several ROS sources and level of cell respiration; and identification of proteins upstream and downstream of CSL during oxidative stress response.

The results acquired during this study are summarized below:

- It was shown that cells lacking *cbf11* are resistant to hydrogen peroxide, but not to menadione whereas the  $\Delta cbf12$  mutant does not show differential sensitivity compared to WT cells upon ROS treatment.
- Measurement of oxygen consumption of CSL mutants revealed, that the  $\Delta cbf11$  mutant has almost undetectable respiration in complex media but this defect is suppressed when cells are grown on nonfermentable carbon source.
- Microscopic analysis of the *cbf11* knock-out unveiled that the mitochondrial morphology is altered in this mutant.
- Twenty-two double knock-outs and deletion mutant of *ctt1* were prepared to analyze genetic interactions of CSL with oxidative stress response genes.
- Sty1 mitogen-activated kinase and Pap1 transcription factor were found to be the key regulators conferring resistance to hydrogen peroxide to the  $\Delta cbf11$  strain.
- Pka1 and Cbf11 were observed to act as negative regulators of oxidative stress response with non-additive effects on the cellular resistance to hydrogen peroxide.
- Sulfiredoxin and catalase were determined to be crucial for the resistance of the *cbf11* knock-out to hydrogen peroxide.
- The energetic metabolism is likely disrupted in cells lacking *cbf11* by transcriptional downregulation of respiration and upregulation of glycolysis and gluconeogenesis.

## 7 References

- Anastasiou, D. *et al.* (2011). Inhibition of pyruvate kinase M2 by reactive oxygen species contributes to cellular antioxidant responses. *Science* (80-. ). *334*, 1278–1283.
- Aravind, L., Watanabe, H., Lipman, D. J., and Koonin, E. V (2000). Lineage-specific loss and divergence of functionally linked genes in eukaryotes. *Proc. Natl. Acad. Sci. U. S. A.* *97*, 11319–11324.
- Aroor, A. R., and DeMarco, V. G. (2014). Oxidative stress and obesity: The chicken or the egg? *Diabetes* *63*, 2216–2218.
- Ayer, A., Tan, S.-X., Grant, C. M., Meyer, A. J., Dawes, I. W., and Perrone, G. G. (2010). The critical role of glutathione in maintenance of the mitochondrial genome. *Free Radic. Biol. Med.* *49*, 1956–1968.
- Balaban, R. S., Nemoto, S., and Finkel, T. (2005). Mitochondria, oxidants and aging. *Cell* *120*, 483–495.
- Barba, G., Soto, T., Madrid, M., Núñez, A., Vicente, J., Gacto, M., and Cansado, J. (2008). Activation of the cell integrity pathway is channelled through diverse signalling elements in fission yeast. *Cell. Signal.* *20*, 748–757.
- Bedard, K., and Krause, K.-H. (2007). The NOX family of ROS-generating NADPH oxidases: physiology and pathophysiology. *Physiol. Rev.* *87*, 245–313.
- Bienert, G. P., Møller, a. L. B., Kristiansen, K. a., Schulz, A., Møller, I. M., Schjoerring, J. K., and Jahn, T. P. (2007). Specific aquaporins facilitate the diffusion of hydrogen peroxide across membranes. *J. Biol. Chem.* *282*, 1183–1192.
- Birnboim, H., and Doly, J. (1979). A rapid alkaline extraction procedure for screening recombinant plasmid DNA. *Nucleic Acids Res.* *7*, 1513–1523.
- Boland, M. L., Chourasia, A. H., and Macleod, K. F. (2013). Mitochondrial dysfunction in cancer. *Front. Oncol.* *3*, 1–28.
- Boldogh, I. R., and Pon, L. A. (2006). Interactions of mitochondria with the actin cytoskeleton. *Biochim. Biophys. Acta - Mol. Cell Res.* *1763*, 450–462.
- Boronat, S. *et al.* (2014). Thiol-based H<sub>2</sub>O<sub>2</sub> signalling in microbial systems. *Redox Biol.* *2*, 395–399.
- Bozonet, S. M., Findlay, V. J., Day, A. M., Cameron, J., Veal, E. A., and Morgan, B. A. (2005). Oxidation of a eukaryotic 2-Cys peroxiredoxin is a molecular switch controlling the transcriptional response to increasing levels of hydrogen peroxide. *J. Biol. Chem.* *280*, 23319–23327.
- Brown, J. D., Day, A. M., Taylor, S. R., Tomalin, L. E., Morgan, B. A., and Veal, E. A. (2013). A peroxiredoxin promotes H<sub>2</sub>O<sub>2</sub> signaling and oxidative stress persistence by oxidizing a thioredoxin family protein. *Cell Rep.*, 1–11.

- Buck, V., Quinn, J., Pino, T. S., Martin, H., Saldanha, J., Makino, K., Morgan, B. A., and Millar, J. B. A. (2001). Peroxide sensors for the fission yeast stress-activated mitogen-activated protein kinase pathway. *Mol. Biol. Cell* *12*, 407–419.
- Byrne, S. M., and Hoffman, C. S. (1993). Six *git* genes encode a glucose-induced adenylate cyclase activation pathway in the fission yeast *Schizosaccharomyces pombe*. *J. Cell Sci.* *105*, 1095–1100.
- Calvo, I. a, Ayté, J., and Hidalgo, E. (2013a). Reversible thiol oxidation in the H<sub>2</sub>O<sub>2</sub> -dependent activation of the transcription factor Pap1. *J. Cell Sci.* *126*, 2279–2284.
- Calvo, I. A. *et al.* (2009). Genome-wide screen of genes required for caffeine tolerance in fission yeast. *PLoS One* *4*.
- Calvo, I. A., Boronat, S., Domenech, A., García-Santamarina, S., Ayté, J., and Hidalgo, E. (2013b). Dissection of a redox relay: H<sub>2</sub>O<sub>2</sub>-dependent activation of the transcription factor Pap1 through the peroxidatic Tpx1-thioredoxin cycle. *Cell Rep.* *1*, 1413–1424.
- Calvo, I. A., García, P., Ayté, J., and Hidalgo, E. (2012). The transcription factors Pap1 and Prr1 collaborate to activate antioxidant, but not drug tolerance, genes in response to H<sub>2</sub>O<sub>2</sub>. *Nucleic Acids Res.* *40*, 4816–4824.
- Castro, F. a V, Mariani, D., Panek, A. D., Eleutherio, E. C. a, and Pereira, M. D. (2008). Cytotoxicity mechanism of two naphthoquinones (menadione and plumbagin) in *Saccharomyces cerevisiae*. *PLoS One* *3*.
- Coant, N. *et al.* (2010). NADPH oxidase 1 modulates WNT and NOTCH1 signaling to control the fate of proliferative progenitor cells in the colon. *Mol. Cell. Biol.* *30*, 2636–2650.
- Coluzzi, E., Colamartino, M., Cozzi, R., Leone, S., Meneghini, C., O’Callaghan, N., and Sgura, A. (2014). Oxidative stress induces persistent telomeric DNA damage responsible for nuclear morphology change in mammalian cells. *PLoS One* *9*, e110963.
- Costa, A., Scholer-Dahirel, A., and Mechta-Grigoriou, F. (2014). The role of reactive oxygen species and metabolism on cancer cells and their microenvironment. *Semin. Cancer Biol.*, 1–10.
- Day, A. M., Brown, J. D., Taylor, S. R., Rand, J. D., Morgan, B. A., and Veal, E. A. (2012). Inactivation of a peroxiredoxin by hydrogen peroxide is critical for thioredoxin-mediated repair of oxidized proteins and cell survival. *Mol. Cell* *45*, 398–408.
- Day, A. M., and Veal, E. A. (2010). Hydrogen peroxide-sensitive cysteines in the Sty1 MAPK regulate the transcriptional response to oxidative stress. *J. Biol. Chem.*
- Degols, G., and Russell, P. (1997). Discrete roles of the Spc1 kinase and the Atf1 transcription factor in the UV response of *Schizosaccharomyces pombe*. *Mol. Cell. Biol.* *17*.
- Degols, G., Shiozaki, K., and Russell, P. (1996). Activation and regulation of the Spc1 stress-activated protein kinase in *Schizosaccharomyces pombe*. *Mol. Cell. Biol.* *16*, 2870–2877.

- DeVoti, J., Seydoux, G., Beach, D., and McLeod, M. (1991). Interaction between *ran1+* protein kinase and cAMP dependent protein kinase as negative regulators of fission yeast meiosis. *EMBO J.* *10*, 3759–3768.
- Di, Y., Holmes, E. J., Butt, A., Dawson, K., Mironov, A., Kotiadis, V. N., Gourlay, C. W., Jones, N., and Wilkinson, C. R. M. (2012). H<sub>2</sub>O<sub>2</sub> stress-specific regulation of *S. pombe* MAPK Sty1 by mitochondrial protein phosphatase Ptc4. *EMBO J.* *31*, 563–575.
- Dickinson, B. C., and Chang, C. J. (2011). Chemistry and biology of reactive oxygen species in signaling or stress responses. *Nat. Chem. Biol.* *7*.
- Dixon, S. J., Costanzo, M., Baryshnikova, A., Andrews, B., and Boone, C. (2009). Systematic mapping of genetic interaction networks. *Annu. Rev. Genet.* *43*, 601–625.
- Eletto, D., Chevet, E., Argon, Y., and Appenzeller-Herzog, C. (2014). Redox controls UPR to control redox. *J. Cell Sci.* *127*, 3649–3658.
- Eshaghi, M., Lee, J. H., Zhu, L., Poon, S. Y., Li, J., Cho, K.-H., Chu, Z., Karuturi, R. K. M., and Liu, J. (2010). Genomic binding profiling of the fission yeast stress-activated MAPK Sty1 and the bZIP transcriptional activator Atf1 in response to H<sub>2</sub>O<sub>2</sub>. *PLoS One* *5*, e11620.
- Finkel, T. (2011). Signal transduction by reactive oxygen species. *J. Cell Biol.* *194*.
- Finkel, T., and Holbrook, N. J. (2000). Oxidants, oxidative stress and the biology of ageing. *Nature* *408*, 239–247.
- Forman, H. J., Ursini, F., and Maiorino, M. (2014). An overview of mechanisms of redox signaling. *J. Mol. Cell. Cardiol.*
- Friis, R. M. N., Glaves, J., Huan, T., Li, L., Sykes, B. D., and Schultz, M. C. (2014). Rewiring AMPK and mitochondrial retrograde signaling for metabolic control of aging and histone acetylation in respiratory-defective cells. *Cell Rep.* *7*, 565–574.
- Fujita, M., and Yamamoto, M. (1998). *S. pombe sck2+*, a second homologue of *S. cerevisiae SCH9* in fission yeast, encodes a putative protein kinase closely related to PKA in function. *Curr. Genet.* *248*–254.
- Gabaldón, T., Rainey, D., and Huynen, M. a. (2005). Tracing the evolution of a large protein complex in the eukaryotes, NADH:ubiquinone oxidoreductase (Complex I). *J. Mol. Biol.* *348*, 857–870.
- Gaits, F., Degols, G., Shiozaki, K., and Russell, P. (1998). Phosphorylation and association with the transcription factor Atf1 regulate localization of Spc1/Sty1 stress-activated kinase in fission yeast. *Genes Dev.* *12*, 1464–1473.
- Gaits, F., Shiozaki, K., and Russell, P. (1997). Protein phosphatase 2C acts independently of stress-activated kinase cascade to regulate the stress response in fission yeast. *J. Biol. Chem.* *272*, 17873–17879.
- Gazave, E., Lapébie, P., Richards, G. S., Brunet, F., Ereskovsky, A. V., Degnan, B. M., Borchiellini, C., Vervoort, M., and Renard, E. (2009). Origin and evolution of the Notch signalling pathway: an overview from eukaryotic genomes. *BMC Evol. Biol.* *9*, 249.

- Gomez, M. *et al.* (2014). Malfunctioning of the iron-sulfur cluster assembly machinery in *Saccharomyces cerevisiae* produces oxidative stress via an iron-dependent mechanism, causing dysfunction in respiratory complexes. *PLoS One* 9, e111585.
- Grant, C. M., Quinn, K. A., and Dawes, I. W. (1999). Differential protein S-thiolation of glyceraldehyde-3-phosphate dehydrogenase isoenzymes influences sensitivity to oxidative stress. *Mol. Cell. Biol.* 19, 2650–2656.
- Gregan, J., Rabitsch, P. K., Rumpf, C., Novatchkova, M., Schleiffer, A., and Nasmyth, K. (2006). High-throughput knockout screen in fission yeast. *Nat. Protoc.* 1.
- Groitel, B., and Jakob, U. (2014). Thiol-based redox switches. *Biochim. Biophys. Acta.*
- Halliwell, B., and Aruoma, O. I. (1991). DNA damage by oxygen-derived species. *Febs* 281, 9–19.
- Hamanaka, R., and Glasauer, A. (2013). Mitochondrial reactive oxygen species promote epidermal differentiation and hair follicle development. *Sci. Signal.* 6.
- Harman, D. (1956). Aging: a theory based on free radical and radiation chemistry. *J. Gerontol.* 11, 298–300.
- Hayles, J., Wood, V., Jeffery, L., Hoe, K.-L., Kim, D.-U., Park, H.-O., Salas-Pino, S., Heichinger, C., and Nurse, P. (2013). A genome-wide resource of cell cycle and cell shape genes of fission yeast. *Open Biol.* 3, 130053.
- Heckman, D. S., Geiser, D. M., Eidell, B. R., Stauffer, R. L., Kardos, N. L., and Hedges, S. B. (2001). Molecular evidence for the early colonization of land by fungi and plants. *Science* 293, 1129–1133.
- Hentges, P., Driessche, B. Van, Tafforeau, L., Vandenhoute, J., and Carr, A. M. (2005). Three novel antibiotic marker cassettes for gene disruption and marker switching in *Schizosaccharomyces pombe*. *Yeast*, 1013–1019.
- Heslot, H., Goffeau, a., and Louis, C. (1970a). Respiratory Metabolism of a “Petite Negative” Yeast *Schizosaccharomyces pombe* 972h-1. *J. Bacteriol.* 104, 473–481.
- Heslot, H., Goffeau, A., and Louis, C. (1970b). Segregational respiratory-deficient mutants of a “petite-negative” yeast *Schizosaccharomyces pombe* 972h-. *J. Bacteriol.* 104, 473–481.
- Holmström, K. M., and Finkel, T. (2014). Cellular mechanisms and physiological consequences of redox-dependent signalling. *Nat. Rev. Mol. Cell Biol.* 15, 411–421.
- Hori, K., Sen, A., and Artavanis-Tsakonas, S. (2012). Notch signaling at a glance. *J. Cell Sci.*
- Chaudière, J., and Ferrari-Iliou, R. (1999). Intracellular antioxidants: From chemical to biochemical mechanisms. *Food Chem. Toxicol.* 37, 949–962.
- Chen, B.-R., and Runge, K. W. (2009). A new *Schizosaccharomyces pombe* chronological lifespan assay reveals that caloric restriction promotes efficient cell cycle exit and extends longevity. *Exp. Gerontol.*

- Chen, D., Toone, W. M., Mata, J., Lyne, R., Burns, G., Kivinen, K., Brazma, A., Jones, N., and Bahler, J. (2003). Global transcriptional responses of fission yeast to environmental stress. *Mol. Biol. Cell* *14*, 214–229.
- Chen, D., Wilkinson, C. R. M., Watt, S., Penkett, C. J., Toone, W. M., Jones, N., and Bahler, J. (2008). Multiple pathways differentially regulate global oxidative stress responses in fission yeast. *Mol. Biol. Cell* *19*, 308–317.
- Ikner, A., and Shiozaki, K. (2005). Yeast signaling pathways in the oxidative stress response. *Mutat. Res.* *569*, 13–27.
- Imlay, J. A. (2013). The molecular mechanisms and physiological consequences of oxidative stress: lessons from a model bacterium. *Nat. Rev. Microbiol.* *11*, 443–454.
- Jain, R., Vanamee, E. S., Dzikovski, B. G., Buku, A., Johnson, R. E., Prakash, L., Prakash, S., and Aggarwal, A. K. (2013). An iron-sulfur cluster in the polymerase domain of yeast DNA polymerase  $\epsilon$ . *J. Mol. Biol.*
- Jin, M., Fuji, M., Culley, B. M., Apolinario, E., Yamamoto, M., Maundrell, K., and Hoffman, C. S. (1995). *sck1*, a high copy number suppressor of defects in the cAMP-dependent protein kinase pathway in fission yeast, encodes a protein homologous to the *SCH9* kinase. *Genetics* *467*, 457–467.
- Jomova, K., and Valko, M. (2011). Advances in metal-induced oxidative stress and human disease. *Toxicology* *283*, 65–87.
- Joseph-Horne, T., Hollomon, D. W., and Wood, P. M. (2001). Fungal respiration: A fusion of standard and alternative components. *Biochim. Biophys. Acta - Bioenerg.* *1504*, 179–195.
- Jourdain, I., Gachet, Y., and Hyams, J. S. (2009). The dynamin related protein Dnm1 fragments mitochondria in a microtubule-dependent manner during the fission yeast cell cycle. *Cell Motil. Cytoskeleton* *66*, 509–523.
- Kanoh, J., Watanabe, Y., Ohsugi, M., Iino, Y., and Yamamoto, M. (1996). *Schizosaccharomyces pombe gad7+* encodes a phosphoprotein with a bZIP domain, which is required for proper G1 arrest and gene expression under nitrogen starvation. *Genes to Cells Devoted to Mol. Cell. Mech.* *1*, 391–408.
- Knutsen, J. H. J., Rein, I. D., Rothe, C., Stokke, T., Grallert, B., and Boye, E. (2011). Cell-cycle analysis of fission yeast cells by flow cytometry. *PLoS One* *6*, e17175.
- Kovall, R. A., and Hendrickson, W. A. (2004). Crystal structure of the nuclear effector of Notch signaling, CSL, bound to DNA. *EMBO J.* *23*, 3441–3451.
- Krisko, A., and Radman, M. (2013). Phenotypic and genetic consequences of protein damage. *PLoS Genet.* *9*.
- Labbé, S., Pelletier, B., and Mercier, A. (2007). Iron homeostasis in the fission yeast *Schizosaccharomyces pombe*. *Biometals* *20*, 523–537.
- Lawrence, C. L., Jones, N., and Wilkinson, C. R. M. (2009). Stress-induced phosphorylation of *S. pombe* Atf1 abrogates its interaction with F Box protein Fbh1. *Curr. Biol.* *19*, 1907–1911.

- Lawrence, C. L., Maekawa, H., Worthington, J. L., Reiter, W., Wilkinson, C. R. M., and Jones, N. (2007). Regulation of *Schizosaccharomyces pombe* Atf1 protein levels by Sty1-mediated phosphorylation and heterodimerization with Pcr1. *J. Biol. Chem.* *282*, 5160–5170.
- Lee, S.-Y., Song, J.-Y., Kwon, E.-S., and Roe, J.-H. (2007). Gpx1 is a stationary phase-specific thioredoxin peroxidase in fission yeast. *Biochem. Biophys. Res. Commun.* *367*, 67–71.
- Looke, M., Kristjuhan, K., and Kristjuhan, A. (2011). Extraction of genomic DNA from yeasts for PCR-based applications. *Biotechniques* *50*, 325–328.
- López-Avilés, S., Grande, M., González, M., Helgesen, A. L., Alemany, V., Sanchez-Piris, M., Bachs, O., Millar, J. B. a, and Aligue, R. (2005). Inactivation of the Cdc25 phosphatase by the stress-activated Srk1 kinase in fission yeast. *Mol. Cell* *17*, 49–59.
- López-Maury, L., Marguerat, S., and Bähler, J. (2008). Tuning gene expression to changing environments: from rapid responses to evolutionary adaptation. *Nat. Rev. Genet.* *9*, 583–593.
- Louvi, A., and Artavanis-Tsakonas, S. (2012). Notch and disease: A growing field. *Semin. Cell Dev. Biol.* *23*, 473–480.
- Madrid, M., Fernández-Zapata, J., Sánchez-Mir, L., Soto, T., Franco, A., Vicente-Soler, J., and Cansado, J. (2013). Role of the fission yeast cell integrity MAPK pathway in response to glucose limitation. *BMC Microbiol.*
- Madrid, M., Núñez, A., Soto, T., Vicente-Soler, J., Gacto, M., and Cansado, J. (2007). Stress-activated protein kinase-mediated down-regulation of the cell integrity pathway mitogen-activated protein kinase Pmk1p by protein phosphatases. *Mol. Biol. Cell* *18*, 4405–4419.
- Madrid, M., Soto, T., Khong, H. K., Franco, A., Vicente, J., Pérez, P., Gacto, M., and Cansado, J. (2006). Stress-induced response, localization, and regulation of the Pmk1 cell integrity pathway in *Schizosaccharomyces pombe*. *J. Biol. Chem.* *281*, 2033–2043.
- Maeda, T., Watanabe, Y., Kunitomo, H., and Yamamoto, M. (1994). Cloning of the *pka1* gene encoding the catalytic subunit of the cAMP-dependent protein kinase in *Schizosaccharomyces pombe*. *J. Biol. Chem.* *269*, 9632–9637.
- Magalhaes, J. P. De, and Church, G. M. (2006). Cells discover fire: Employing reactive oxygen species in development and consequences for aging. *Exp. Gerontol.* *41*, 1–10.
- Millar, J. B. A., Buck, V., and Wilkinson, M. G. (1995). Pyp1 and Pyp2 PTPases dephosphorylate an osmosensing MAP kinase controlling cell size at division in fission yeast. *Genes Dev.* *9*, 2117–2130.
- Miller, E. W., Dickinson, B. C., and Chang, C. J. (2010). Aquaporin-3 mediates hydrogen peroxide uptake to regulate downstream intracellular signaling. *Proc. Natl. Acad. Sci. U. S. A.* *107*, 15681–15686.
- Moen, R. J., Cornea, S., Oseid, D. E., Binder, B. P., Klein, J. C., and Thomas, D. D. (2014). Redox-sensitive residue in the actin-binding interface of myosin. *Biochem. Biophys. Res. Commun.*

- Morigasaki, S., Shimada, K., Ikner, A., Yanagida, M., and Shiozaki, K. (2008). Glycolytic enzyme GAPDH promotes peroxide stress signaling through multistep phosphorelay to a MAPK cascade. *Mol. Cell* 30, 108–113.
- Mourer, T., Jacques, J.-F., Brault, A., Bisailon, M., and Labbe, S. (2015). Shu1 is a cell-surface protein involved in iron acquisition from heme in *Schizosaccharomyces pombe*. *J. Biol. Chem.*, jbc.M115.642058.
- Mudge, D. K., Yang, F., Currie, B. M., Kim, J. M., Yeda, K., Bashyakarla, V. K., Ivey, F. D., and Hoffman, C. S. (2013). Sck1 negatively-regulates Gpa2-mediated glucose signaling in *Schizosaccharomyces pombe*. *Eukaryot. Cell*.
- Murphy, M. P. *et al.* (2011). Unraveling the biological roles of reactive oxygen species. *Cell Metab.*, 361–366.
- Mutoh, N., Nakagawa, C. W., and Yamada, K. (1999). The role of catalase in hydrogen peroxide resistance in fission yeast *Schizosaccharomyces pombe*. *Can. J. Microbiol.* 45, 125–129.
- Nakagawa, C. W., Yamada, K., and Mutoh, N. (2000). Role of Atf1 and Pap1 in the induction of the catalase gene of fission yeast *Schizosaccharomyces pombe*. *J. Biochem.* 238, 233–238.
- Nathan, C., and Cunningham-Bussel, A. (2013). Beyond oxidative stress: an immunologist's guide to reactive oxygen species. *Nat. Rev. Immunol.* 13, 349–361.
- Neely, L. A., and Hoffman, C. S. (2000). Protein kinase A and mitogen-activated protein kinase pathways antagonistically regulate fission yeast *fbp1* transcription by employing different modes of action at two upstream activation sites. *Mol. Cell. Biol.* 20, 6426–6434.
- Nelson, D. L., Lehninger, A. L., and Cox, M. M. (2008). Principles of Biochemistry.
- Nickel, A., Kohlhaas, M., and Maack, C. (2014). Mitochondrial reactive oxygen species production and elimination. *J. Mol. Cell. Cardiol.*
- Ntziachristos, P., Lim, J. S., Sage, J., and Aifantis, I. (2014). From fly wings to targeted cancer therapies: a centennial for notch signaling. *Cancer Cell* 25, 318–334.
- O'Donnell, P., Do, K. Q., and Arango, C. (2014). Oxidative/nitrosative stress in psychiatric disorders: Are we there yet? *Schizophr. Bull.*, 8–10.
- Ohmiya, R., Kato, C., Yamada, H., Aiba, H., and Mizuno, T. (1999). A fission yeast gene (*prrr1+*) that encodes a response regulator implicated in oxidative stress response. *J. Biochem.* 1066, 1061–1066.
- Oravcová, M., Teska, M., Půta, F., Folk, P., and Převorovský, M. (2013). Fission yeast CSL proteins function as transcription factors. *PLoS One* 8.
- Pancaldi, V., Sarac, O. S., Rallis, C., McLean, J. R., Převorovsky, M., Gould, K., Beyer, a., and Bahler, J. (2012). Predicting the fission yeast protein interaction network. *G3; Genes|Genomes|Genetics* 2, 453–467.

- Papadakis, M. a, and Workman, C. T. (2014). Oxidative stress response pathways: Fission yeast as archetype. *Crit. Rev. Microbiol.* 7828, 1–16.
- Paulo, E., García-Santamarina, S., Calvo, I. a, Carmona, M., Boronat, S., Domènech, A., Ayté, J., and Hidalgo, E. (2014). A genetic approach to study H<sub>2</sub>O<sub>2</sub> scavenging in fission yeast--distinct roles of peroxiredoxin and catalase. *Mol. Microbiol.* 92, 246–257.
- Penton, A. L., Leonard, L. D., and Spinner, N. B. (2012). Notch signaling in development and disease. *Semin. Cell Dev. Biol.* 14, 320–328.
- Petersen, J. (2009). TOR signalling regulates mitotic commitment through stress-activated MAPK and Polo kinase in response to nutrient stress. *Biochem. Soc. Trans.* 37, 273–277.
- Poljšak, B., and Fink, R. (2014). The protective role of antioxidants in the defence against ROS/RNS-mediated environmental pollution. *Oxid. Med. Cell. Longev.* 2014.
- Poole, R. K., and Lloyd, D. (1973). Oscillations of enzyme activities during the cell-cycle of a glucose-repressed fission-yeast *Schizosaccharomyces pombe* 972h-. *Biochem. J.* 136, 195–207.
- Převorovský, M., Groušl, T., Staňurová, J., Ryneš, J., Nellen, W., Půta, F., and Folk, P. (2009). Cbf11 and Cbf12 , the fission yeast CSL proteins, play opposing roles in cell adhesion and coordination of cell and nuclear division. *Exp. Cell Res.* 315, 1533–1547.
- Převorovský, M., Půta, F., and Folk, P. (2007). Fungal CSL transcription factors. *BMC Genomics* 12, 1–12.
- Pulliam, D. A., Bhattacharya, A., and Remmen, H. Van (2013). Mitochondrial Dysfunction in Aging and Longevity: A Causal or Protective Role? *Antioxidants Redox Signal.* 19.
- Quinlan, C. L., Perevoshchikova, I. V, Hey-Mogensen, M., Orr, A. L., and Brand, M. D. (2013). Sites of reactive oxygen species generation by mitochondria oxidizing different substrates. *Redox Biol.* 1, 304–312.
- Quinn, J., Findlay, V. J., Dawson, K., Millar, J. B. A., Jones, N., Morgan, B. A., and Toone, W. M. (2002). Distinct regulatory proteins control the graded transcriptional response to increasing H<sub>2</sub>O<sub>2</sub> levels in fission yeast *Schizosaccharomyces pombe*. *Mol. Biol. Cell* 13, 805–816.
- Quinn, J., Cheetham, J., Buck, V., Malakasi, P., Smith, D. A., Millar, J. B. A., and Morgan, B. A. (2011). Two-component mediated peroxide sensing and signal transduction in fission yeast. *Antioxid. Redox Signal.* 15.
- Radtke, F., MacDonald, H. R., and Tacchini-Cottier, F. (2013). Regulation of innate and adaptive immunity by Notch. *Nat. Rev. Immunol.* 13, 427–437.
- Rallis, C., Codlin, S., and Bahler, J. (2013a). TORC1 signaling inhibition by rapamycin and caffeine affect lifespan, global gene expression, and cell proliferation of fission yeast. *Aging Cell*, 563–573.
- Rallis, C., López-Maury, L., Georgescu, T., Pancaldi, V., and Bahler, J. (2013b). Systematic screen for mutants resistant to TORC1 inhibition in fission yeast reveals genes involved in cellular ageing and growth. *Biol. Open*.

- Reczek, C. R., and Chandel, N. S. (2015). ROS-dependent signal transduction. *Curr. Opin. Cell Biol.* 33, 8–13.
- Rhee, S. G. (2013). H<sub>2</sub>O<sub>2</sub>, a necessary evil for cell signaling. *Science* (80-. ). 1882.
- Rosini, M., Simoni, E., Milelli, A., Minarini, A., and Melchiorre, C. (2013). Oxidative stress in Alzheimer's disease: are we connecting the dots? *J. Med. Chem.*
- Roux, A. E., Quissac, A., Chartrand, P., Ferbeyre, G., and Rokeach, L. A. (2006). Regulation of chronological aging in *Schizosaccharomyces pombe* by the protein kinases Pka1 and Sck2. *Aging Cell*, 345–357.
- Sabatinos, S. A., and Forsburg, S. L. (2010). Molecular genetics of *Schizosaccharomyces pombe*. In: *Guide to yeast genetics: Functional genomics, Proteomics, and other systems analysis*, Elsevier Inc, 759–795.
- Samejima, I., Mackie, S., and Fantes, P. A. (1997). Multiple modes of activation of the stress-responsive MAP kinase pathway in fission yeast. *EMBO J.* 16, 6162–6170.
- Samejima, I., Mackie, S., Warbrick, E., Weisman, R., and Fantes, P. a (1998). The fission yeast mitotic regulator *win1+* encodes an MAP kinase kinase kinase that phosphorylates and activates Wis1 MAP kinase kinase in response to high osmolarity. *Mol. Biol. Cell* 9, 2325–2335.
- Sansó, M., Gogol, M., Ayté, J., Seidel, C., and Hidalgo, E. (2008). Transcription factors Pcr1 and Atf1 have distinct roles in stress- and Sty1-dependent gene regulation. *Eukaryot. Cell* 7, 826–835.
- Shieh, J. C., Wilkinson, M. G., Buck, V., Morgan, B. a., Makino, K., and Millar, J. B. a (1997). The Mcs4 response regulator coordinately controls the stress-activated Wak1-Wis1-Sty1 MAP kinase pathway and fission yeast cell cycle. *Genes Dev.* 11, 1008–1022.
- Shiozaki, K., and Russell, P. (1995). Cell-cycle control linked to extracellular environment by MAP kinase pathway in fission yeast. *Nature* 378, 739–743.
- Shiozaki, K., and Russell, P. (1996). Conjugation, meiosis, and the osmotic stress response are regulated by Spc1 kinase through Atf1 transcription factor in fission yeast. *Genes Dev.* 10, 2276–2288.
- Smethurst, D. G. J., Dawes, I. W., and Gourlay, C. W. (2013). Actin - a biosensor that determines cell fate in yeasts. *FEMS Yeast Res.* 14, 89–95.
- Smith, D. A., Toone, W. M., Chen, D., Bähler, J., Jones, N., Morgan, B. A., and Quinn, J. (2002). The *Srk1* Protein Kinase Is a Target for the *Sty1* Stress-activated MAPK in Fission Yeast. *J. Biol. Chem.* 277, 33411–33421.
- Stincon, A. *et al.* (2014). The return of metabolism: biochemistry and physiology of the pentose phosphate pathway. *Biol. Rev. Camb. Philos. Soc.*
- Takeda, T., Toda, T., Kominami, K., Kohnosu, A., Yanagida, M., and Jones, N. (1995). *Schizosaccharomyces pombe atf1+* encodes a transcription factor required for sexual development and entry into stationary phase. *EMBO J.* 14, 6193–6208.

- Toda, T., Dhut, S., Superti-Furga, G., Gotoh, Y., Nishida, E., and Sugiura, R. (1996). The fission yeast *pmk1+* gene encodes a novel mitogen-activated protein kinase homolog which regulates cell integrity and functions coordinately with the protein kinase C pathway. *Mol. Cell. Biol.*
- Toda, T., Shimanuki, M., and Yanagida, M. (1991). Fission yeast genes that confer resistance to staurosporine encode an AP-1-like transcription factor and a protein kinase related to the mammalian ERK1/MAP2 and budding yeast FUSS3 and KSS1 kinases. *Yeast* 2, 60–73.
- Toone, W. M., Kuge, S., Samuels, M., Morgan, B. A., Toda, T., and Jones, N. (1998). Regulation of the fission yeast transcription factor Pap1 by oxidative stress: requirement for the nuclear export factor Crm1 (Exportin) and the stress-activated MAP kinase Sty1/Spc1. *Genes Dev.* 12.
- Valko, M., Leibfritz, D., Moncol, J., Cronin, M. T. D., Mazur, M., and Telser, J. (2007). Free radicals and antioxidants in normal physiological functions and human disease. *Int. J. Biochem. Cell Biol.* 39, 44–84.
- Valko, M., Morris, H., and Cronin, M. T. D. (2005). Metals, Toxicity and Oxidative Stress. *Curr. Med. Chem.*, 1161–1208.
- Veal, E. a, Day, A. M., and Morgan, B. a (2007). Hydrogen peroxide sensing and signaling. *Mol. Cell* 26, 1–14.
- Veal, E. A., Findlay, V. J., Day, A. M., Bozonet, S. M., Evans, J. M., Quinn, J., and Morgan, B. A. (2004). A 2-Cys Peroxiredoxin Regulates Peroxide-Induced Oxidation and Activation of a Stress-Activated MAP Kinase. *Mol. Cell* 15, 129–139.
- Veal, E. A., Toone, W. M., Jones, N., and Morgan, B. A. (2002). Distinct roles for glutathione S -transferases in the oxidative stress response in *Schizosaccharomyces pombe*. *J. Biol. Chem.*
- Vivancos, A. P., Castillo, E. a, Biteau, B., Nicot, C., Ayté, J., Toledano, M. B., and Hidalgo, E. (2005). A cysteine-sulfinic acid in peroxiredoxin regulates H<sub>2</sub>O<sub>2</sub> -sensing by the antioxidant Pap1 pathway. *Proc. Natl. Acad. Sci. U. S. A.* 102, 8875–8880.
- Vivancos, A. P., Castillo, E. A., Jones, N., Ayté, J., and Hidalgo, E. (2004). Activation of the redox sensor Pap1 by hydrogen peroxide requires modulation of the intracellular oxidant concentration. *Mol. Microbiol.* 52, 1427–1435.
- Vivancos, A. P., Jara, M., Zuin, A., Sansó, M., and Hidalgo, E. (2006). Oxidative stress in *Schizosaccharomyces pombe*: different H<sub>2</sub>O<sub>2</sub> levels, different response pathways. *Mol. Genet. Genomics* 276, 495–502.
- Watson, J. D. (2014). Type 2 diabetes as a redox disease. *Lancet* 383, 841–843.
- Wei, N. *et al.* (2014). Oxidative stress diverts tRNA synthetase to nucleus for protection against DNA damage. *Mol. Cell*, 1–10.
- Weisman, R. (2010). Chapter 13 - Fission yeast TOR and rapamycin. In: *The Enzymes*, Elsevier Inc., 251–269.

- Wells, M. L., Huang, W., Li, L., Gerrish, K. E., Fargo, D. C., Oszolak, F., and Blackshear, P. J. (2012). Post-transcriptional regulation of cell-cell interaction protein-encoding transcripts by Zfs1p in *S. pombe*. *Mol. Cell. Biol.* *32*, 4206–4214.
- Wilkinson, M. G., Samuels, M., Takeda, T., Toone, W. M., Shieh, J.-C., Toda, T., Millar, J. B. A., and Jones, N. (1996). The Atf1 transcription factor is a target for the Sty1 stress-activated MAP kinase pathway in fission yeast. *Genes Dev.* *10*, 2289–2301.
- Wood, V. *et al.* (2012). PomBase: A comprehensive online resource for fission yeast. *Nucleic Acids Res.* *40*, 695–699.
- Zadzinski, R., Fortuniak, A., Bilinski, T., Grey, M., and Bartosz, G. (1998). Menadione toxicity in *Saccharomyces cerevisiae* cells: Activation by conjugation with glutathione. *Biochem. Mol. Biol. Int.* *44*, 747–759.
- Zaitsevskaya-Carter, T., and Cooper, J. A. (1997). Spm1, a stress-activated MAP kinase that regulates morphogenesis in *S. pombe*. *EMBO J.* *16*, 1318–1331.
- Zuin, A., Carmona, M., Morales-Ivorra, I., Gabrielli, N., Vivancos, A. P., Ayté, J., and Hidalgo, E. (2010a). Lifespan extension by calorie restriction relies on the Sty1 MAP kinase stress pathway. *EMBO J.* *29*, 981–991.
- Zuin, A., Castellano-Esteve, D., Ayté, J., and Hidalgo, E. (2010b). Living on the edge: Stress and activation of stress responses promote lifespan extension. *Aging (Albany, NY)*. *2*, 231–237.
- Zuin, A., Gabrielli, N., Calvo, I. a, García-Santamarina, S., Hoe, K.-L., Kim, D. U., Park, H.-O., Hayles, J., Ayté, J., and Hidalgo, E. (2008). Mitochondrial dysfunction increases oxidative stress and decreases chronological life span in fission yeast. *PLoS One* *3*, e2842.

## 8 List of supplements

1. Supplementary Table 1. *Schizosaccharomyces pombe* strains used in this study
2. Manuscript CSL transcription factors regulate periodic gene expression and cell-cycle progression in the fission yeast, submitted for publication in MBoC (2015)

**Supplementary Table 1. *Schizosaccharomyces pombe* strains used in this study**

<b>ID</b>	<b>Genotype</b>	<b>Experiments</b>	<b>Source/Reference</b>
<b>JB32</b>	h <sup>+</sup> s	spot tests, respiration	Lab stock
<b>MP21</b>	h <sup>+</sup> s $\Delta cbf12::natR$	spot tests, respiration, strain construction	Převorovský, Tvarůžková <i>et al.</i> *
<b>MP25</b>	h <sup>+</sup> s $\Delta cbf11::kanR \Delta cbf12::natR$	spot tests, respiration	Převorovský, Tvarůžková <i>et al.</i> *
<b>MP44</b>	h <sup>+</sup> s $\Delta cbf11::kanR$	strain construction	Převorovský, Tvarůžková <i>et al.</i> *
<b>MP114</b>	h <sup>+</sup> s $\Delta cbf11::natR$	spot tests, respiration, strain construction, FACS	Převorovský, Tvarůžková <i>et al.</i> *
<b>MP73</b>	h <sup>+</sup> $\Delta cbf12::natR ura4-D18 leu1-32$	strain construction	Lab stock
<b>MP83</b>	h <sup>+</sup> $\Delta cbf11::natR ura4-D18 leu1-32$	strain construction	Lab stock
<b>JB146</b>	h <sup>-</sup> $\Delta atf1::ura4 ura4-D18$	strain construction, spot tests	Lab stock
<b>JB147</b>	h <sup>-</sup> $\Delta pap1::ura4 ura4-D18$	strain construction, spot tests	Lab stock
<b>JB148</b>	h <sup>-</sup> $\Delta prr1::his7 his7-?$	strain construction, spot tests	Lab stock
<b>JB149</b>	h <sup>-</sup> $\Delta sty1::ura4 ura4-D18$	strain construction, FACS, spot tests	Lab stock
<b>JB554</b>	h <sup>-</sup> $\Delta pmk1::KanMX6$	strain construction, spot tests	Lab stock
<b>JB669</b>	h <sup>-</sup> $\Delta hrs1::hygB$	strain construction, spot tests	Lab stock
<b>JB725</b>	h <sup>-</sup> $\Delta pka1::KanMX6$	strain construction, spot tests	Lab stock
<b>JB996</b>	h <sup>-</sup> $\Delta sck1::KanMX4$	strain construction, spot tests	Lab stock
<b>JB997</b>	h <sup>-</sup> $\Delta sck2::KanMX4$	strain construction, spot tests	Lab stock
<b>MP326</b>	h <sup>-</sup> $gar2-mCherry:kanR leu1 ura4$	microscopy	Lab stock
<b>MP328</b>	h <sup>-</sup> $\Delta cbf12::natR \Delta sck1::kanMX4$	spot tests	This study
<b>MP330</b>	h <sup>-</sup> $\Delta cbf12::natR \Delta sck2::kanMX4$	spot tests	This study
<b>MP332</b>	h <sup>-</sup> $\Delta cbf11::natR \Delta sck1::kanMX4$	spot tests	This study
<b>MP344</b>	h <sup>+</sup> $\Delta cbf11::natR gar2-GFP:kanR$	microscopy	Lab stock
<b>MP351</b>	h <sup>-</sup> $\Delta cbf11::natR \Delta pka1::kanMX6$	spot tests	This study; Převorovský, Tvarůžková <i>et al.</i> *
<b>MP354</b>	h <sup>-</sup> $\Delta cbf11::natR \Delta prr1::his7 his7-?$	spot tests	This study
<b>MP355</b>	h <sup>-</sup> $\Delta cbf12::natR \Delta prr1::his7 his7-?$	spot tests	This study
<b>MP358</b>	h <sup>-</sup> $\Delta cbf12::natR \Delta pka1::kanMX6$	spot tests	This study
<b>MP360</b>	h <sup>-</sup> $\Delta cbf11::natR \Delta sck2::kanMX4$	spot tests	This study
<b>MP361</b>	h <sup>-</sup> $\Delta cbf12::natR \Delta hrs1::hygB$	spot tests	This study
<b>MP362</b>	h <sup>-</sup> $\Delta cbf11::natR \Delta hrs1::hygB$	spot tests	This study

\* manuscript submitted for publication

**Supplementary Table 1. *Schizosaccharomyces pombe* strains used in this study - continued**

<b>ID</b>	<b>Genotype</b>	<b>Experiments</b>	<b>Source/Reference</b>
<b>MP363</b>	h- $\Delta cbf11::natR \Delta pmk1::KanMX6$	spot tests	This study
<b>MP364</b>	h- $\Delta cbf12::natR \Delta pmk1::KanMX6$	spot tests	This study
<b>MP365</b>	h- $\Delta cbf12::natR \Delta atf1::ura4 ura4-D18$	spot tests	This study
<b>MP366</b>	h- $\Delta cbf12::natR \Delta pap1::ura4 ura4-D18$	spot tests	This study
<b>MP367</b>	h- $\Delta cbf11::natR \Delta atf1::ura4 ura4-D18$	spot tests	This study
<b>MP368</b>	h- $\Delta cbf11::natR \Delta pap1::ura4 ura4-D18$	spot tests	This study
<b>MP376</b>	h- $\Delta cbf12::natR \Delta sty1::ura4 ura4-D18$	spot tests	This study
<b>MP382</b>	h- $\Delta cbf11::natR \Delta sty1::ura4 ura4-D18$	FACS, spot tests	This study; Převedrovský, Tvarůžková <i>et al.</i> *
<b>MP431</b>	h- $\Delta srx1::ura4 ade6-M216 his7-366 leu1-32 ura4-D18$	strain construction, spot tests	Bozonet <i>et al.</i> , 2005
<b>MP432</b>	h+ $\Delta gpx1::ura4 ade6-M210 his7-366 leu1-32 ura4-D18$	strain construction, spot tests	Bozonet <i>et al.</i> , 2005
<b>MP433</b>	h+ $\Delta gst2::ura4 ade6-210 his7-366 leu1-32 ura4-D18$	strain construction, spot tests	Veal <i>et al.</i> , 2002
<b>MP464</b>	h- $\Delta cbf11::natR \Delta srx1::ura4 ade6-M216 his7-366 leu1-32 ura4-D18$	spot tests	This study
<b>MP465</b>	h+ $\Delta cbf11::natR \Delta gpx1::ura4 ade6-M210 his7-366 leu1-32 ura4-D18$	spot tests	This study
<b>MP466</b>	h+ $\Delta cbf11::natR \Delta gst2::ura4 ade6-210 his7-366 leu1-32 ura4-D18$	spot tests	This study
<b>MP471</b>	h+ $\Delta ctt1::natR$	spot tests	This study
<b>MP472</b>	h+ $\Delta cbf11::kanR \Delta ctt1::natR$	spot tests	This study

\* manuscript submitted for publication